Functional outcomes of *Cadps* A-to-I RNA editing in the nervous and endocrine systems

By

Kayla M. Shumate

Dissertation

Submitted to the Faculty of the

Graduate School of Vanderbilt University

in partial fulfillment of the requirements

for the degree of

DOCTOR OF PHILOSOPHY

in

Pharmacology

May 14, 2021

Nashville, Tennessee

Approved:

Ronald B. Emeson, PhD

Carrie K. Jones, PhD

Heidi E. Hamm, PhD

Ege T. Kavalali, PhD

David M. Miller III, PhD

ACKNOWLEDGEMENTS

To my mentor, Dr. Ronald Emeson, thank you for providing a supportive learning environment that encouraged the tenacious pursuit of hypotheses while demanding rigorous experimental design. You have deeply shaped my approach to scientific problem solving and have instilled in me an appreciation for rigorous, reproducible research. I am certain that your mantra “You must first convince yourself the effect is real” will serve me well throughout my scientific career.

To my committee chair, Dr. Carrie Jones, thank you for your unwavering dedication to my success as a graduate student. The hours spent designing experiments, reviewing data, and preparing for presentations made a profound impact on my training, and I am very grateful for your service as my committee chair, mentor, and advocate.

To my collaborator and committee member, Dr. Ege Kavalali, thank you for the engaging, insightful conversations about synaptic transmission and for welcoming me into the rich scientific community of your lab. It has been invigorating to be surrounded by exceptionally talented and kind individuals who are share an enthusiasm for scientific discovery.

To my committee members, Drs. Heidi Hamm and David Miller III, thank you for your thoughtful input at our meetings and help in critically shaping the direction of this work.

To my colleagues, Kathleen Patterson, Dr. Turnee Malik, and Christopher Hofmann, thank you for your extensive technical assistance, countless whiteboard sessions, and importantly, for your endless capacity to create a fun work environment.

To my husband, Timothy Rodriguez, thank you for your constant encouragement and your steadfast enthusiasm for my pursuit of my career goals. Be it a partner to celebrate with, a shoulder to cry on, or a warm meal to come home to, your day-to-day support has made graduate school profoundly more manageable and for that I am extremely grateful.

To my parents, Allen and Phyllis Shumate, thank you for encouraging me to dream big and for the sacrifices you made in support of those dreams. You taught me to boldly approach new challenges and to work hard to achieve my goals, while giving me the space to succeed or fail by providing a safety net of unconditional love. I can never thank you enough.

TABLE OF CONTENTS

LIST OF TABLES

LIST OF FIGURES

CHAPTER 1

Introduction

Neuronal communication by chemical neurotransmission

The human brain is comprised of approximately 100 billion neurons which direct complex behaviors, from planning and executing motor movements to feeling and emoting happiness. Cognition and behavior require the coordination of neuronal circuits that span different regions of the brain. As such, communication between neurons is essential for proper function. Neuronal communication occurs predominantly by chemical neurotransmission, a process in which the release of chemicals by one neuron is sensed by adjacent neurons. The chemical message is translated to an electrical signal that is transduced down the length of a neuron. Once the electrical signal reaches the synapse, or terminal ends of the neuron, the signal is again translated into a chemical message and is released to communicate to the next neuron in the circuit.

The process of chemical neurotransmission has been studied for decades and a consensus view of the cycle of regulated neurotransmitter release, exocytosis, has been established (Figure 1). Secretory vesicles, small intracellular organelles with discrete membranes, are formed by membrane budding off endosomes or through local recycling. Vesicles traffic to the synapse and are then loaded with chemical neurotransmitters. Next, vesicles undergo docking and priming at the active zone, a specialized site of release containing a dense collection of proteins required to facilitate release. Docking and priming reactions position vesicles directly opposed to the plasma membrane in preparation to respond to calcium influx. When nearby voltage gated Ca^{2+} channels open, calcium sensors activate and trigger merging of vesicle and plasma membranes. A fusion pore is created, connecting the vesicle lumen and extracellular space, to permit release of vesicle contents into the synaptic cleft therefore completing exocytosis. Vesicles are re-generated through multiple endocytotic pathways and can re-enter the cycle of

regulated exocytosis. (Sudhof, 2004). In summary, chemical neurotransmission is a cellular process that translates electrical signals into chemical neurotransmitter release which allows neurons to communicate, therefore providing the foundation for nervous system function.

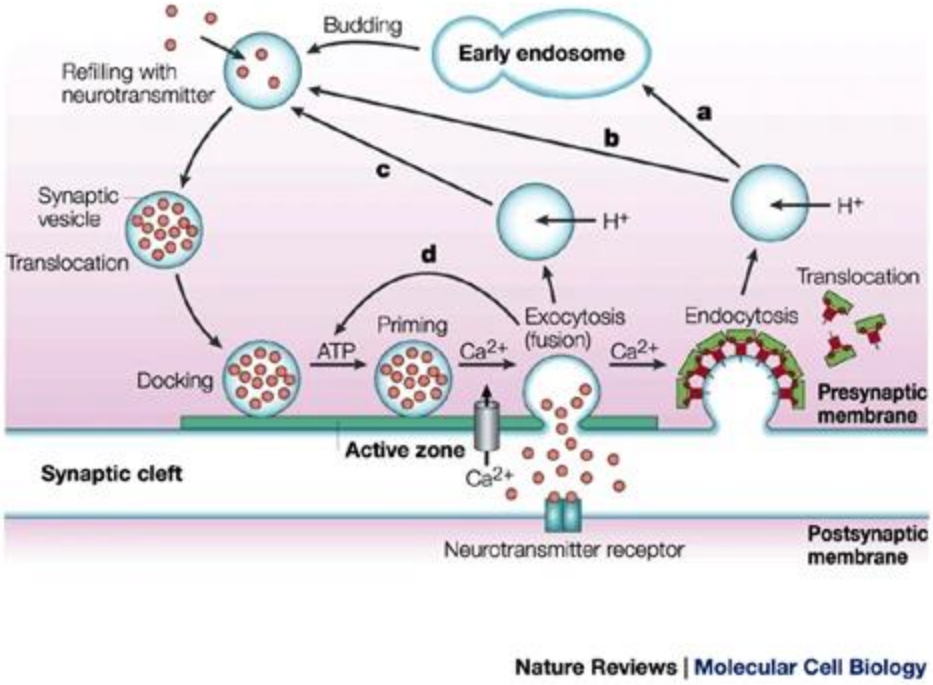

Figure 1. The synaptic vesicle cycle. Synaptic vesicles bud off the early endosome or are recycled from the plasma membrane and are filled with neurotransmitter. Vesicles traffic to the active zone where they undergo docking and ATP-dependent priming. Once primed, vesicles can rapidly respond to Ca^{2+} influx through voltage gated calcium channels by fusing with the plasma membrane to release neurotransmitter into the synaptic cleft. Vesicles can undergo clatherin-dependent endocytosis to return to the synaptic vesicle cycle. Image source (Gundelfinger, Kessels, & Qualmann, 2003), reprinted with copyright permission.

Vesicle docking and priming by SNARE and accessory proteins

During chemical neurotransmission, vesicles undergo docking and priming at the active zone. Docking and priming of vesicles is methodically orchestrated through a multitude of protein-protein interactions that enable eventual fusion of vesicle and plasma membranes. Once trafficked to the synapse, vesicles are tethered and docked at the active zone through interactions between cytomatrix active zone-enriched proteins, including bassoon and piccolo, Rab-Interacting Molecules (RIMs), RIM binding proteins (RIM-BPs), the CAST/ELKS/Brunchpilot proteins, Liprin-αs, and munc13s, and vesicle bound proteins including Rab3s and Rab27b (Gundelfinger, Kessels, & Qualmann, 2003; Kaeser et al., 2011; Mukherjee et al., 2010; Pavlos et al., 2010; Siksou et al., 2009; Y. Wang, Okamoto, Schmitz, Hofmann, & Sudhof, 1997). Vesicles then undergo priming through the coordinated actions of **s**oluble **N**-ethylmaleimide sensitive factor **a**ttachment protein **re**ceptors, SNARE, and SNARE assembly proteins including munc-13s, munc18s, and CAPS (Augustin, Rosenmund, Sudhof, & Brose, 1999; Gerber et al., 2008; Jockusch et al., 2007). T-SNAREs, located on the target or plasma membrane, and v-SNAREs, located on the vesicle membrane, contribute alpha helices that zipper together at least partially into a tetrahelical bundle, termed the trans-SNARE complex to complete vesicle priming (Sollner, Bennett, Whiteheart, Scheller, & Rothman, 1993; Sutton, Fasshauer, Jahn, & Brunger, 1998). The canonical neuronal SNARE complex is comprised of four parallel alpha helices: one from the v-SNARE synaptobrevin-2 (syb-2), one from the t-SNARE syntaxin-1 (stx-1) and two from the t-SNARE SNAP-25 (Sutton et al., 1998). Docking and priming of vesicles require sequential protein-protein interactions that are necessary for proper SNARE complex formation.

Through the work of many groups, the molecular interactions underlying the formation of the trans-SNARE complex have been identified, and a model of trans-complex assembly has been proposed. First, stx-1 must transition from an auto-inhibited, “closed” state to an open state in which the SNARE domain, H3, is exposed and available to interact with cognate SNARE domains (Dulubova et al., 1999; Misura, Scheller, & Weis, 2000; B. Yang, Steegmaier, Gonzalez

Jr., & Scheller, 2000). Subsequently, the SNARE domains of SNAP-25 and syb2 bind to stx-1 H3 domain and partially zipper together, which locks vesicles within 1-3 nm of the plasma membrane (Imig et al., 2014). At this stage, vesicles are primed and poised to rapidly respond to a Ca^{2+} stimulus and fuse with the plasma membrane to complete the cycle of regulated exocytosis.

SNARE accessory proteins, including munc-13s, munc-18s, and CAPS, aid in proper SNARE complex assembly by stabilizing assembly intermediates, accelerating protein conformation state transitions, and templating tetrahelical bundle formation (Figure 2). Munc18-1 interacts with the auto-inhibitory H_{abc} domain of stx-1 to lock stx-1 in the "closed" conformation (Dulubova et al., 1999; Hata, Slaughter, & Sudhof, 1993; B. Yang, Steegmaier, Gonzalez, & Scheller, 2000). This interaction stabilizes membrane bound stx-1 and prevents formation of non-productive SNARE domain interactions such as 2:1 heteromers generated between 2 copies of stx-1 and 1 copy of SNAP-25 (Ma, Su, Seven, Xu, & Rizo, 2013). Munc13-1 accelerates protein conformation state transitions by opening stx-1 to permit interactions between stx-1 H3 and cognate SNARE domains (Ma, Li, Xu, & Rizo, 2011; X. Yang et al., 2015). *In vitro* studies have also identified roles for munc13-1 and munc18 in promoting parallel tetrahelix assembly and proper helix registration by templating insertion of syb2 and/or SNAP25 SNARE domains into a nascent SNARE complex (Jiao et al., 2018; Lai et al., 2017; Shu, Jin, Rothman, & Zhang, 2020; S. Wang et al., 2019). These two functions promote the formation of functional instead of misassembled, non-functional SNARE complexes. In summary, SNARE accessory proteins interact with SNARE proteins to promote formation of functional, properly assembled SNARE complexes.

While SNARE accessory proteins play an auxiliary role in vesicle priming, they are essential for regulated exocytosis, neuronal communication, and animal viability. For example, knockout of munc13-1 in mice leads to a loss of vesicle priming, a 90% reduction in evoked excitatory neurotransmission, and perinatal lethality (Augustin et al., 1999). All spontaneous and evoked excitatory and inhibitory neurotransmission is lost in munc13-1/2 double knockout

neurons, suggesting that the remaining neurotransmission in munc13-1 KO is due to munc13-2 activity (Varoqueaux et al., 2002). Similarly, knockout of munc18-1 in mice leads to loss of evoked excitatory neurotransmission, neuronal degeneration, and perinatal lethality (Verhage et al., 2000) Therefore the SNARE accessory proteins munc13-1 and munc18-1 are essential, and necessary for regulated exocytosis.

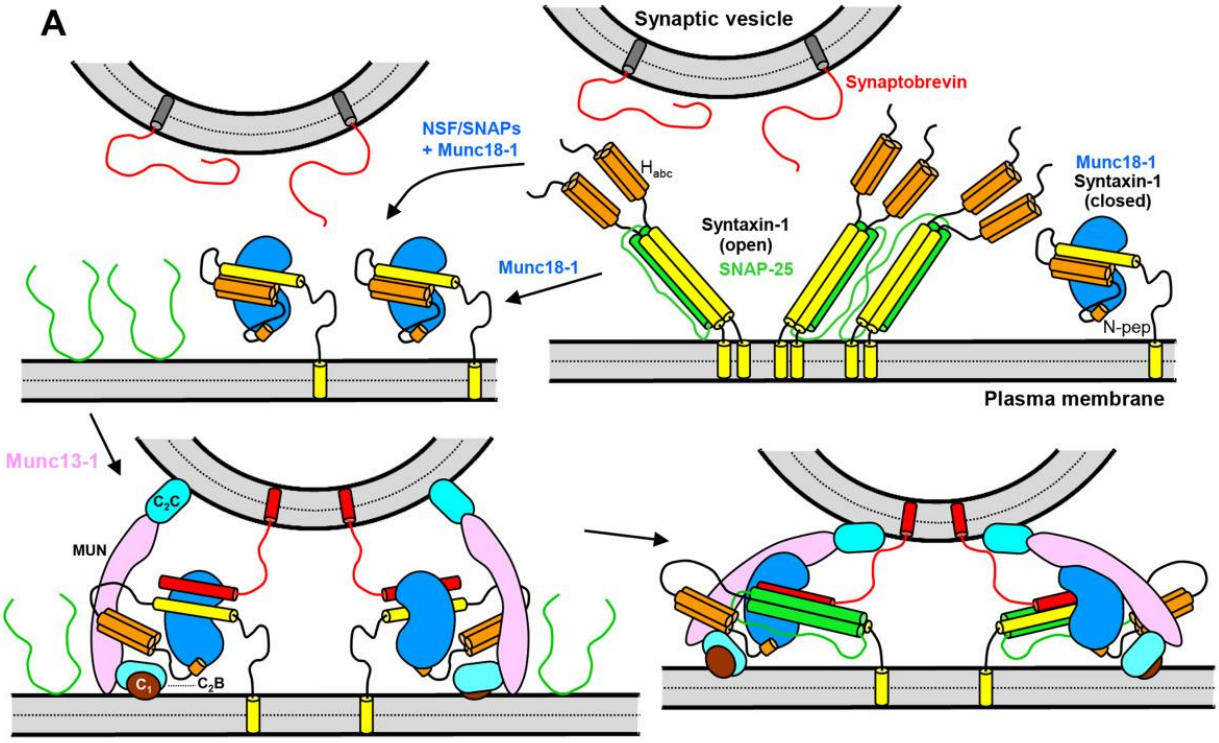

Figure 2. SNARE and SNARE accessory proteins mediate synaptic vesicle priming. *Upper right panel.* In the absence of munc18-1, the SNARE domains of syntaxin-1 (yellow) and SNAP-25 (green) form non-productive heteromers. *Upper left panel.* Munc18-1 (blue) binds the SNARE domain and Habc domain (orange) of syntaxin-1 to lock it in a closed state in the first step of SNARE priming. *Lower left panel.* Addition of munc13-1 (purple) mediates opening of syntaxin-1 through Habc and linker domain interactions and mediates vesicle and plasma membrane bridging through C_1 (brown) and C_2C domain (cyan) interactions with phospholipids. Munc18-1 templates alignment of synaptobrevin (red) and syntaxin (yellow) SNARE domains to further SNARE priming. *Lower right panel.* Addition of SNAP-25 SNARE domains (green) complete SNARE complex formation and SNARE priming. Adapted from (Rizo, 2018), reprinted with copyright permission.

Calcium-dependent Activator Protein for Secretion

CAPS Family

Another SNARE accessory protein is **C**alcium-dependent **a**ctivator **p**rotein for **s**ecretion, CAPS. There are two mammalian CAPS paralogs, CAPS1 and CAPS2, which are expressed throughout the central nervous system and in peripheral endocrine tissues (Cisternas, Vincent, Scherer, & Ray, 2003; Sadakata et al., 2006; Speidel et al., 2003; J. H. Walent, B. W. Porter, & T. F. Martin, 1992a). Specifically, CAPS1 is expressed widely throughout the CNS and high levels of expression are detected in the adrenal glands as well. CNS expression of CAPS2 is more limited, with high expression noted in the cerebellum. CAPS1 and CAPS2 largely exhibit discrete developmental and tissue specific expression patterns in mice, but limited examples of cellular co-expression have been reported (Sadakata et al., 2006; Shaib et al., 2018; Speidel et al., 2008). Although CAPS1 and CAPS2 contain the same functional domains and exhibit about 80% amino acid sequence identity, when co-expressed in the same cell, they regulate neurotransmission at distinct release sites (Shaib et al., 2018; Speidel et al., 2003). For example, in dorsal root ganglia neurons CAPS1 regulates release of glutamate from SVs, while CAPS2 promotes release of neuropeptides from LDCVs (Shaib et al., 2018). Therefore, the two mammalian CAPS family members, CAPS1 and CAPS2, exhibit discrete expression profiles and when they are co-expressed, they likely perform non-redundant cellular functions.

CAPS1 Domain Architecture & Synaptic Function

Mammalian CAPS1 was discovered as a 145 kDa cytosolic factor derived from rat brain lysate that reconstituted norepinephrine release from cracked PC12 cells (J. H. Walent, B. W. Porter, & T. F. J. Martin, 1992b). Once cloned, the rat *Cadps* gene was recognized as an ortholog of *unc-31*, a *C. elegans* gene first identified by Sydney Brenner while performing a mutagenesis screen for the uncoordinated phenotype (Ann, Kowalchyk, Loyet, & Martin, 1997; Brenner, 1974).

Human *CADPS,* identified in 2004, shares 98% sequence identity with mouse *Cadps*, suggesting that the functional properties of the protein identified in mice are relevant to the human protein (Cisternas et al., 2003).

Global ablation of CAPS1 expression [CAPS1 knockout (KO) mice] provide insight into the physiologic importance and *in vivo* function of CAPS1. Pups from heterozygous matings are born at normal mendelian ratios, yet CAPS1 KO mice are lethargic and have labored breathing, leading to perinatal lethality. There are no gross alterations in brain, heart, lung, or adrenal gland morphology demonstrating that CAPS1, like munc13-1/2 and munc18, is not necessary for normal development but is required for survival (Speidel et al., 2005). The synaptic function of CAPS1 in vesicle docking/priming is illustrated by imaging studies of CAPS1 null synapses, which show a decrease in the number of docked vesicles (Imig et al., 2014; Shinoda et al., 2016). Electrophysiology studies also support a role for CAPS1 in vesicle priming, as demonstrated by a reduction in the size of the readily releasable pool, or primed, vesicles in CAPS1 KO neurons (Jockusch et al., 2007). Therefore, CAPS1 is an essential protein that functions similarly to munc13s and munc18s in facilitating vesicle priming in neurons.

CAPS1 contains four discrete protein domains that modulate lipid and protein interactions: a C2 domain, a pleckstrin homology (PH) domain, a Munc-homology domain (MHD), and a C-terminal domain (CTD) (Figure 3). These domains direct CAPS1 binding to the plasma membrane, SNARE complex, and vesicles to promote priming and exocytosis.

In neuronal proteins, canonical C2 domains are autonomously folded, Ca^{2+}-dependent phospholipid binding modules (Rizo & Sudhof, 1998). However, these C2 domain functions remain mostly unexplored in CAPS, and other functions have been attributed to it. As for calcium binding, CAPS1 has two Ca^{2+} binding sites with affinities of 270 µM and 4.3 mM (Ann et al., 1997). Early studies found CAPS1 binds to hydrophobic chromatography columns in a Ca^{2+}-dependent manner and exhibits differential proteolysis when exposed to Ca^{2+}, suggesting that CAPS1 undergoes a conformational shift upon Ca^{2+} binding (Ann et al., 1997; Walent et al., 1992a).

Whether CAPS1 docking/priming function is Ca^{2+} dependent remains debated as there are data to support both conclusions using different variations of *in vitro* liposome fusion assays (James, Kowalchyk, Daily, Petrie, & Martin, 2009; Kreutzberger et al., 2017). No studies have directly assessed Ca^{2+} or phospholipid binding of the CAPS1 C2 domain. Instead, recent work has shown the C2 domain mediates homodimerization of CAPS1, in a manner analogous to the C2 domain of munc13-1 (Lu et al., 2006; Petrie et al., 2016). The majority of active CAPS1 is dimerized, based on characterization of PC12 membrane bound CAPS, and deletion of the C2 domain impairs CAPS1-dependent exocytosis in PC12s (Petrie et al., 2016). Furthermore, mutations in the C2 domain impair release of norepinephrine from permeable PC12 cells, decrease release of NPY-mCherry from cultured neurons, and cause significant neuronal dysfunction in *C. elegans* (L. Avery, Bargmann, & Horvitz, 1993; Grishanin et al., 2004; van Keimpema, Kooistra, Toonen, & Verhage, 2017). Therefore, the CAPS1 C2 domain is necessary for vesicle priming and CAPS1 homodimerization, but it remains unknown if it acts as a canonical C2 domain to modulate Ca^{2+} or phospholipid binding.

A CAPS1 domain that has been attributed to phospholipid binding is the pleckstrin-homology or PH domain. The CAPS1 PH domain binds nonspecifically to acidic phospholipids, such as phosphoinositides and phosphoserines, and exhibits preference for $PI(4,5)P_2$ over PI(5)P, $PI(3,5)P_2$, and $PI(3,4,5)P_3$ (Grishanin et al., 2002; Loyet et al., 1998). Interaction of the CAPS1 PH domain with phosphoserine is important for PM targeting and PH domain mutants with disrupted phosphoserine binding fail to rescue exocytosis in CAPS1/2 DKO neurons and cracked PC12 cells (Grishanin et al., 2002; van Keimpema et al., 2017). CAPS1 synaptic function is dependent on PIP_2 interactions, as PIP_2 cleavage by PLCŋ2 during high frequency stimulation leads to CAPS1 independent exocytosis in PC12 cells (Kabachinski, Yamaga, Kielar-Grevstad, Bruinsma, & Martin, 2014). In summary, the PH domain of CAPS1 enables phosphoserine and phosphoinositide lipid interactions at the active zone that support CAPS1-dependent exocytosis.

Another membrane targeting domain is the carboxy-terminal or CTD of CAPS1. This domain is important for vesicle interactions, as the CTD alone is sufficient for DCV association in PC12 cells (Grishanin et al., 2002). CAPS1 is thought to traffic to synapses with vesicles in PC12 cells, and CTD deletion impairs synaptic enrichment of CAPS1 in hippocampal neurons (Kabachinski, Kielar-Grevstad, Zhang, James, & Martin, 2016; van Keimpema et al., 2017). The CTD is essential for CAPS1 function in SV and DCV exocytosis, as deletion impairs exocytosis in PC12s and hippocampal neurons (Grishanin et al., 2002; van Keimpema et al., 2017). The CTD also interacts with septins, a family of neuronally expressed small GTPase proteins that form structural filaments (Hosono et al., 2016; Kinoshita, Noda, & Kinoshita, 2000). Multiple septins are localized pre-synaptically and function in regulated exocytosis, including septin-8 (Beites, Xie, Bowser, & Trimble, 1999; Tsang et al., 2001). Septin-8 interacts with the v-SNARE syb2 and is thought to promote SNARE complex formation through interactions with SNARE complex intermediates containing syb2, stx-1, and synaptophysin (Ito et al., 2009). Although this hypothesis has not been formally tested, it is intriguing to speculate that CAPS1 CTD interaction(s) with septins could be the molecular link between the CTD and vesicles. CAPS1 CTD is an essential domain and mediates interactions with vesicles, potentially through a complex with septin proteins.

The MHD domain of CAPS1 interacts with multiple SNARE proteins and plays a central role in CAPS1 function of promoting SNARE complex formation. It will be discussed in more detail below. In summary, CAPS1 is a large, multi-domain protein that homodimerizes via its C2 domain and functions in vesicle exocytosis through interactions with the plasma membrane, SNARE complex, and vesicles via interactions with the PH domain, MHD domain, and CTD, respectively.

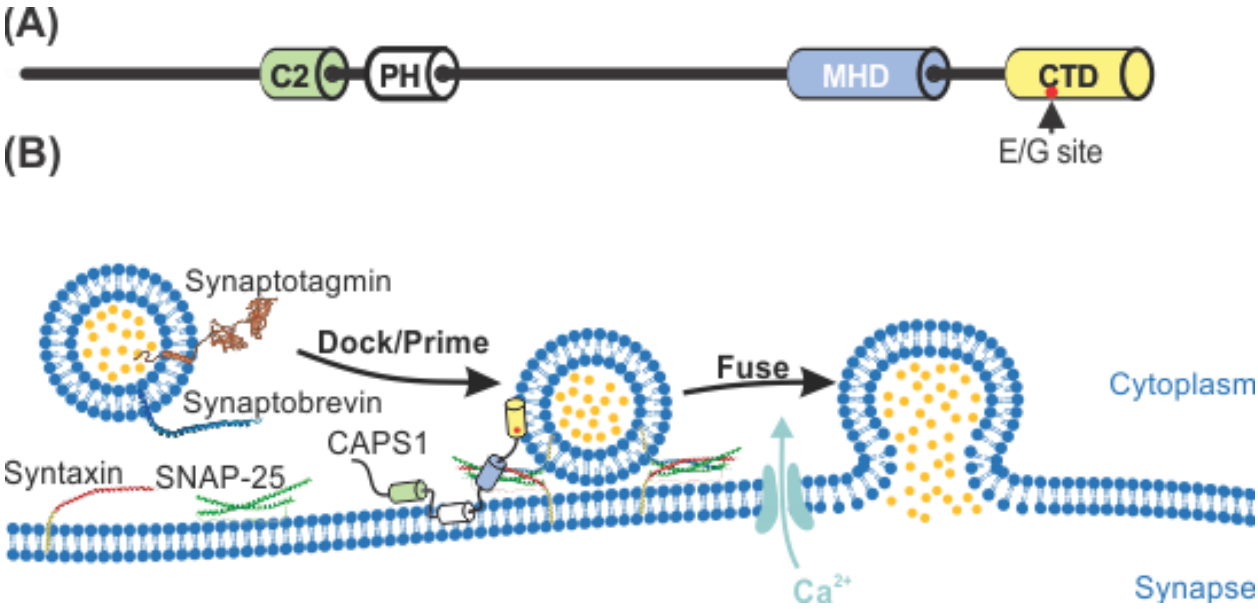

Figure 3. CAPS1 domain structure and interactions during vesicle priming. (**A**) Domain structure of CAPS1 showing the C2 (green), pleckstrin-homology (white), munc-homology (blue), and carboxy-terminal domains (yellow). The location of the E/G editing site is indicated (•). (**B**) CAPS1 domain interactions during vesicle priming showing the PH domain interaction with the plasma membrane, the MHD interaction with the SNARE complex, and the CTD interacting with the SV membrane.

CAPS1 as a SNARE accessory protein

While munc-13s and munc18 are key SNARE accessory proteins that participate in SNARE complex formation, specific roles for CAPS1 in this process also have been identified. The CAPS1 MHD domain is required for CAPS1-dependent vesicle exocytosis and interacts with all the canonical SNARE proteins. Deletion of CAPS1-MHD impairs exocytosis in cracked PC12 cells, whereas expression of MHD alone does not support exocytosis, signifying that the CAPS1-MHD is necessary, but not sufficient, for CAPS1-dependent exocytosis (Grishanin et al., 2002). Additionally, exocytosis of BDNF-GFP is impaired in PC12 cells expressing a truncated CAPS1ΔMHD, demonstrating the importance of the MHD in intact cells (Khodthong, Kabachinski, James, & Martin, 2011). In summary, the MHD domain is required for CAPS1-dependent exocytosis.

CAPS1-MHD mediates interactions with all canonical SNARE proteins, including stx-1, syb2, and SNAP-25, in modes that are distinct from munc13 and munc18 binding. CAPS1 binds to full-length, membrane bound stx-1a with an affinity 220 nM (Daily, Boswell, James, & Martin, 2010). The H3 (SNARE domain) and transmembrane domain linker region of stx-1 are CAPS1 binding sites, and CAPS1 interactions with closed stx-1 are very weak, suggesting CAPS1 binds the exposed H3 and linker region when stx-1 is in an open conformation (Daily et al., 2010; Parsaud et al., 2013). Further, CAPS1 selectivity interacts with syntaxins-1, -2, and -4, but not syntaxins-3 and -6, which may confer synapse specificity (Daily et al., 2010). Truncated forms of CAPS1, containing the MHD domain, can outcompete full length CAPS1 binding to stx-1 liposomes and inhibit liposome fusion, illustrating the requirement of the MHD domain-stx-1 interaction for CAPS1 function (James et al., 2009).

Full length and MHD domain fragments of CAPS1 also interact with syb2 liposomes, with a binding affinity of 212 nM. This interaction is sensitive to botulinum neurotoxin D, indicating residues 1-60 of syb2 are important for the interaction (Daily et al., 2010; Khodthong et al., 2011). SNAP-25 liposomes and full length CAPS1 interact with an apparent K_D of ~400 nM (Daily et al.,

2010) and the N-terminal SNARE helix, SN1, is the likely SNAP-25 binding site for CAPS1 (Daily et al., 2010). Therefore, the CAPS1 MHD domain interacts with all canonical SNARE proteins, as demonstrated by *in vitro* biochemical studies, and interactions with stx-1 serve an essential role in CAPS1 function.

Beyond mapping binding interactions between CAPS1 and canonical SNAREs, many studies have described a role of CAPS1 in mediating trans-SNARE complex formation. In liposome fusion and lipid mixing assays, CAPS1 enhances the rate of lipid mixing and fusion between donor v-SNARE containing liposomes and acceptor t-SNARE containing liposomes (James et al., 2009). Addition of CAPS1 to a mixture of donor and acceptor liposomes also results in increased in SNARE complex formation (James et al., 2009). Furthermore, in an alternative *in vitro* assay system using purified DCVs and supported lipid bilayers containing t-SNAREs, removal of CAPS significantly impedes Ca^{2+}-dependent vesicle exocytosis, through impaired vesicle docking/priming, not fusion (Kreutzberger et al., 2017). In a recent study by Zhou and colleagues, a crystal structure of the CAPS1 DAMH domain (domain of unknown function, DUF+MHD) was solved and structure-guided studies were performed to characterize the role of the DAMH in SNARE complex assembly. The authors identified inhibitory and faciliatory roles of CAPS1 in trans-SNARE complex formation through interactions with the munc13-1 MUN domain and SNARE complex intermediates. CAPS1 DAMH domain binds to the munc13-1 MUN domain and inhibits the ability of the munc13-1 MUN domain to open stx-1 through displacement of munc-18-1 (H. Zhou et al., 2019). In a lipid mixing assay, CAPS1 inhibits munc13-1 MUN domain induced lipid mixing between stx-1/munc-18 liposomes and syb2 liposomes (H. Zhou et al., 2019).These data suggest an inhibitory role for CAPS1 in initial opening of stx-1 by munc-13-1. As for a role in promoting trans-SNARE complex formation, CAPS1 DAMH stabilizes a SNARE complex reaction intermediate consisting of stx-1 – SNAP-25 heteromers and protects this intermediate from degradation by munc-18 (H. Zhou et al., 2019). Mutations in the DAMH region that abrogate binding to the stx-1/SNAP-25 intermediate fail to rescue DCV exocytosis in CAPS1

knockdown PC12 cells, demonstrating the physiological significance of this interaction ((H. Zhou et al., 2019). Therefore, the CAPS1 DAMH domain has two distinct roles in trans-SNARE complex formation. In the future, it will be interesting to see if the interaction between the munc13-1 MUN domain and the CAPS1 DAMH domain is of physiologic relevance.

Whether CAPS1 function is redundant with munc13 and/or other SNARE accessory proteins is a long-standing debate in the vesicle priming field. Munc13 and CAPS proteins share several functional domains, including the SNARE binding MHD domain and C2 domains. Phylogenetic analysis suggests a conserved role of munc13 and CAPS MUN domains, extended versions of the MHD, as tethering complexes acting at synapses (Pei, Ma, Rizo, & Grishin, 2009; Stevens & Rettig, 2009). However, several lines of evidence refute functional redundancy. First, CAPS1 binds to SNAREs in conformations or at binding sites that are distinct from other SNARE accessory proteins. Binding of CAPS1 to t-SNARE and v-SNARE liposome mixtures is not outcompeted by addition of munc18-1 or complexin-1, indicating that CAPS1 binds SNAREs in distinct regions or in distinct modes from munc18-1 and complexin-1 (Daily et al., 2010). Additionally, munc13-1 MUN domain and syb2 and SNAP-25 interactions occur at sites that are distinct from CAPS1 binding locations (S. Wang et al., 2019). Studies in primary hippocampal neurons have also shown CAPS1 overexpression cannot rescue munc13-1/2 loss of function in regulated exocytosis and conversely, munc13-1 overexpression cannot rescue CAPS1 loss of function (Jockusch et al., 2007). Together, data from these studies show that CAPS1-SNARE binding sites are distinct from other SNARE accessory proteins and support the notion that CAPS1 acts in a similar, yet non-redundant manner to munc13s in regulating exocytosis.

A-to-I RNA Editing

CAPS1 transcripts are subject to co-transcriptional modifications including alternative splicing and RNA editing that increase the diversity of cellular CAPS1 protein isoform expression (Ann et al., 1997; Miyake et al., 2016). RNA editing was first identified in mammals in 1987 when

a C-to-U alteration in the mRNA sequence of apolipoprotein B was discovered in intestinal lysates. As uracil base pairs with adenine during translation, a C-to-U transition in the mRNA coding sequence results in alteration of the encoded amino acid. C-to-U editing in Apo-B results in generation of a pre-mature stop codon, resulting in a truncated form of Apo-B that is expressed in a tissue specific manner (Powell et al., 1987). Subsequently, several types of RNA editing have been identified, with adenosine-to-inosine (A-to-I) RNA editing recognized as the most abundant modification in mammalian transcripts (Bahn et al., 2012; Park, Williams, Wold, & Mortazavi, 2012). In A-to-I RNA editing, select adenosines undergo hydrolytic deamination at the C6 position of the purine ring to generate an inosine nucleoside (Polson, Crain, Pomerantz, McCloskey, & Bass, 1991). Inosine preferentially base pairs with cytosine and is therefore recognized by most cellular machinery, including tRNA anticodon loops, as guanosine (Basilio, Wahba, Lengyel, Speyer, & Ochoa, 1962). A-to-I RNA editing is mediated by a family of enzymes termed ADARs, adenosine deaminases that act on RNA (Hough & Bass, 1994; Kim et al., 1994; Melcher, Maas, Herb, Sprengel, Seeburg, et al., 1996; O'Connell et al., 1995). There are three mammalian ADARs, but only ADAR1 and ADAR2 are catalytically active (Chen et al., 2000; Melcher, Maas, Herb, Sprengel, Higuchi, et al., 1996). ADARs are expressed throughout the central nervous system and contain two key domains, double stranded RNA binding domains and a catalytic adenosine deaminase domain (Melcher, Maas, Herb, Sprengel, Higuchi, et al., 1996; O'Connell & Keller, 1994). ADARs bind selectively to dsRNA duplexes, which are typically formed through *cis* interactions of inverted sequence repeats near the editing site and in downstream introns (Lomeli et al., 1994). Double-stranded RNA duplex elimination abolishes ADAR binding and A-to-I RNA editing (Herb, Higuchi, Sprengel, & Seeburg, 1996; Higuchi et al., 1993; Rueter, Burns, Coode, Mookherjee, & Emeson, 1995; Rueter, Dawson, & Emeson, 1999). In summary, A-to-I RNA editing is a co-transcriptional process mediated by ADAR interactions with dsRNA duplexes resulting in catalytic deamination of adenosine to inosine.

Due to the base changing nature of A-to-I RNA editing, the effects on mRNA transcripts vary widely. Most frequently, editing events occur in intronic sequences and Alu repeats and have no known function (Park et al., 2012; Ramaswami et al., 2013). However, there are several well characterized examples of A-to-I editing that result in changes in translated protein sequence, including splice site alterations, pre-mature stop codon generation, and non-synonymous amino acid substitutions (Rueter et al., 1995). A-to-I editing of GluA2 mRNA, encoding a subunit of the AMPA subtype of ionotropic glutamate receptor, results in a non-synonymous glutamine to arginine alteration in the amino acid sequence and is the best characterized example of a coding change mediated by editing (Rueter et al., 1995). GluA2 Q/R site editing renders AMPA receptors containing the edited subunit impermeable to Ca^{2+}, which is critical for proper nervous system function (Brussa et al., 1995; Sommer, Kohler, Sprengel, & Seeburg, 1991). Additional A-to-I RNA editing sites in the mammalian transcriptome that result in nonsynonymous substitutions include sites in the 2C-subtype of the serotonin receptor, the K_v 1.1 voltage-gated potassium channel, the metabotropic glutamate receptor subtype 4, and CAPS1 itself.

CAPS1 E/G Site RNA Editing

In a 2009 publication, Li and colleagues identified a potential A-to-I RNA editing site within human CAPS1 by comparing genomic DNA sequences to RNA sequences from seven tissues of a single individual (Li et al., 2009). Within exon 28 of the human *CADPS* gene, guanosine was detected in cDNA transcripts generated from RNA while adenosine was detected in the genomic DNA sequence. This nucleotide alteration is predicted to cause a non-synonymous change in the amino acid sequence at position 1250, resulting in a glutamate to glycine substitution. The human CAPS1 E/G site was also identified in a 2013 study aimed at mapping A-to-I RNA editing events using RNA sequencing alone (Ramaswami et al., 2013). Our lab has shown that CAPS1 E/G site editing is conserved across mammalian species, making it well suited to study using rodent model systems.

CAPS1 E/G site RNA editing has been characterized in greater detail by our lab and in a 2016 publication by Miyake and colleagues (Miyake et al., 2016). The minimal sequence required for duplex formation and RNA editing is located within a region encompassing portions of human exon 28 and intron 28, which align with mouse exon 27 and intron 27. CAPS1 E/G site editing occurs in mice and humans, with tissue specific levels of editing ranging from ~80% in human adrenal glands to <20% in total brain. Editing of CAPS1 can be mediated by both ADAR1 and ADAR2 in mice (Miyake et al., 2016), though a recent study using variations of ADAR1 and ADAR2 knockout mice found CAPS1 is preferentially edited by ADAR2 (Cruz, Kato, Nakahama, Shibuya, & Kawahara, 2020). In summary, *Cadps* transcripts in mice and humans are subject to RNA editing by ADAR2 and the frequency of editing varies by tissue.

To investigate the physiologic effect of CAPS1 E/G site editing, mice that solely express the edited isoform of CAPS1, CAPS1(G), were generated by substituting a guanosine for adenosine at the editing site. Homozygous mice bearing the CAPS1(G) allele are hyperactive and males are lean due to loss of white adipose tissue mass. This correlates with increased energy expenditure as measured by increases in $V0_2$ consumption. Administration of 0.5 mg/kg haloperidol, a dopamine D2 receptor antagonist, normalized hyperactivity and energy expenditure in CAPS1(G) mice (Miyake et al., 2016). No differences were identified in other neurobehavioral assays performed, including tests for motor coordination, anxiety, spatial learning and memory and thermal nociception. In summary, increased CAPS1(G) expression has physiologic effects in mice, including enhanced locomotor activity and energy expenditure.

The impact of CAPS1 E/G site editing on CAPS1 cellular function has been studied using adrenal chromaffin cells and striatal synaptosome preparations. Edited CAPS1 increases release of norepinephrine in PC12 cells when compared to non-edited CAPS1, and primary adrenal chromaffin cells isolated from CAPS1(G) mice have an increase in the number of exocytosis events. Assessment of DCV distribution in chromaffin cells by electron microscopy found no differences in number of vesicles within 100nm of the plasma membrane, though it should be

noted that vesicle counts at this depth include those located in several pools, including the reserve and readily releasable vesicle pools. It's been shown that CAPS1/2 DKO neurons have no differences in the absolute number of vesicles located within 100 nm of an active zone, but breakdown of this distribution in smaller bins shows a distinct decrease in vesicles 0-5 nm from the active zone, indicating absence of docked/primed vesicles, with a commensurate increase in vesicle counts in the 10-20 nm, 20-30 nm, and 30-40 nm bins (Imig et al., 2014). Therefore, further characterization of CAPS1(G) expressing PC12 cells is required to draw conclusions about effects on vesicle docking/priming. Stimulated release of dopamine from striatal synaptosomes prepared from CAPS1(G) mice was also increased, demonstrating a role of CAPS1 editing regulating exocytosis in endocrine and neural cells.

To elucidate a molecular mechanism by which CAPS1 E/G site editing increases CAPS1 function, Miyake and colleagues investigated interactions between CAPS1 and syntaxin1. Recombinant edited CAPS1 pulled down more endogenous stx-1 from mouse brain lysates than non-edited CAPS1. In line with previous studies, purified edited CAPS1 interacted more with recombinantly-expressed open stx-1 than with closed stx-1 (Daily et al., 2010). Additionally, edited CAPS1 has enhanced interactions with open stx-1 when compared to non-edited CAPS1. In summary, CAPS1 E/G site editing alters *in vitro* interactions with stx-1 which may contribute to enhanced exocytosis, given the essential role of stx-1 in neurotransmission.

A preliminary study focused of the functional effects of CAPS1 E/G site editing identified increased release of dopamine and norepinephrine that is potentially driven by enhanced interactions of edited CAPS1 with open stx-1. Many questions remain about the role of CAPS1 editing in neurotransmission, including how editing impacts spontaneous and evoked release of neurotransmitters and hormones in intact cells and tissue, which neurotransmitter/hormone systems are impacted by editing, and whether physiologically relevant outcomes, other than locomotor activity, are altered by increased or decreased levels of CAPS1 editing. In this body of this work, I will attempt to address these questions and will also seek to reproduce key findings

presented by Miyake and colleagues. These studies will provide more insight into how dysregulation of *Cadps* editing would affect nervous and endocrine system function thereby impacting human health.

CHAPTER 2

Functional effects of *Cadps* editing on fast neurotransmission

Modified from: Shumate *et al*. “RNA editing-mediated regulation of CAPS1 localization and its impact on synaptic transmission” (under review, 2021).

Introduction

Fast neurotransmission is rapid inter-neuronal signaling by glutamate, GABA, and glycine that occurs in less than 1 millisecond. Signaling through these neurotransmitters is extremely rapid due the ionotropic nature of post-synaptic receptors and precise spatial alignment of pre-synaptic release sites with post-synaptic receptor-containing densities. Key tenets of the synaptic vesicle cycle and regulated exocytosis have been elucidated by studying fast neurotransmission. Therefore, it is a logical starting point for our studies of the functional effects of *Cadps* editing. Historically, primary hippocampal neurons have been a popular model system for studying fast neurotransmission. For example, the role of CAPS1 as a synaptic vesicle priming protein was first elucidated using primary hippocampal neuron cultures generated from CAPS1 knockout mice (Jockusch et al., 2007). Therefore, we will characterize spontaneous and evoked, excitatory and inhibitory neurotransmission in primary hippocampal neurons cultured from mice solely expressing either non-edited or edited CAPS1 to gain further insight into how *Cadps* editing regulates fast neurotransmission.

The role of CAPS1 in regulating fast, excitatory spontaneous and evoked exocytosis has been studied extensively. CAPS1 deletion in primary hippocampal neurons decreases the frequency and amplitude of spontaneous release events, reduces the amplitude of evoked release events, and alters short term synaptic plasticity (Jockusch et al., 2007). These observations are further supported *in vivo,* as region-specific knockout of CAPS1 leads to a decrease in excitatory neurotransmission at hippocampal CA3-CA1 synapses (Shinoda et al., 2016) and cerebellar climbing fiber-Purkinje cell synapses (Sadakata et al., 2013). CAPS1-

mediated short-term synaptic plasticity is physiologically significant, as mutant mice in which CAPS1 expression was selectively ablated from the thalamus exhibited altered short term synaptic depression at thalamocortical layer IV synapses (Nestvogel et al., 2020). Altered synaptic plasticity led to stronger adaptation to visual stimulation in anesthetized animals, illustrating the capacity for changes in pre-synaptic plasticity to have significant neuronal network effects. Thus, CAPS1 promotes excitatory spontaneous and evoked neurotransmission and alters short term synaptic plasticity in both *in vitro* and *in vivo* model systems, which suggests editing of *Cadps* may impact fast neurotransmission.

We also will explore the mechanisms connecting edited CAPS1 to enhanced exocytosis further by characterizing the localization of CAPS1. As the CAPS1 E/G editing site is in the carboxy-terminal domain, we are particularly interested in investigating synaptic localization of CAPS1. Previous studies using cultured neurons have shown that CAPS1 is expressed diffusely in the soma (Eckenstaler, Lessmann, & Brigadski, 2016) and in puncta along neurites which colocalize with several pre-synaptic proteins including the vesicular glutamate transporter 1 (vGlut1) (Farina et al., 2015), synaptobrevin-2 (Shaib et al., 2018), synapsin 1/2 (Shaib et al., 2018), and synaptophysin 1 (van Keimpema et al., 2017). The CTD of CAPS1 is necessary for its synaptic localization in cultured neurons, as deletion of the domain eliminates CAPS1 puncta in neurites and ablates its co-localization with synaptophysin (van Keimpema et al., 2017). Furthermore, neurons expressing a truncated CAPS1 protein lacking its C-terminus fail to support dense core vesicle (DCV) exocytosis (van Keimpema et al., 2017), demonstrating the significance of this domain for proper synaptic localization and function. Therefore, we will test the hypothesis that edited CAPS1 has enhanced synaptic localization compared to its non-edited counterpart.

In conclusion, the effect of *Cadps* RNA editing on exocytosis of synaptic vesicles containing the fast-acting neurotransmitters, glutamate and GABA, and a link between enhanced exocytosis and SNARE protein binding remain uncharacterized. In this chapter, we examine the effect of *Cadps* RNA editing on spontaneous and evoked neurotransmission at excitatory and

inhibitory synapses using primary hippocampal neuron cultures isolated from mutant mice engineered to solely express either edited or non-edited *Cadps* mRNAs. We will also assess CAPS1 synaptic localization and identify a role for neuronal activity in regulating *Cadps* editing levels.

Methods

Animal Information

Mutant mice in which the editing of *Cadps* transcripts was selectively ablated, *Cadps*^{em1Eme} hereafter referred to as termed CAPS1(E) mice, were made using the CRISPR-cas9 system to delete the editing site complementary sequence in intron 27 of the *Cadps* gene (Figure 5a). Two gRNAs (Sigma-Aldrich; Figure 5b), and cas9 mRNA (Sigma-Aldrich, cat. CAS9MRNA) were injected into the cytoplasm of single cell embryos derived from C57Bl/6NHsd mice (Envigo). Embryos were transplanted into pseudo-pregnant foster dams and pups were screened for the desired deletion using the CAPS1(E) genotyping protocol (*described below*) and direct sequencing of PCR amplicons. A founder animal, heterozygous for the mutant *Cadps* allele, was mated with wild-type C57Bl/6NHsd animals to generate heterozygous offspring. Mutant animals were backcrossed to wild-type C57Bl/6NHsd animals to eliminate potential off-target effects and all subsequent offspring were generated by heterozygous mating to maintain the homozygous mutant line and appropriate control littermates.

Mice solely expressing edited CAPS1 transcripts, *Cadps*^{tm1Osb} hereafter referred to as CAPS1(G) mice, were developed using the C57Bl/6NJcl mouse strain and cryopreserved mouse embryos from this line were acquired from the Institute of Physical and Chemical Research (Riken; cat. CDB1091K). Mouse embryos were re-derived by implantation of embryos into pseudo-pregnant foster dams. Pups were screened for the mutant allele using the CAPS1(G)

genotyping protocol (*described below*) and all subsequent offspring were generated by heterozygous mating to maintain the homozygous mutant line and appropriate control littermates.

As CAPS1(E) and CAPS1(G) mice were developed using slightly divergent C57Bl/6N background strains (C57Bl/6NHsd and C57Bl/6NJcl, respectively), all experiments were performed in both mutant and wild-type animals from each respective strain [termed CAPS1(E) WT and CAPS1(G) WT]. Comparisons between wild-type littermates for CAPS1(E) and CAPS1(G) mutant mice were made for every experiment to control for possible strain effects and are reported in Figure 8Figure 10, and Figure 12.

All animal procedures were approved by the Vanderbilt Institutional Animal Care and Use Committee (protocol #s M2000083 and M1500005). Animals were separated by sex at weaning and housed in cages with 2-5 mixed genotype littermates. *Ad libitum* access to food and water was provided with a 12-hour light/dark cycle and standard environmental conditions. All animals were euthanized in accordance with the AVMA Guidelines for the Euthanasia of Animals (2020 edition). 12-week-old mice (3 females and 2 males/genotype; females 17-23 grams, males 23-29 grams) were used for qRT-PCR and *Cadps* editing level quantification experiments. 12-week-old male mice were used for Western blotting analyses.

Mouse genotyping

Genomic DNA from tail or toe biopsy samples was prepared using REDExtract-N-Amp Tissue PCR Kit (Sigma-Aldrich, cat. XNAT) according to the manufacturer's instructions. CAPS1(E) mice were genotyped by PCR amplification using forward (5'-TCCCACTTGTC-CTCTCTCAGATG-3') and reverse (5'-GGAGGCCCCACTGGTGAGTT-3') primers to generate PCR amplicons that span the targeted deletion. Amplification products were resolved by 2% agarose gel electrophoresis to detect amplicons corresponding to the wild-type (177 bp) and CAPS1(E) (127 bp) alleles (Figure 6). Mice bearing the CAPS1(G) allele were genotyped using direct sequence analysis of PCR amplicons containing the editing site, generated using forward

(5'-GATGGACGTGGCCGACGCCTACG-3') and reverse (5'-CTGGGATGCAGACACAGCCACACC-3') primers.

Primary Hippocampal Cell Cultures

Primary dissociated hippocampal neuron cultures were prepared as described previously (Kavalali, Klingauf, & Tsien, 1999; Schoch et al., 2001). Briefly, hippocampi were dissected from 1- to 2-day-old homozygous CAPS1(E), CAPS1(G) mutant mice and wild-type littermates. Dissected hippocampi were dissociated with a trypsin solution (10 mg/mL) for 10 minutes at 37°C. After mechanical trituration by pipetting, the cells were plated on 12 mm glass cover slips coated with Matrigel (Corning Biosciences, Tewksbury, MA) with a ratio of 3 cover slips per hippocampus. The growth medium contained MEM (without phenol red), 5 g/L D-glucose, 0.2 mg/L $NaHCO_3$, 100 mg/L transferrin, 0.5 mM L-glutamine, 2% B27 supplement and 5% fetal bovine serum. 2 µM cytosine arabinoside (Sigma, St. Louis, MO) was added to the medium after 1 day *in vitro* (DIV 1) and the concentration was reduced to 1 µM at DIV 4. Cultures were incubated at 37°C in a humidified incubator with a 95% air/5% CO_2 environment and all experiments were performed at DIV 15-18.

Activity Modulation of Neurons

Primary hippocampal cell cultures from wild-type mice were treated with 40 µM bicuculline (Sigma, cat. 14340), 2 µM TTX (Enzo Life Science, cat. BML-NA120-0001), or an equal volume of 99.5% DMSO (Sigma, cat. D4540) as vehicle control on DIV 15 and were incubated for 48 hours at 37°C in a humidified incubator with a 95% air/5% CO_2 environment.

Quantification of CAPS1 RNA editing

RNA was extracted from flash frozen, sagittally bisected whole brain tissue using Trizol Reagent (Invitrogen, cat. 15596018) according to the manufacturer's instructions. RNA was isolated from neuron cultures using Trizol to harvest cells and phase separate the RNA according to manufacturer's instructions. The aqueous phase from the Trizol separation was added to an equal volume of 70% ethanol and loaded onto a purification column provided with the Rneasy

Micro Kit (Qiagen, cat. 74004), and the remaining steps of purification were carried out according to the manufacturer's instructions. The optional on-column Dnase treatment step was performed using Rnase-free Dnase according to the manufacturer's instructions (Qiagen, cat. 79254). cDNA was prepared from 2 µg (brain tissue) or 200 ng (neuron cultures) of total RNA using the High-Capacity cDNA Reverse Transcription kit (Applied Biosystems, cat. 4368813). RT-PCR amplicons spanning the *Cadps* editing site were generated using forward (5'-GATGGACGTGGCCGACGCCTACG-3) and reverse (5'- CTGTCCTTCATGCTGATA-CCTTGTAAG-3') primers. PCR amplicons were visualized by agarose gel electrophoresis and purified using the SV Wizard PCR and Gel Clean-up Kit according to the manufacturer's instructions (Promega, cat. A9282). Purified PCR amplicons were sequenced using the reverse primer indicated above. Relative peak heights in sequence electropherogram traces were used to quantify RNA editing, as previously described (Malik, Cartailler, & Emeson, 2021).

qRT-PCR

RNA was extracted and cDNA generated from bisected brain tissue and primary neuron cultures, as described above. Quantitative RT-PCR was performed using a *Cadps* probe/primer set (Applied Biosystems, assay Mm00488924_m1) with Eukaryotic 18S rRNA control probe/primer limited set (Applied Biosystems, cat. 4319413E), or *Adar* primer/probe set (Applied Biosystems, assay Mm00508001_m1) and *Adarb1* primer/probe set (Applied Biosystems, assay Mm00504621_m1) with control *Gapdh* primer/probe set (Applied Biosystems, assay Mm99999915_g1) and 2X TaqMan Universal PCR Mastermix (Applied Biosystems, cat. 4304437). Data analysis was performed using the $\Delta\Delta C_t$ method (Livak & Schmittgen, 2001).

Deep Sequencing

Complementary DNA was generated as described above. A two-step RT-PCR strategy was employed to multiplex samples within one Illumina flow cell, as previously described (Hood et al., 2014), using forward (5'-ATTAACCCTCACTAAAGGGATTCTCAGGATGTCCTTCGTGATA-3) and reverse (5'-

TAATACGACTCACTATAGGGTCAGCCACGTGCAGATGATG-3') primers that span the *Cadps* editing site. Data exclusion criteria were pre-defined as any reads that were not identical to the *Cadps* reference gene sequence 15 nucleotides up or downstream from the editing site.

Western Blotting

Whole cell lysates from brain tissue were prepared using RIPA buffer supplemented with cOmplete™, Mini, EDTA-free protease inhibitor tablets (Roche, cat. 4693159001). Equal concentrations of protein samples were resolved by SDS-PAGE electrophoresis using a 4-20% gradient gel (Bio-Rad, cat. 4561094). Proteins were transferred to a nitrocellulose membrane (Cytiva, cat. 10600004) using a semi-dry transfer apparatus. Membranes were air dried for at least 30 minutes, re-hydrated, and blocked for 1 hour with Intercept PBS blocking buffer (LI-COR, cat. 927-70001). Primary and secondary antibodies (Table 1) were diluted in blocking buffer and blots were incubated overnight or for 2 hours with primary and secondary antibodies, respectively. Immunoblots were imaged using an Odyssey CLx infrared imaging system (LI-COR) and quantified using Image Studio Lite (LI-COR).

Immunocytochemistry and Quantitative Colocalization Analysis

DIV16-19 primary hippocampal neurons were washed in PBS and fixed in a buffer containing 1% PFA/7.5% sucrose in PBS (wt/vol). Autofluorescence was reduced with a 50mM glycine solution and cells were permeabilized in 0.0075% (wt/vol) digitonin buffer. Coverslips were blocked with 2% BSA and incubated overnight with primary antibodies diluted in blocking buffer. Primary antibodies used include rabbit anti-CAPS1 (Synaptic Systems, cat. 262 013, 1:200), mouse anti-vGAT (Synaptic Systems, cat. 131 011, 1:200), and guinea pig anti-vGlut1 (Synaptic Systems, cat. 135 304, 1:1,000). After washing, secondary antibodies diluted in blocking buffer were added for 1-2 hours. Secondary antibodies used include goat anti-rabbit Alexa 568 (Invitrogen, cat. A11011, 1:500), donkey anti-mouse Alexa 488 (Invitrogen, cat. 21202, 1:500), and goat anti-guinea pig Alexa 647 (Invitrogen, cat. A21450, 1:1,000). Coverslips were washed and imaged within 48 hours. Cells were imaged using a Zeiss LSM 510 Meta inverted confocal

microscope. Image Z stacks were captured at 1024 x 1024 resolution, using a 63X (na 1.4) oil immersion objective. Images not used for analysis were pre-defined as those in which x, y drift occurred through the Z stack, or those in which obvious fluorescent artifacts (cell debris, aggregates of secondary antibody) were present that could skew proper threshold analysis.

Object-based colocalization was performed using the 3D object counter in Fiji (National Institutes of Health), with slight modifications to the object overlap analysis method previously described (Bolte & Cordelieres, 2006). Briefly, images were segmented using the Moments threshold analysis (Tsai, 1985). Channels were split, and a shape filter (IJ Blob, elongation=0-0.6) (Wagner & Lipinski, 2013) and water-shedding were applied to the green (vGAT) and blue (vGlut1) channels to select for individual, punctate-like structures. 3D objects were counted in the blue and green channels using the 3D object counter. Z stacks of each channel to be co-localized were multiplied (i.e., CAPS1 x vGAT and CAPS1 x vGlut1) to obtain a Z-stack of overlapping pixels. 3D objects were counted in each overlap stack using a size filter to define positive colocalization as an overlap of >15 voxels of two colors in the same object (calibration: 1 voxel = 0.143 × 0.143 × 1 μm). The number of CAPS1-containing puncta was determined by dividing the number of objects counted in the overlap z stack by the number of objects counted in the respective individual z stack for vGlut1 or vGAT. A custom macro was written to automate these procedures and is available upon request.

Electrophysiology

Electrophysiologic recordings were performed on pyramidal neurons from primary hippocampal cell cultures at room temperature. The external solution during the recordings was a modified Tyrode's solution containing (in mM) 150 NaCl, 4 KCl, 10 glucose, 10 HEPES, 2 $MgCl_2$, 2 $CaCl_2$ at pH 7.4 and 310 mOsm. The internal solution for the recording pipette contained (in mM) 15 Cs-$MeSO_3$, 10 CsCl, 5 NaCl, 10 HEPES, 0.6 EGTA, 20 Tetraethylammonium-Cl, 4 Mg-ATP, 0.3 Na_3GTP and 10 QX-314 [N-(2,6-dimethylphenylcarbamoylmethyl)-triethylammonium bromide] at pH 7.35 and 300 mOsm. D-AP5 (50 μM, Abcam, cat. 120003) was used to eliminate

NMDA currents. Picrotoxin (50 μM, Sigma, P1675) and CNQX (10 μM, Sigma, C239) were used to isolate excitatory and inhibitory evoked postsynaptic currents, respectively. For miniature post-synaptic current recordings, TTX (1 μM, Tocris, Bristol, UK) was added to block action potentials. The neurons were voltage-clamped at -70 mV and postsynaptic currents were measured using an Axon Instruments Axopatch 200B amplifier (Molecular Devices, San Jose, CA) with a 2 KHz filter. The signal was digitized using Axon Instruments Digidata 1550B data acquisition system (Molecular Devices) with a sampling rate of 10 kHz. The data was recorded using Clampex 11 software (Molecular Devices). Threshold for mEPSC and mIPSC amplitudes were 5 pA and the rise time threshold was set to 0.3 ms. For evoked experiments, any response where the stimulus was applied during a spontaneous action potential or any recording where the recorded minimum amplitude was higher than the starting baseline were discarded.

Study Design

This study was not preregistered. Unless otherwise stated, no randomization was performed to allocate subjects in the study. The experimenter was blinded to genotype during RNA and protein biochemical experiments. No blinding was performed during imaging or electrophysiology experiments or during statistical analyses. The study was exploratory as no primary or secondary endpoints were pre-specified. Unless otherwise stated, no exclusion criteria were pre-defined.

Statistical Methods

Statistical analyses of data were performed using Prism software, version 9.0 (GraphPad, San Diego, CA). No sample size calculations were performed. Outliers were identified and excluded from the evoked IPSC and EPSC data sets using the ROUT Method, Q= 1%. Data normality was assessed using the Shapiro-Wilk Test, and non-parametric statistical tests were employed to compare non-normal data. Statistical tests are reported in each figure legend. Reported values represent the mean ± SEM unless otherwise stated.

Antibody	Species	Dilution	Vendor	Catalog #
anti-β-actin	goat pab	1:1,000	Santa Cruz	sc-1616
anti-CAPS1	rabbit pab	1:1,000	Synaptic Systems	262 003
anti-Munc18-1	rabbit mab	1:1,000	Cell Signaling Technology	13414
anti-SNAP-25	rabbit pab	1:1,500	Abcam	ab41455
anti-synaptobrevin2	mouse mab	1:1,000	Synaptic Systems	104 211
anti-synaptotagmin1	mouse mab	1:5,000	Synaptic Systems	105 011
anti-syntaxin1a	rabbit mab	1:1,000	Abcam	ab170889
anti-goat 680LT	donkey	1:50,000	LI-COR	926-68024
anti-mouse Alexa 790	goat mab	1:15,000 to 1:50,000	Jackson Immuno	211-652-171
anti-rabbit Alexa 790	mouse mab	1:15,000 to 1:50,000	Jackson Immuno	211-652-171

Table 1. Primary and Secondary Antibodies used in Western Blotting

Results

Activity-Dependent Modulation of *Cadps* Editing

Previous studies have demonstrated an increase in both dopamine release from striatal synaptosomes and DCV exocytosis from adrenal chromaffin cells prepared from mutant mice solely expressing the edited isoform of CAPS1 (CAPS1(G)) (Miyake et al., 2016). Given the broad expression of CAPS1 throughout the brain (Speidel et al., 2003; Wassenberg & Martin, 2002), it is likely that editing-mediated alterations in neurotransmitter release are not limited to catecholaminergic systems. To examine the functional consequences of editing of *Cadps* mRNAs in the glutamatergic and GABAergic systems, primary hippocampal neuron cultures were selected as a model system. In wild-type neuronal cultures, an average of 29.9 ± 4.0% (n=6 cultures) of *Cadps* transcripts were edited. The variability in *Cadps* editing between cultures was not necessarily surprising, as neuronal activity has been shown to modulate RNA editing in primary cortical neurons and hippocampal brain slices for several ADAR targets (Balik, Penn, Nemoda, & Greger, 2013; Sanjana, Levanon, Hueske, Ambrose, & Li, 2012). To examine whether *Cadps* editing was similarly modulated by neuronal activity in primary hippocampal neurons, cultures from wild-type mice were treated for 48 hours with tetrodotoxin (TTX)—a sodium channel blocker—to prevent action potential firing, or bicuculline—a $GABA_A$ receptor antagonist—to alleviate circuit inhibition and promote neuronal activation. *Cadps* editing was significantly decreased following TTX application (22.5 ± 2.1%) compared to vehicle treated cultures (32.1 ±3.2%), and significantly increased following bicuculline application (40.8 ± 2.2%) (Figure 4A, B). As *Cadps* editing is mediated by both ADAR1 and ADAR2 (Miyake et al., 2016), expression of RNA transcripts encoding these proteins was quantified. While the expression of *Adarb1* RNA *(*encoding the ADAR2 protein) decreased with TTX application and increased upon bicuculline treatment, the expression of *Adar* transcripts (encoding the ADAR1 protein) was not altered by pharmacologic manipulation of neuronal activity (Figure 4C). These findings suggest that *Cadps*

editing is modulated by neuronal activity, potentially through changes in ADAR2 expression levels.

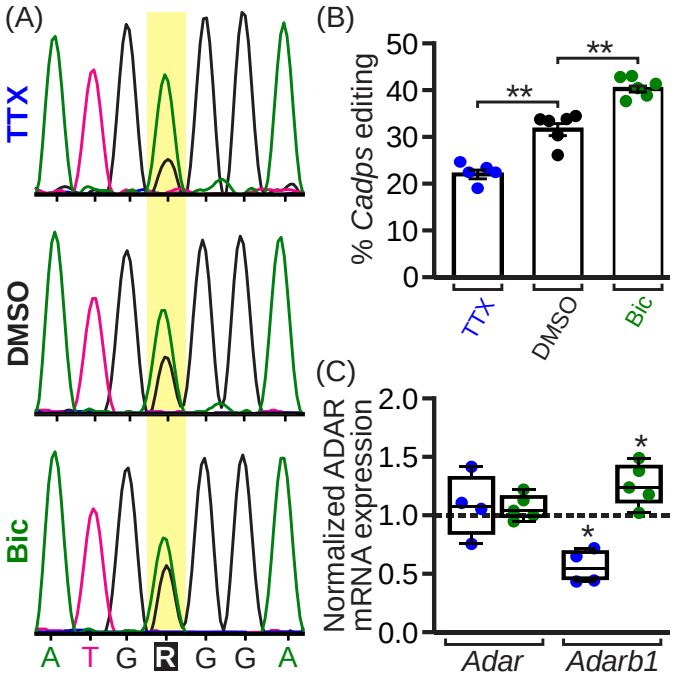

Figure 4. *Cadps* RNA editing is altered by neuronal activity. (**A**) Electropherogram traces from Sanger sequencing of RT-PCR amplicons generated from wild-type neurons treated with tetrodotoxin (TTX), bicuculline (Bic), or vehicle (DMSO) are presented; the position of the editing site is indicated in yellow. (**B**) Quantification of *Cadps* RNA editing level in wild-type neurons treated with Bic (●), TTX (●), or vehicle (●) (n= 5-6 cell preparations per treatment, Holm-Sidak's Multiple Comparison Test, **p<0.01). (**C**) Quantitative RT-PCR analysis of *Adar* and *Adarb1* mRNA levels in wild-type neurons treated with Bic (●), TTX (●) normalized to vehicle is shown (n= 5-6 cell preparations per treatment, paired t-test of ΔC_t values, *p<0.05).

Generation of CAPS1(E) mice

To make direct functional comparisons between CAPS1 proteins encoded by non-edited and edited transcripts, it was essential to develop a model system in which the expression of the encoded CAPS1(E) and CAPS1(G) protein isoforms was limited to a single variant that could not be altered in response to neuronal activity. While mice solely expressing the CAPS1(G) isoform had been developed previously (Miyake et al., 2016), we engineered a mutant mouse model solely expressing the non-edited isoform of *Cadps*, encoding the CAPS1(E) protein variant. A CRISPR-Cas9 based approach using two single guide RNAs (sgRNAs) was employed to excise the editing site complementary sequence (ECS) in intron 27 of the mouse *Cadps* gene, a region critical for formation of the RNA duplex required for ADAR-mediated editing of *Cadps* transcripts (Figure 5A, B) (Miyake et al., 2016). Sequence analysis of genomic DNA-derived PCR amplicons generated from CAPS1(E) mice confirmed deletion of the expected 54 nucleotides and revealed an insertion of four additional nucleotides within the intron, presumably resulting from non-homologous end joining (Figure 5B).

To confirm that mutant mice bearing the modified *Cadps* allele solely express transcripts encoding the CAPS1(E) isoform of the protein, RT-PCR amplification of the *Cadps* editing site from whole-brain derived RNA was performed and the resulting amplicons were sequenced directly. Complementary DNA from wild-type animals exhibited overlapping adenosine/guanosine peaks in electropherogram traces resulting from a mixture of non-edited and edited *Cadps* transcripts (16.7% editing), whereas cDNAs from CAPS1(E) animals showed only the non-edited adenosine nucleotide at the editing site (Figure 5C). To further confirm the absence of editing in CAPS1(E) animals, deep sequencing was used to survey a large population of editing site containing RT-PCR amplicons generated from whole brain RNA. Of 737,158 total *Cadps* reads, 99.89% contained a non-edited adenosine residue at the editing site, while the remaining 0.11% of reads contained either G (0.04%), T (0.01%), or C (0.06%), likely representing experimental background created by reverse transcriptase or DNA polymerase errors made during generation

and sequencing of the library. Offspring from the mating of heterozygous CAPS1(E) animals were genotyped at weaning (Figure 6) and demonstrated a normal Mendelian distribution, indicating that the CAPS1(E) mutation does not result in embryonic or early postnatal lethality.

To assess whether the lack of editing of *Cadps* mRNAs affects steady-state *Cadps* mRNA or CAPS1 protein expression levels, quantitative RT-PCR and Western blotting strategies were used to compare brain samples from CAPS1(E) and wild-type mice. Results from these analyses revealed that sole expression of non-edited *Cadps* transcripts did not significantly alter either *Cadps* mRNA or CAPS1 protein expression in CAPS1(E) mice when compared to wild-type littermates (Figure 5D-F). As we sought to use this mouse model to investigate pre-synaptic function, we also analyzed expression levels of canonical SNARE proteins (syntaxin-1, SNAP-25, synaptobrevin-2), a synaptic calcium sensor (synaptotagmin-1), and a SNARE accessory protein (munc18). Expression levels of all pre-synaptic proteins analyzed were unaltered in the CAPS1(E) mutant animals (Figure 5E-F).

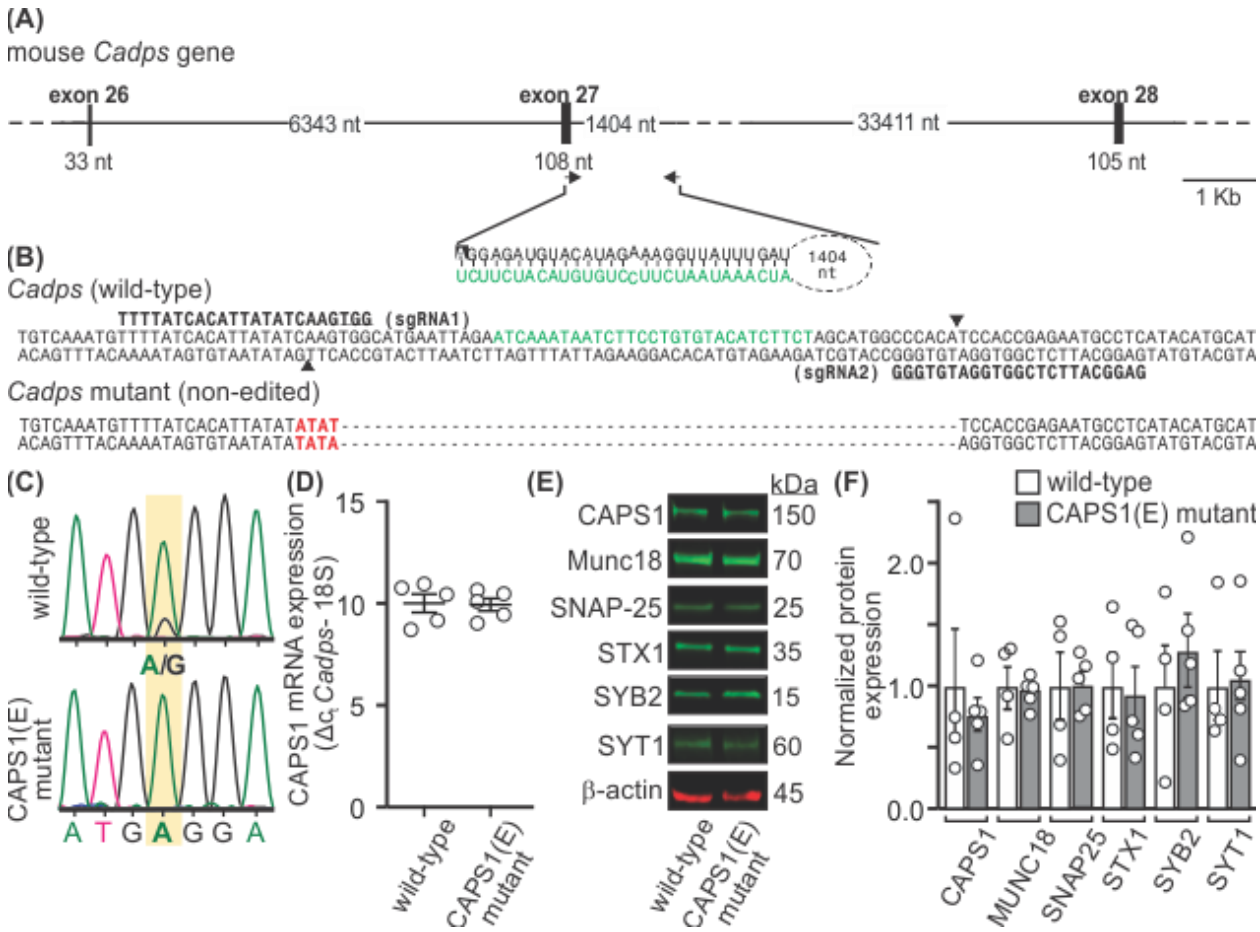

Figure 5. Generation of a mutant mouse line solely expressing the non-edited isoform of CAPS1, CAPS1(E). (**A**) A schematic diagram for a portion of the mouse *Cadps* gene is presented illustrating the location of a dsRNA duplex formed by an inverted repeat (arrows) within exon 27 and intron 27 (*green lettering*). The adenosine subject to site-specific A-to-I RNA editing (*inverse lettering*) is located at the 5'-end of the duplex within exon 27. The lengths of the presented exons and introns in nucleotides (nt) are shown. (**B**) Two sgRNAs were used to direct CRISPR/Cas9-mediated excision of the editing site complementary sequence (ECS), the intronic portion of the dsRNA duplex (*green lettering*). The protospacer-adjacent motifs (NGG) are underlined, and the predicted Cas9-mediated cleavage sites are indicated with arrowheads. The resulting mutant *Cadps* allele with the desired deletion (- - -) and an insertion of 4 random nucleotides (*red lettering*) by non-homologous end joining is shown. (**C**) Electropherogram traces from Sanger sequencing of RT-PCR amplicons generated from whole brain RNA are shown; the position of the editing site is indicated in yellow. (**D**) Quantitative RT-PCR analysis of *Cadps* mRNA levels in CAPS1(E) and wild-type mice (n= 5 animals/genotype, unpaired t-test, p>0.05). (**E**) Representative western blots and (**F**) quantitative analysis of the expression of major pre-synaptic exocytosis-regulating proteins, including CAPS1, munc-18, SNAP-25, syntaxin-1 (STX1), synaptobrevin-2 (SYB2), and synaptotagmin-1 (SYT1), in CAPS1(E) and wild-type mice, normalized to actin expression (n= 4-5 animals/genotype; Mann-Whitney test with Holm-Sidak's Multiple Comparison Correction, p>0.05).

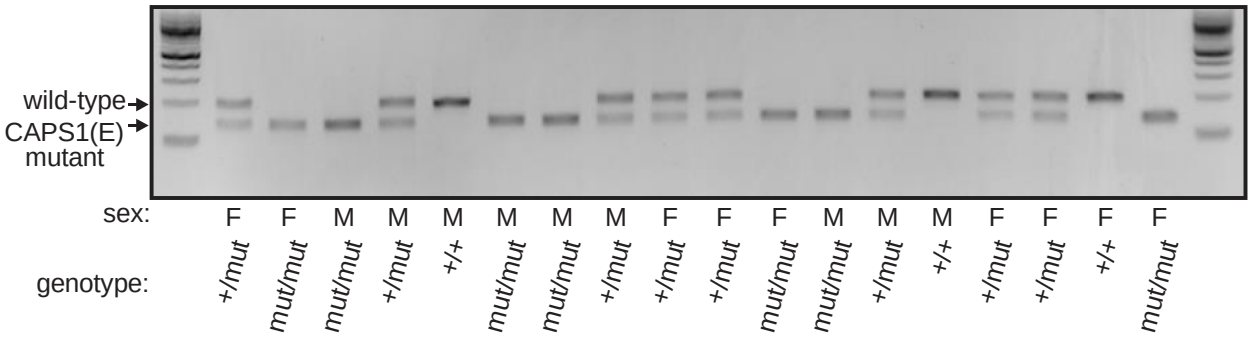

Figure 6. Genotype analysis of the CAPS1(E) mutant mouse line. Electrophoretic resolution of genomic DNA-derived PCR amplicons from wild-type (177bp) and CAPS1(E) mutant alleles (127bp) is shown, denoting the expected migration positions on a 2% agarose gel visualized with ethidium bromide. The sex and genotype of offspring animals are indicated.

Effect of *Cadps* Editing on Evoked Neurotransmission and Short-term Plasticity

Previous studies have demonstrated a role for CAPS1 in regulating glutamatergic neurotransmission and synaptic plasticity (Jockusch et al., 2007), however GABAergic neurotransmission has not been studied. As CAPS1 is present in a substantial number of GABAergic synapses (see below, Figure 11H and Figure 12D), we investigated the effect of *Cadps* editing on evoked inhibitory neurotransmission by analyzing whole cell recordings from pyramidal neurons in hippocampal cultures derived from CAPS1(E) and CAPS1(G) and wild-type littermate mice. A train of 10 action potentials was delivered from 1 to 20 Hz to elicit multiple forms of short-term plasticity and the data was analyzed to study various aspects of evoked neurotransmission. There were no detectable changes in IPSC amplitudes measured from the initial stimulus (at 1 Hz) in CAPS1(G) neurons compared to CAPS(E) neurons (Figure 7a, b). Paired-pulse ratios of the first two IPSC amplitudes were decreased in CAPS1(G) neurons compared to CAPS1(E) neurons, suggesting enhanced release probability in CAPS1(G) neurons (Figure 7C). All stimulation frequencies elicited short-term depression at inhibitory synaptic terminals, and CAPS1(G) neurons undergo enhanced synaptic depression compared to CAPS1(E) neurons during high frequency stimulation at 20 Hz (Figure 7D). No effect of strain was found in baseline neurotransmission, paired-pulse ratios, or short-term plasticity in comparisons of CAPS1(E) WT and CAPS1(G) WT neurons (Figure 8A-C). Overall, these results are consistent with the premise that *Cadps* editing enhances release probability and short-term depression at inhibitory synapses.

In parallel electrophysiology studies, the effect of *Cadps* editing on glutamatergic neurotransmission also was assessed. Analysis of the response to the first stimulation at 1 Hz showed no change in EPSC amplitudes in CAPS1(G) neurons compared to CAPS1(E) neurons (Figure 7e, f). Paired-pulse ratios of EPSC amplitudes from the first two responses show no difference between CAPS1(E) and CAPS1(G) neurons across all stimulation frequencies tested (Figure 7g), although a strain effect is noted when comparing paired-pulse ratios of CAPS1(E) WT

to CAPS1(G) WT which prevents any conclusions from being drawn (Figure 8e). No significant differences in short-term plasticity at excitatory synapses between CAPS1(E) and CAPS1(G) neurons were observed in response to a train of action potentials at 1- 20Hz (Figure 7h). No effect of strain was found in baseline neurotransmission or short-term plasticity in comparisons between CAPS1(E) WT and CAPS1(G) WT neurons (Figure 8d, f). These results demonstrate that *Cadps* editing has no significant effect on baseline glutamatergic neurotransmission or high frequency stimulation-driven synaptic plasticity.

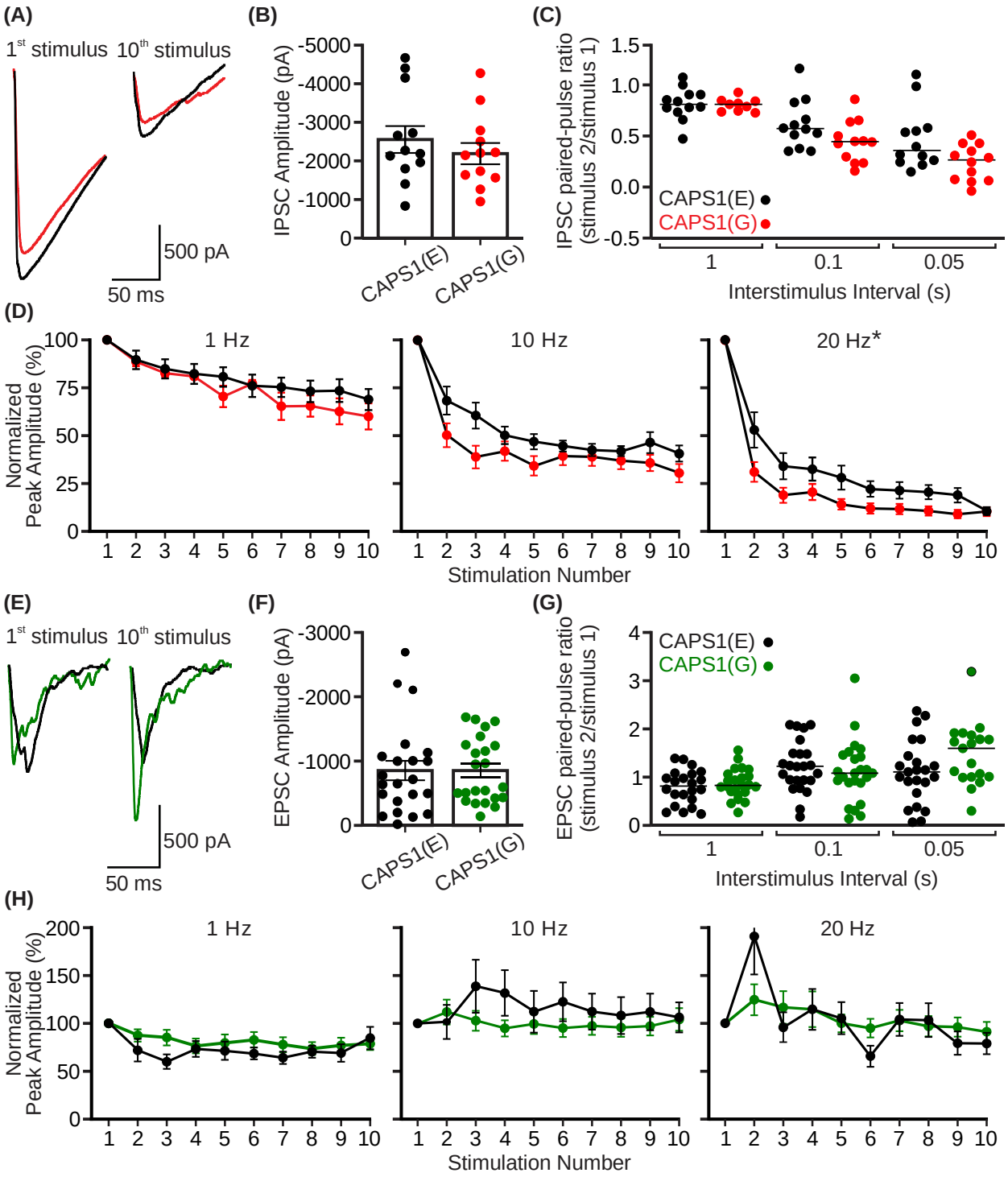

Figure 7. Effect of *Cadps* RNA editing on evoked neurotransmission. (A) Representative IPSC traces of the first and last peak elicited by a train of 10 action potentials when delivered at 10 Hz, with CAPS1(E) (●) and CAPS1(G) (●) responses shown. **(B)** IPSC amplitudes elicited by a single action potential. (n= 12 neurons from 2 independent cell preparations; unpaired t-test, p>0.05). **(C)** Paired-pulse ratios calculated from IPSC amplitudes generated by stimulus 2/stimulus 1 responses with interstimulus intervals from 1-0.05 seconds are presented. (n= 12 neurons per genotype from 2 cell preparations, Two-way ANOVA,

genotype effect F (1, 63) = 7.642, **p<0.01). **(D)** Normalized peak amplitudes plotted by stimulation number elicited by a train of 10 action potentials delivered at 1 Hz, 10 Hz, and 20 Hz. (n= 12 neurons per genotype from 3 cell preparations; Mixed Effects Analysis, 1 Hz genotype effect F (1, 22) = 1.839, p>0.05, 10 Hz genotype effect F (1, 22) = 3.514, p>0.05, 20 Hz genotype effect F (1, 22) = 4.695, *p<0.05). **(E)** Representative EPSC traces of the first and last peak elicited by a train of 10 action potentials when delivered at 10 Hz, with CAPS1(E) (●) and CAPS1(G) (●) responses shown. **(F)** EPSC amplitudes elicited by a single action potential (n= 24 neurons from 6 independent cell preparations; Mann-Whitney test, p>0.05). **(G)** Paired-pulse ratios calculated from EPSC amplitudes generated by stimulus 2/stimulus 1 with interstimulus intervals from 1- 0.05 seconds are presented (n= 24 neurons per genotype from 6 cell preparations, Two-way ANOVA, genotype effect F (1, 129) = 1.383, p>0.05). **(H)** Normalized peak amplitudes plotted by stimulation number elicited by a train of 10 action potentials delivered at 1 Hz, 10 Hz, and 20 Hz. (n= 24 neurons per genotype from 6 cell preparations; Mixed Effects Analysis, 1 Hz genotype effect F (1, 46) = 0.6246, p>0.05, 10 Hz genotype effect F (1, 46) = 0.6580, p>0.05, 20 Hz genotype effect F (1, 46) = 0.4589, p>0.05).

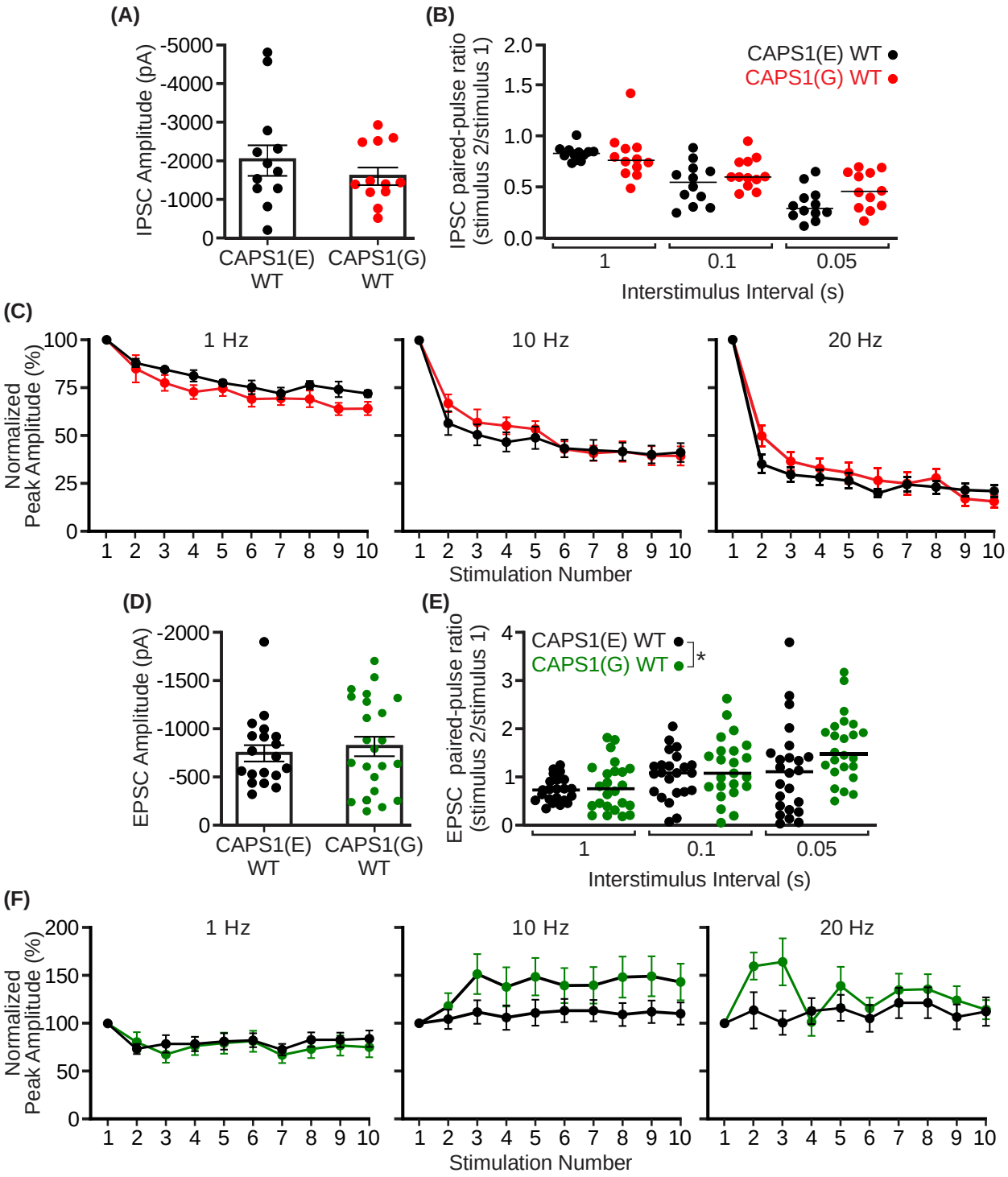

Figure 8. Evoked neurotransmission in CAPS1(E) WT and CAPS(G) WT hippocampal neurons. (**A**) IPSC amplitudes elicited by a single action potential are presented. (n= 12 neurons from 2 independent cell preparations; unpaired t-test, p>0.05). (**B**) Paired-pulse ratios calculated from IPSC amplitudes generated by stimulus 2/stimulus 1 responses with interstimulus intervals from 1- 0.05 seconds are shown. (n= 12 neurons per genotype from 2 cell preparations, Two-way ANOVA, genotype effect F (1, 87) = 2.348, p>0.05). (**C**) Normalized peak amplitudes plotted by stimulation number elicited by a train of 10 action potentials delivered at 1 Hz, 10 Hz, and 20 Hz are presented. (n= 12 neurons per genotype

from 3 cell preparations; Mixed Effects Analysis, 0.1 Hz genotype effect $F(1, 22) = 1.206$, $p>0.05$, 1 Hz genotype effect $F(1, 22) = 2.347$, $p>0.05$, 10 Hz genotype effect $F(1, 22) = 0.1815$, $p>0.05$, 20 Hz genotype effect $F(1, 22) = 0.4415$, $p>0.05$). (**D**) EPSC amplitudes elicited by a single action potential are shown (n= 24 neurons from 6 independent cell preparations; Mann-Whitney test, $p>0.05$). (**E**) Paired-pulse ratios calculated from EPSC amplitudes generated by stimulus 2/stimulus 1 with interstimulus intervals from 1- 0.05 seconds are presented (n= 24 neurons per genotype from 6 cell preparations, Two-way ANOVA, genotype effect $F(1, 135) = 4.532$, $*p<0.05$). (**F**) Normalized peak amplitudes plotted by stimulation number elicited by a train of 10 action potentials delivered at 1 Hz, 10 Hz, and 20 Hz are shown (n= 24 neurons per genotype from 6 cell preparations; Mixed Effects Analysis, 1 Hz genotype effect $F(1, 46) = 0.0929$, $p>0.05$, 10 Hz genotype effect $F(1, 46) = 2.351$, $p>0.05$, 20 Hz genotype effect $F(1, 46) = 1.946$, $p>0.05$).

Effects of *Cadps* Editing on Spontaneous Neurotransmission

In addition to its role in evoked neurotransmission, CAPS1 also regulates spontaneous neurotransmission as deletion of the protein in cultured hippocampal neurons results in reduced mEPSC frequency and amplitude (Jockusch et al., 2007). To assess the effect of *Cadps* editing on spontaneous neurotransmission, miniature IPSCs and EPSCs were recorded from pyramidal neurons in hippocampal cultures derived from CAPS1(E), CAPS1(G), and wild-type littermate animals (Figure 9A, D). Analysis of mIPSC recordings found no change in frequency (Figure 9B), and an increase in mIPSC amplitude in CAPS1(G) neurons compared to CAPS1(E) expressing neurons (Figure 9C). No strain effects were observed in mIPSC measurements (Figure 10B, C). While no *Cadps* editing-dependent changes were found in mEPSC frequency or amplitude (Figure 9E, F), a strain effect was noted in which neurons from CAPS1(G) WT had reduced mEPSC amplitudes compared to those from CAPS1(E) WT neurons (Figure 10F). Therefore, while a strain effect precludes drawing conclusions about *Cadps* editing-dependent effects on spontaneous glutamatergic neurotransmission, increased mIPSC amplitudes in CAPS1(G) neurons suggests *Cadps* editing alters spontaneous transmission at inhibitory synapses.

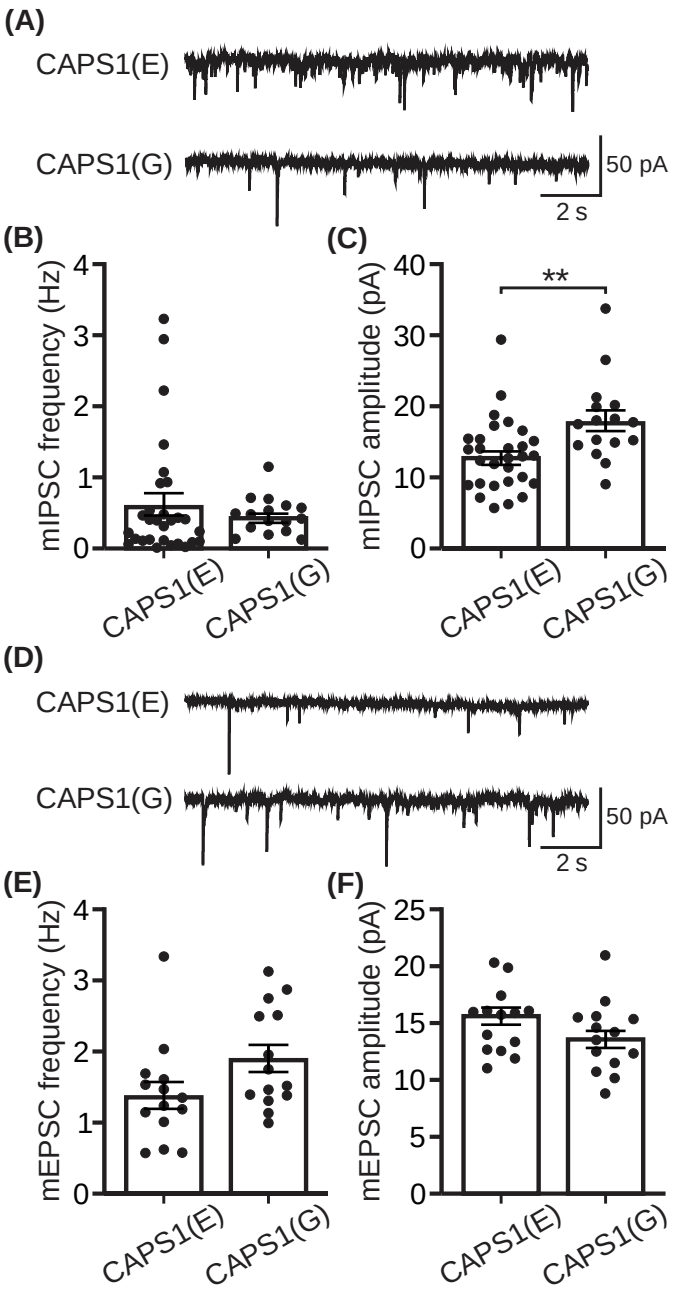

Figure 9. Effect of *Cadps* RNA editing on spontaneous neurotransmission. (**A**) Representative mIPSC traces recorded from CAPS1(E) and CAPS1(G) expressing neurons. (**B**) An analysis of mIPSC frequency is shown. (n= 16-29 neurons per genotype from 8 cell preparations; Mann-Whitney test, p>0.05). (**C**) An analysis of mIPSC amplitudes is presented (n= 16-29 neurons per genotype from 8 cell preparations; Mann-Whitney test, **p<0.01). (**D**) Representative mEPSC traces recorded from CAPS1(E) and CAPS1(G) expressing neurons. (**E**) An analysis of mEPSC frequency is shown (n= 14 neurons per genotype from 6 cell preparations; Mann-Whitney test, p>0.05). (**F**) An analysis of mEPSC amplitude is presented. (n= 14 neurons per genotype from 6 cell preparations; Unpaired t test, p>0.05).

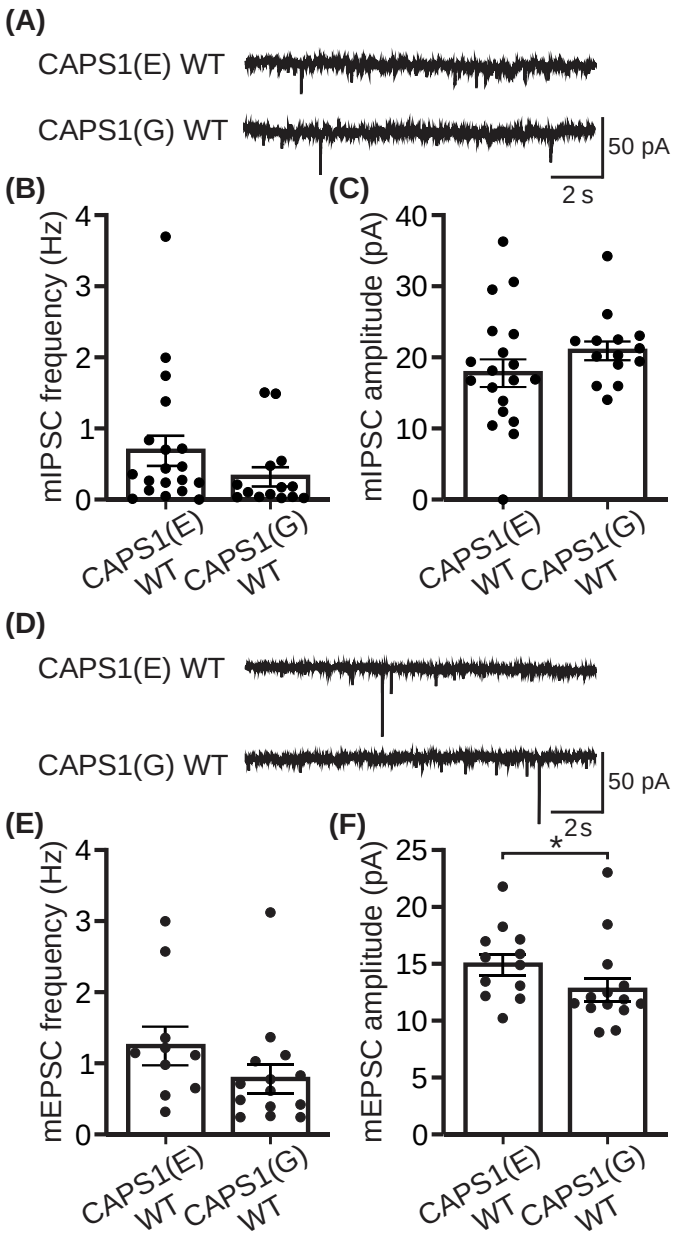

Figure 10. Spontaneous neurotransmission in CAPS1(E) WT and CAPS1(G) WT hippocampal neurons. (**A**) Representative mIPSC traces recorded from CAPS1(E) WT and CAPS1(G) WT neurons are provided. (**B**) An analysis of mIPSC frequency is shown (n= 14-19 neurons per genotype from 8 cell preparations; Mann-Whitney test, p>0.05). (**C**) An analysis of mIPSC amplitudes is presented (n= 14-19 neurons per genotype from 8 cell preparations; Unpaired t test, p>0.05). (**D**) Representative mEPSC traces recorded from CAPS1(E) WT and CAPS1(G) WT neurons are provided. (**E**) An analysis of mEPSC frequency is shown (n= 10-14 neurons per genotype from 6 cell preparations; Mann-Whitney test, p>0.05). (**F**) An analysis of mEPSC amplitude is shown (n= 10-14 neurons per genotype from 6 cell preparations; Mann-Whitney test, *p<0.05).

Effect *Cadps* Editing on Synaptic Localization

CAPS1 is selectively expressed in some, but not all, excitatory synapses in wild-type neurons (Farina et al., 2015) and the carboxyl-terminal region of CAPS1 (residues 654-1355) is essential for synaptic localization and subsequent vesicle exocytosis (van Keimpema et al., 2017). As editing of *Cadps* RNA results in a glutamate-to-glycine substitution (1252 aa) within the C-terminal domain, we hypothesized that *Cadps* RNA editing may play a role in modulating the targeting of CAPS1 to synapses. CAPS1 synaptic localization was examined by taking advantage of primary cultures of hippocampal neurons prepared from CAPS1(E), CAPS1(G), and wild-type mice. CAPS1 synaptic localization was assessed by immunocytochemical analysis using antibodies targeting CAPS1 and both excitatory and inhibitory synapse markers, the vesicular glutamate transporter 1 (vGlut1) and the vesicular GABA transporter (vGAT), respectively. In agreement with previous studies, CAPS1 was expressed in puncta along neurites in cultures from wild-type neurons (Figure 11A), and similar localization was found in CAPS1(E) and CAPS1(G) neurons (Figure 12A, B*)*. CAPS1 co-localized with vGlut1 (Figure 11B, C) and vGAT (belowFigure 11D, E), and interestingly much greater co-localization was seen in vGAT than vGlut1 synapses in primary hippocampal neurons.

The extent of CAPS1 synaptic localization was measured using object-based colocalization analysis applied to immunofluorescent images of CAPS1(E) and CAPS1(G) cultures (Bolte & Cordelieres, 2006), allowing quantification of the number of vGlut1 and vGAT synapses that contained CAPS1 within a field of view. Results from this analysis showed an editing-dependent increase in CAPS1-containing vGlut1 puncta (Figure 11F). CAPS1(G) neurons had a significantly higher percentage of CAPS1-containing vGlut1 synapses (8.9 ±0.9%) compared to CAPS1(E) neurons (2.9 ±0.6%). Furthermore, the percentage of $CAPS1^{+}/vGlut1^{+}$ puncta in wild-type neurons (4.0 ±0.8% CAPS1(E) WT and 6.0 ±0.9% CAPS1(G) WT) was intermediate to that observed in CAPS1(E) and CAPS1(G) neurons, presumably resulting from the intermediate level of editing (~30%) found in wild-type cultures. The change in co-localization

of CAPS1 in excitatory pre-synapses did not result from an alteration in total vGlut1 puncta count (Figure 11G). Additionally, no strain effect was found when comparing the percentage of $CAPS1^+/vGlut1^+$ puncta from CAPS1(E) WT to CAPS1(G) WT neurons (Figure 12C). Together, these results demonstrate that *Cadps* editing enhances glutamatergic synaptic localization of CAPS1.

Parallel analysis of CAPS1 localization in GABAergic synapses also revealed an editing-dependent increase in the percentage of CAPS1-containing vGAT puncta (Figure 11H). In CAPS1(E) neurons, CAPS1 co-localized with an average of 70.0 ±4.8% vGAT puncta, whereas in CAPS1(G) neurons an average of 92.5 ±4.1% vGAT puncta contain CAPS1. Once again, the level of CAPS1 co-localization with the GABAergic synapse marker was at an intermediate level in neurons isolated from wild-type littermates, 87.3 ±3.1% and 81.7 ±2.7% from CAPS1(E) WT and CAPS1(G) WT neurons, respectively, when compared to neurons expressing CAPS1(E) and CAPS1(G). The change in percentage of $CAPS1^+$ puncta did not result from a change in the total number of vGAT synapses (Figure 11I). As before, no strain effect was found when comparing the percentage of positive CAPS1 puncta in vGAT synapses between CAPS1(E) WT and CAPS1(G) WT neurons (Figure 12D). These results show that CAPS1(G) exhibits increased GABAergic synaptic localization compared to CAPS1(E) in a manner similar to what is seen in glutamatergic synapses.

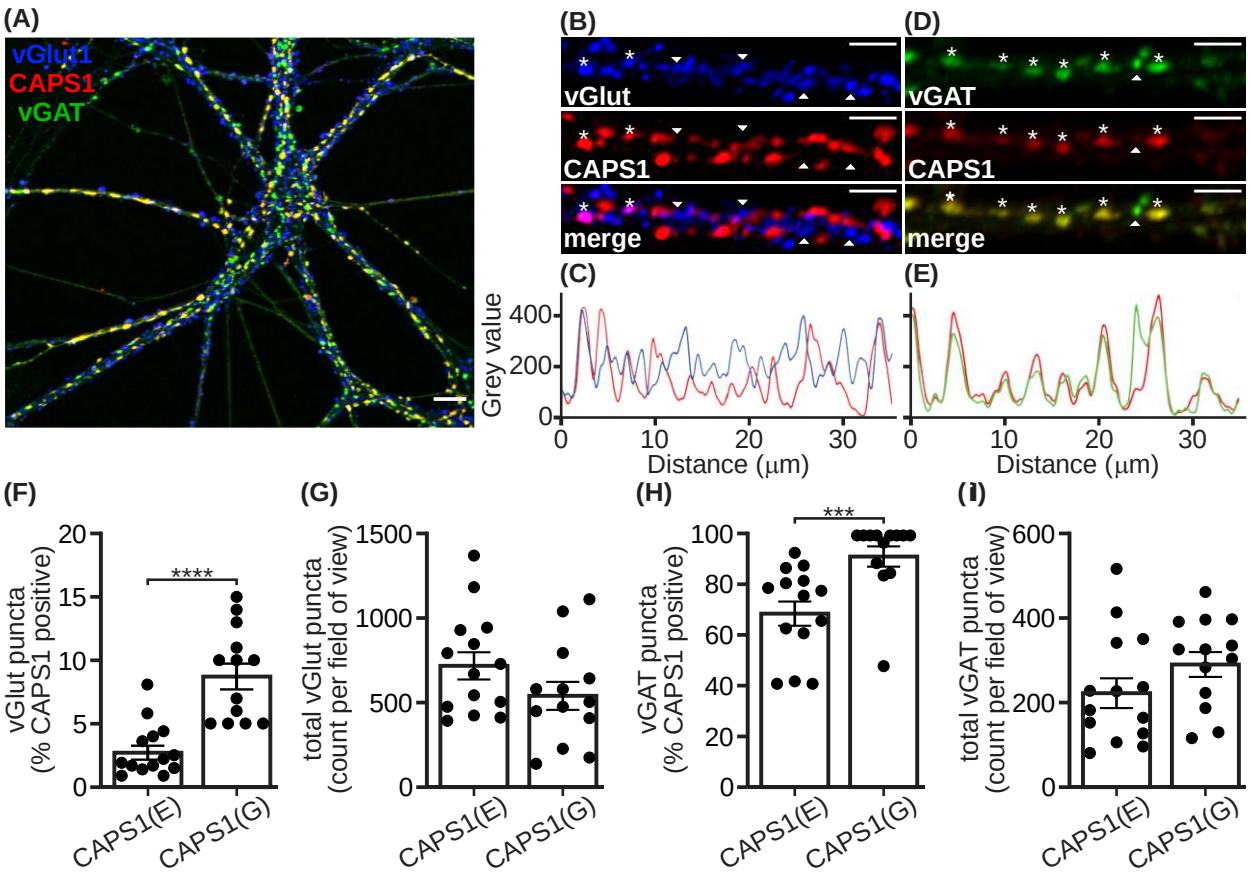

Figure 11. Enhancement of CAPS1(G) synaptic localization in cultured hippocampal neurons. (**A**) Representative immunofluorescent image of cultured wild-type hippocampal neurons labelled using affinity purified antibodies targeting CAPS1 (*red*), a glutamatergic synapse marker, vGlut1 (*blue*), and a GABAergic synapse marker, vGAT (*green*); scale bar = 10 µm. (**B**) Magnified view of a neurite labelled for CAPS1 and vGlut1; vGlut1 and CAPS1 overlapping regions (*asterisks*) and vGlut1 puncta not enriched for CAPS1 (*arrowheads*) are shown; scale bar = 5 µm. (**C**) Line scan of CAPS1 (*red*) and vGlut1 (*blue*) pixel intensity across the neurite shown in panel b. (**D**) Magnified view of a neurite labelled for CAPS1 and vGAT. vGAT and CAPS1 overlapping domains (*asterisks*) and vGAT puncta not enriched for CAPS1 (*arrowheads*) are shown; scale bar = 5 µm. (**E**) Line scan of CAPS1 (*red*) and vGAT (*green*) pixel intensity across the neurite shown in panel d. (**F**) Quantification of CAPS1 localization in vGlut1 puncta; CAPS1(E) 2.9 ± 0.6%, CAPS1(G) 8.9 ± 1.0% (n=13-14 fields of view from 2 independent cell preparations; Mann-Whitney test, ****p<0.0001). (**G**) Quantification of total vGlut1 puncta; CAPS(E) 731.1 ± 80.5, CAPS1(G) 553.9 ± 78.6 (n= 13-14 fields of view from 2 independent cell preparations, unpaired t-test, p>0.05). (**H**) Quantification of CAPS1 localization in vGAT puncta; CAPS1(E) 69.9 ± 4.8%, CAPS1(G) 92.5 ± 4.1% (n=13-14 fields of view from 2 independent cell preparations; Mann-Whitney test, ***p<0.001). (**I**) Quantification of total vGAT puncta; CAPS(E) 229.4 ± 35.2, CAPS1(G) 298.0 ± 30.0 (n=13-14 fields of view in 2 independent cell preparations; unpaired t-test, p>0.05).

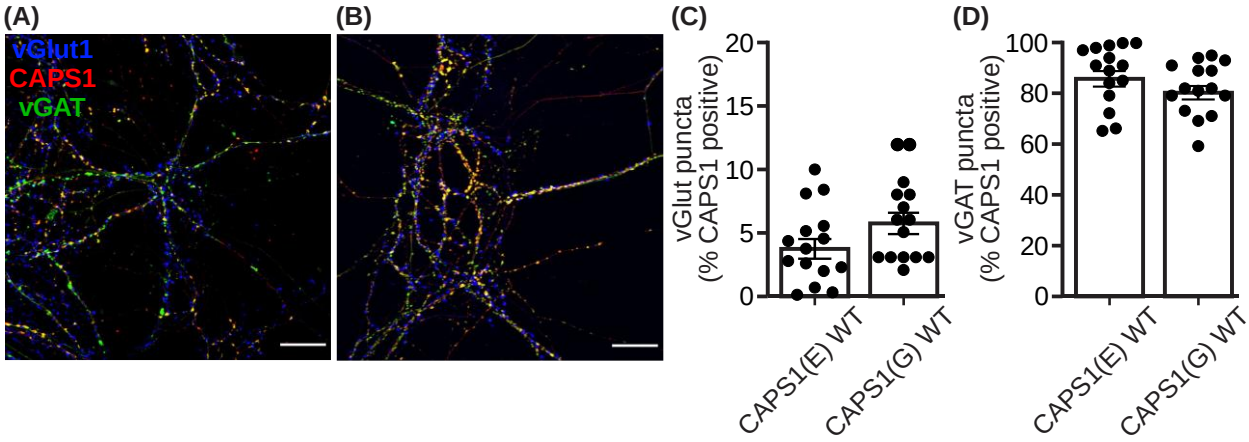

Figure 12. CAPS1 localization in CAPS1(E) and CAPS1(G) neurons and quantification of CAPS1 in CAPS1(E) WT and CAPS1(G) WT neurons. (**A-B**) Representative immunofluorescent images of cultured CAPS(E) (**A**) and CAPS1(G) (**B**) hippocampal neurons labelled using affinity purified antibodies targeting CAPS1 (*red*), a glutamatergic synapse marker, vGlut1 (*blue*), and a GABAergic synapse marker, vGAT (*green*); scale bar = 20 µm. (**C**) Quantification of CAPS1 localization in vGlut1 puncta; CAPS1(E) WT 4.0 ± 0.8%, CAPS1(G)WT 6.0 ± 0.9% (n=15 fields of view from 2 independent cell preparations; unpaired t-test, p>0.05). (**D**) Quantification of CAPS1 localization in vGAT puncta; CAPS1(E) WT 87.3 ± 3.1%, CAPS1(G) WT 81.7 ± 2.70% (n=15 fields of view from 2 independent cell preparations; unpaired t-test, p>0.05).

Discussion

In this chapter, a novel mouse model solely expressing the glutamate-containing isoform of the CAPS1 protein, CAPS1(E), was developed to assess the full extent of *Cadps* editing-dependent changes to synaptic localization and neurotransmission by comparison to mutant mice solely expressing the CAPS1(G) isoform. This experimental paradigm provides an advantage over the study of a single mutant mouse line in which comparisons are made to control animals, since neurons from wild-type mice exhibit an intermediate level of A-to-I conversion in *Cadps* transcripts and such post-transcriptional modifications can be controlled by neuronal activity (Figure 4A, B), thus making comparisons to wild-type neurons problematic. Additionally, this approach provides the greatest possible range in *Cadps* editing, either 0% or 100%, to distinguish functional differences between mutant mouse lines that express CAPS1 isoforms encoded by non-edited or edited *Cadps* transcripts, respectively.

The importance of CAPS1 as a SNARE accessory protein, to augment the release of neurotransmitters and peptide hormones, has been well-established (Elhamdani, Martin, Kowalchyk, & Artalejo, 1999; Jockusch et al., 2007; Nestvogel et al., 2020; Rupnik et al., 2000; Sadakata et al., 2013; Shaib et al., 2018; Speidel et al., 2005; Tandon et al., 1998). *Cadps* RNA editing is known to enhance catecholaminergic neurotransmitter release in *ex vivo* synaptosome preparations and in cultured primary adrenal chromaffin cells (Miyake et al., 2016). Building on these findings, the effect of *Cadps* editing on neurotransmission was investigated further by exploring spontaneous and evoked neurotransmission and short-term plasticity at excitatory and inhibitory synapses. Taking advantage of cultured primary hippocampal neurons, our studies have indicated that *Cadps* editing does not have a detectable impact on baseline evoked neurotransmission amplitudes but alters short-term synaptic depression in inhibitory synapses (Figure 7). *Cadps* editing enhances synaptic depression in response to high frequency stimulation in inhibitory synapses while decreasing the paired pulse ratio, indicating an enhanced release probability. Short-term depression primarily is mediated presynaptically by depletion of the

readily-releasable pool of vesicles, and enhanced synaptic depression is generally attributed to an increase in release probability or a decrease in the size of the readily-releasable pool of vesicles (Regehr, 2012). At inhibitory synapses, *Cadps* editing increases the release-probability, thus providing a likely explanation for increased short-term depression at these synapses. In agreement with previous studies that showing CAPS1 mediates synaptic plasticity (Jockusch et al., 2007; Nestvogel et al., 2020), these studies further indicate that *Cadps* editing modulates a specific type of plasticity, short-term depression at inhibitory synapses.

Regarding spontaneous inhibitory neurotransmission, miniature IPSC amplitudes were increased in CAPS1(G) cultures with no change in event frequency (Figure 9). The factors most commonly shown to affect mPSC amplitudes are post-synaptic receptor populations and vesicular neurotransmitter content (Nusser, Cull-Candy, & Farrant, 1997; Wojcik et al., 2006; Wojcik et al., 2004). Several studies have demonstrated a role of CAPS1 in regulating monoaminergic vesicle content through modulation of vMAT1/2 transporter function or intravesicular transmitter stability (Brunk, Blex, Speidel, Brose, & Ahnert-Hilger, 2009; Speidel et al., 2005), although other studies have refuted these findings (Fujita et al., 2007). Additionally, a decrease in mEPSC amplitude but no change in amplitude generated in response to exogenously applied glutamate, kainate, or GABA were reported in CAPS1 knockout neurons (Jockusch et al., 2007). These observations indicate a deficiency in vesicle loading, not post-synaptic receptor populations, underlie decreased mEPSC amplitudes in these neurons. Therefore, while the effect CAPS1 in vGAT-mediated neurotransmitter loading has not been explicitly investigated, our studies suggest a possible modulatory role for *Cadps* editing in this process.

The C-terminal domain of CAPS1 is necessary for synapse localization and exocytosis of DCVs in cultured hippocampal neurons (van Keimpema et al., 2017). As editing in *Cadps* mRNA results in a non-synonymous E-to-G amino acid substitution within this C-terminal region, the effect of *Cadps* editing on synaptic localization was investigated. CAPS1(G) localized to a significantly greater proportion of both glutamatergic and GABAergic synapses than the

CAPS1(E) isoform (Figure 11F, H). This effect is not explained by altered glutamatergic or GABAergic synapse count (Figure 11G, I), suggesting the effect is solely driven by enhanced CAPS1 synaptic localization. Results from these studies also revealed that CAPS1 is more highly associated with GABAergic rather than glutamatergic synapses (Figure 11F, H), which is consistent with electrophysiologic analyses where more significant effects are seen in inhibitory rather than excitatory neurotransmission (Figure 7, Figure 9).

Previous *in vitro* studies have shown that the affinity of CAPS1(G) for syntaxin-1 is greater than that of CAPS1(E) (Miyake et al., 2016). While it is possible that interactions between syntaxin-1 and CAPS1 drive enhanced synaptic localization of CAPS1(G), as another SNARE accessory protein, munc18, is thought to traffic to synapses with syntaxin-1 (Cijsouw et al., 2014), these observations also may be correlative. In CAPS2—a CAPS1 paralog—the dynactin-binding domain is necessary for proper axonal trafficking (Sadakata, Washida, Iwayama, et al., 2007), whereas the synaptic enrichment of another family of SNARE priming proteins with a high homology to CAPS proteins—munc13s —is mediated by C2 domain interactions with RIM1s (Andrews-Zwilling, Kawabe, Reim, Varoqueaux, & Brose, 2006) or an N-terminal coiled-coil domain interaction with ELK1 (Kawabe et al., 2017). As CAPS1 synaptic trafficking and enrichment is poorly understood beyond the identification of a critical role for the C-terminal domain in synapse localization (van Keimpema et al., 2017), additional studies will be required to examine whether the editing of *Cadps* transcripts alters interactions between CAPS1 and other key trafficking/enrichment proteins. More broadly, it remains to be determined whether the editing-dependent enhancement of neurotransmission mediated by CAPS1(G) is due to altered vesicle priming—as suggested by enhanced interactions with syntaxin-1 (Miyake et al., 2016) —or due to increased synaptic localization of CAPS1 (Figure 11F, H), or both. Overexpression of CAPS1 in wild-type DRG neurons is sufficient to increase DCV release probability and exocytosis (Shaib et al., 2018), suggesting that increasing CAPS1 abundance and increased synaptic enrichment alone could drive enhanced neurotransmission. While the precise molecular mechanism(s) by

which CAPS1(G) enhances neurotransmission remain unknown, the present studies reveal a possible role for editing-dependent enhancement of CAPS1 synaptic localization in this process.

ADAR-mediated RNA editing is subject to modulation by neuronal activity, with chronic activation generally leading to global increases in editing, whereas chronic silencing generally causes a global decrease in editing levels (Balik et al., 2013; Sanjana et al., 2012). Consistent with these observations, *Cadps* editing in wild-type hippocampal cultures increased after 48 hours of bicuculline treatment and decreased after 48 hours of TTX treatment (Figure 4A, B). While the direction of change for *Cadps* editing is consistent with previous reports, the magnitude of change in cultured hippocampal neurons (±10%) was far greater than previously observed in cultured cortical neurons (±2-3%) (Sanjana et al., 2012), despite comparable treatment conditions. Changes in the expression of *Adarb1*, but not *Adar*, were found in both model systems (Figure 4C) (Sanjana et al., 2012). Since *Cadps* RNAs are subject to editing by both enzymes (Miyake et al., 2016), alterations in *Adarb1* expression alone could account for the observed changes in A-to-I conversion. Alternatively, as suggested by differences in the effect size, additional regulatory factors may be involved. Numerous studies spanning the past decade have consistently concluded that changes in ADAR expression do not fully account for differences in the extent of A-to-I editing and the identification of such regulatory factors remains an active area of research for the field (Hood et al., 2014; Li & Church, 2013; Porath et al., 2019; Sapiro et al., 2020; Schaffer et al., 2020; Tan et al., 2017; Wahlstedt, Daniel, Enstero, & Ohman, 2009).

Overall, these studies provide further insight into the regulation of *Cadps* editing and examine *Cadps* editing-dependent changes in neurotransmission and CAPS1 subcellular localization. Significant changes in brain *Cadps* editing levels have been reported in individuals with Fragile X syndrome (Tran et al., 2019) and in the hippocampus and frontal cortex of *Fmr1* knockout mice, a model of Fragile X syndrome (Filippini et al., 2017). Additionally, dysregulation of global RNA editing has been reported in several neurological disorders including Alzheimer's disease and amyotrophic lateral sclerosis (Hideyama et al., 2012; Khermesh et al., 2016).

Expanding our knowledge of the functional outcomes of *Cadps* RNA editing in fast-acting neurotransmission provides insight into the potential role(s) alterations in *Cadps* editing may play in such disease states.

CHAPTER 3

Functional effects of *Cadps* editing on neuromodulatory synaptic signaling

Introduction

The majority of neurotransmission that occurs in the CNS is driven by release of the fast-acting transmitters glutamate, GABA, and glycine. However, another category of neurotransmitters, neuromodulatory transmitters, also play a critical role in normal CNS function. The neurons releasing neuromodulatory transmitters comprise only thousands of neurons in the rodent brain, a very tiny fraction of the roughly 70 million neurons that make up the mouse central nervous system (M. C. Avery & Krichmar, 2017). Yet these systems are imperative for many higher ordered cognitive processes including attention, motivation, long-term planning, and decision making, and emotion. Neuromodulatory systems include noradrenergic, cholinergic, dopaminergic, and serotonergic neurons that largely reside in small, discrete nuclei and send projections to vast regions of the brain. These systems provide another layer of information input, in addition to excitation or inhibition by glutamate or GABA, which neurons integrate to maintain normal behavioral responses. As such, understanding the mechanisms that control release of these transmitters is essential to understanding brain function. Additionally, several psychiatric disorders are thought to be rooted in dysfunction of neuromodulatory transmission, including schizophrenia and autism (Fuccillo, 2016; Howes & Kapur, 2009). As such, understanding regulation of neuromodulatory systems more deeply could contribute to developing treatments for these disorders.

A well characterized neuromodulatory system, the dopaminergic system, encompasses four projection pathways that direct a variety of cognitive outcomes. In the nigrostriatal pathway, dopamine neurons originate in the substantia nigra pars compacta (SN) and project to the dorsal striatum, a brain region encompassing the caudate nucleus, putamen, and globus pallidus (GP).

This pathway is critical for motor control, sequential motor task execution, habit formation, and social behaviors (Graybiel & Grafton, 2015; Howe & Dombeck, 2016; Lee et al., 2018; Ogura et al., 2005), and impaired dopamine signaling in the nigrostriatal pathway is implicated in movement disorders such as Parkinson's disease (Blesa & Przedborski, 2014). In the mesolimbic and mesocortical pathways, dopamine neurons originate in the ventral tegmental area (VTA). In the mesolimbic pathway, dopamine projections terminate in the nucleus accumbens (NAcc). Signaling in this pathway is important for motivated and reward-driven behaviors as dysregulation plays a role in addiction, schizophrenia, and depression (Eshel & Roiser, 2010; Salamone & Correa, 2012; J. Wang et al., 2015). In the mesocortical pathway, dopamine projections terminate in the prefrontal cortex (PFC) where they modulate attention and working memory (Puig, Rose, Schmidt, & Freund, 2014). The tuberoinfundibular pathway denotes dopamine projections from the arcuate nucleus of the hypothalamus to the pituitary gland which controls release of several hormones, including prolactin and ACTH (Gudelsky, 1981; Olah et al., 2009). The nigrostriatal, mesolimbic, mesocortical, and tuberoinfundibular dopamine projection pathways permit communication between distinct brain regions to mediate a variety of physiological and cognitive processes.

The molecular basis of neuromodulatory transmission was traditionally thought to mirror fast neurotransmission, however recent studies have concluded that while the general principles of regulated exocytosis are maintained in dopaminergic synapses, some structural and molecular properties of the systems differ. Similar to fast acting transmitters, dopamine is loaded into synaptic vesicles through a vesicular transporter, vesicular monoamine transporter 2 (vMAT2) in the CNS (Y. Liu et al., 1992), and dopamine release is quantal (Pothos, Davila, & Sulzer, 1998). Dopamine release is also calcium-dependent (Rice et al., 1994) and occurs through SNARE-mediated exocytosis (Bergquist, Niazi, & Nissbrandt, 2002; Fortin, Desrosiers, Yamaguchi, & Trudeau, 2006). However, the specific Ca^{2+} channels engaged in axonal dopamine release differ from fast-acting synapses (Brimblecombe, Gracie, Platt, & Cragg, 2015) and axonal specific

dopamine Ca^{2+} sensors have not been identified. There are also similar modes of transmitter release with both spontaneous, or action-potential independent, and evoked release, or action-potential dependent, described in both systems (Crawford & Connor, 1973; Gantz, Bunzow, & Williams, 2013; Grace & Bunney, 1984a, 1984b; J. T. Yorgason, Zeppenfeld, & Williams, 2017). Thus, dopamine packaging in synaptic vesicles, Ca^{2+}-triggered quantal release, SNARE-mediated exocytosis, and dual modes of release are properties of neuromodulatory, dopaminergic neurotransmission that mirror fast synapses.

Through several decades of work, features distinguishing dopamine synapses and neurotransmission from fast transmission synapses have been identified. Key differences between the systems emerge when structural properties of the synapse and molecular components of the exocytosis machinery were investigated. Dopamine neurotransmission is often described as volume transmission, as dopamine diffuses down a concentration gradient in the extracellular space to signal to distant receptors. This slower and far-reaching volume transmission is in direct contrast to wiring transmission that occurs at glutamatergic synapses where post-synaptic receptors are precisely aligned with pre-synaptic release sites for rapid signal transduction between neurons (Tang et al., 2016). Indeed, it has been shown that dopamine pre-synaptic sites do not align directly with post-synaptic specializations containing dopamine receptors (Caille, Dumartin, & Bloch, 1996; Uchigashima, Ohtsuka, Kobayashi, & Watanabe, 2016), suggesting the transmitter must diffuse farther than glutamate and GABA to engage its receptors. This property, along with the metabotropic nature of dopamine receptors, contributes to the temporally slower nature of post-synaptic dopamine signaling. Therefore, due to the slower signaling properties of dopamine transmission, tight coupling of an action potential stimulus to vesicle release may not be necessary at dopamine synapses which suggests the active zone machinery that mediates this coupling in glutamatergic and GABAergic synapses may not be present in dopamine terminals. However recent studies have found evoked dopamine release occurs from synapses that contain active zone-like structures (Banerjee et al., 2020; C. Liu,

Kershberg, Wang, Schneeberger, & Kaeser, 2018). The molecular components required for dopamine release are still being elucidated, and initial studies indicate overlap in the composition yet altered functions of molecular components of the dopamine active zone when compared to glutamatergic and GABAergic active zones.

Understanding dopamine release at the molecular level is a relatively new field, with key components identified in fast neurotransmitter release now being evaluated in dopaminergic systems. A seminal study published in 2018 by Pascal Kaeser's lab was the first to address the molecular components of the dopamine active zone and release machinery. Using striatal brain slices from dopamine neuron-specific conditional knockout animals and three dimensional super resolution microscopy, the group concluded that dopamine synapses, termed varicosities, contain the active zone proteins RIM1/2, bassoon, and ELKS1/2α (C. Liu et al., 2018). RIM1/2 were shown to be necessary for any evoked dopamine release in the dorsal striatum, through disrupted scaffolding of bassoon and munc13 at active zone-like release sites, while ELKS1/2α ablation did not impact dopamine release (C. Liu et al., 2018). These results contrast with the roles of RIM1/2 and ELKS1/2α in classical transmitter release, where glutamatergic transmission is decreased but not completely absent in RIM1/2 knockout and ELKS1/2α knockout hippocampal synapses (Acuna, Liu, & Sudhof, 2016; Held, Liu, & Kaeser, 2016).

A role for CAPS1 in regulating dopamine release from central neurons has not been explicitly examined, nor has a role for CAPS1 in regulating release of any of the other neuromodulatory transmitters been investigated in vertebrates. Studies performed in *C. elegans* suggest that CAPS plays an important role in release of acetylcholine (Charlie, Schade, Thomure, & Miller, 2006; Miller et al., 1996). However, it should be noted that a single CAPS protein exists in this species, thus these conclusions can be generally applied to the CAPS-family of proteins but do not explicitly implicate CAPS1 or CAPS2. Studies investigating the expression of CAPS1 and CAPS2 in murine dopaminergic neurons are inconclusive. A 2003 study by Speidel and colleagues shows *Cadps* expression in the striatum of P21 mice, while *Cadps2* is absent (Speidel

et al., 2003). Given mRNAs can undergo axonal transport for local synaptic translation in neurons (Bassell et al., 1998) and the low resolution of ISH imaging, it is possible that *Cadps* expression in the striatum is due to axonal transport from dopaminergic cell bodies. Alternatively, the *Cadps* transcripts may be expressed in GABAergic medium spiny neurons and cholinergic interneurons, the primary striatal cell populations. A more detailed investigation of striatal CAPS1 and CAPS2 protein expression found a dense network of CAPS1-positive fibers in the striatum along with cell bodies that were CAPS1 and CAPS2 positive (Sadakata et al., 2006). In the same study, CAPS1 staining was not detected in dopamine neuron cell bodies located in the VTA and SN while CAPS2 staining in these cells was extensive (Sadakata et al., 2006). Furthermore, clear expression of CAPS2 but not CAPS1 was found in dopaminergic neurons in DIV 27 mesencephalic-striatal co-cultures (Sadakata et al., 2006). Therefore, it remains unclear if CAPS1 expression in striatal fibers is due to expression in dopaminergic axons, and if CAPS1 is expressed in the dopaminergic neurons of the SN or VTA, the level of expression is expected to be low.

While the expression data does not suggest a strong role for CAPS1 in regulating dopamine release, an investigation of the effect of *Cadps* editing on dopamine release identified a functional role for the protein in this process. Using striatal synaptosomes prepared from CAPS1(G) mice, Miyake and colleagues found an increase in high potassium-evoked dopamine release when compared to release from wild-type derived synaptosomes (Miyake et al., 2016). This established a clear role for CAPS1 in regulating striatal dopamine release. A physiological effect of increased striatal dopamine signaling was noted in CAPS1(G) mice which display significant hyperactivity that was modulated by administration of a dopamine receptor type 2, D2R, antagonist (Miyake et al., 2016). Together these results provide the foundation for the studies described in this chapter. I investigated the expression of CAPS1 in dopaminergic neurons located in the VTA and SN and characterized *Cadps* editing levels in these brain regions. I also examined the role of *Cadps* editing in modulating dopamine release *in vivo* and characterized dopamine-mediated behaviors in CAPS1(G) mice.

Methods

Tissue Collection

Brain samples from 8-13 weeks old CAPS1(G) male mice and corresponding CAPS1(G) WT littermates were collected for monoamine content analysis; samples from 13 week old male CAPS1(G) mice and CAPS1(G) WT littermates were used for SN CAPS1 protein expression and *Cadps* editing analysis, samples from 10-16 week old CAPS1(G) WT female mice were used for VTA *Cadps* editing analysis, and samples from 10-12 week old male C57Bl/6N mice (JAX) were used to assess cocaine-mediated effects on *Cadps* editing in the VTA and NAcc. Animals were transferred from a central housing facility to the laboratory and acclimated to the novel environment for 2 hours with dissections beginning at 11am. Mice were deeply anesthetized with isoflurane before rapid decapitation and brain removal. Brains were sectioned coronally using an adult mouse brain slicer (Zivic Instruments), and punches were taken from appropriate sections to collect the PFC, striatum, NAcc, and SN. Tissue enriched for VTA neurons was collected from the ventral midbrain portion a 2mm thick coronal slice taken at the junction of the hypothalamus and cerebellum. Punches/ regions from both hemispheres were collected in a single 1.5 mL Eppendorf tube for PFC, NAcc, VTA, and striatum samples, while each hemisphere SN sample was placed in a separate 1.5 mL tube. Tubes were submerged in liquid nitrogen directly after tissue collection for rapid freezing. Samples were stored at -80°C.

CAPS1 protein expression

A single hemisphere SN sample per animal was thawed on ice and protein extracted in 150µL of RIPA buffer supplemented with cOmplete™, EDTA-free protease inhibitor cocktail (Roche, cat. 4693159001). Samples were sonicated briefly, rocked for 15 minutes at 4°C, and centrifuged at 21,000 xg for 20 minutes. The resulting supernatant was collected, and 10µL was prepared with β-mercaptoethanol containing Laemmli sample buffer and loaded onto a 4-20% gradient SDS-PAGE gel. Proteins were transferred to a nitrocellulose membrane using a semi-

dry transfer apparatus (Bio-Rad). Membranes were dried for 30 minutes, re-hydrated with water, and blocked for 1 hour with PBS Intercept blocking buffer diluted 1:1 in PBS (Licor). Primary antibodies targeting CAPS1 (1:500, Synaptic Systems, cat. 262 003) and β-actin (1:1000, Santa Cruz, cat. sc-1616) were diluted in blocking buffer and applied to membranes overnight. Fluorescently conjugated secondary antibodies were diluted in blocking buffer and applied to membranes for 2 hours (anti-rabbit Alexa 790 1:15,000, Jackson Immuno, 211-652-171 and anti-goat 680LT 1:50,000, LI-COR, 926-68024). Blots were washed and imaged on a LI-COR Clx Instrument and band intensities were quantified using Image Studio Lite (LI-COR). Data are presented as CAPS1/β-actin, normalized to WT animals.

Cadps RNA editing levels

RNA was extracted from brain tissue punches/sections using brief sonication in Trizol Reagent (Invitrogen, cat. 15596018) and phase separation of RNA according to manufacturer's instructions. The aqueous phase from the Trizol separation was added to an equal volume of 70% ethanol and loaded onto a purification column provided with the RNeasy Micro Kit (Qiagen, cat. 74004, 2019-2020), and the remaining steps of purification were carried out according to the manufacturer's instructions. The optional on-column DNase treatment step was performed using RNase-free DNase according to the manufacturer's instructions (Qiagen, cat. 79254). cDNA was prepared from 2 µg RNA using the High-Capacity cDNA Reverse Transcription kit (Applied Biosystems, cat. 4368813). RT-PCR amplicons spanning the *Cadps* editing site were generated using forward (5'-GATGGACGTGGCCGACGCCTACG-3) and reverse (5'-CTGTCCTTCATGCT-GATACCTTGTAAG-3') primers. PCR amplicons were visualized after agarose gel electrophoresis and purified using the SV Wizard PCR and Gel Clean-up Kit according to the manufacturer's instructions (Promega, cat. A9282). Purified PCR amplicons were sequenced using the reverse primer indicated above. Relative peak heights in sequence electropherogram traces were used to quantify RNA editing, as previously described (Malik et al., 2021).

Immunohistochemistry

CAPS1(G) WT male mice were anesthetized with isoflurane and perfused transcardially with 10 mL of PBS followed by 20 mL of freshly prepared 4% PFA in PBS. Brains were dissected and placed in 4% PFA overnight at 4°C and then moved to 30% sucrose for storage at 4°C. Thirty-micron coronal sections containing the striatum, VTA, and SN were cut using a freezing microtome (Leica) and were stored in PBS at 4°C. Free floating sections were washed in TBS and antigen retrieval was performed in a sodium citrate buffer (10 mM sodium citrate, 0.05% Tween 20, pH 6.0) for 20 minutes at 85-95°C. Sections were washed again in TBS, and blocked for 20 minutes in blocking buffer (TBS, 0.2% Triton X-100, 4% horse serum). Sections were incubated by rocking in primary antibodies diluted in blocking buffer for 48 hours at 4°C, followed by washing and incubating by rocking in secondary antibodies diluted in blocking buffer for 120 minutes at room temperature. Primary antibodies used were as follows: rabbit anti-CAPS1 (1:500, Synaptic Systems, 262 013) and guinea pig anti-tyrosine hydroxylase (1:1000, Synaptic Systems, 213 104) and secondary antibodies used were goat anti-rabbit Alexa 568 (1:1000, Invitrogen, A11011) and goat anti-guinea pig Alexa 647 (1:1,000, Invitrogen, A21450). After a final wash, sections were mounted on charged slides and dried in the dark overnight at room temperature. Coverslips were applied with Vectashield with DAPI mounting media. Slides were imaged using a Zeiss LSM 510 Meta inverted confocal microscope and image Z stacks used for analysis were captured at 1024 x 1024 resolution, using a 63X (na 1.4) oil immersion objective. TH density was analyzed in Image J using a custom macro to measure the area of staining. Briefly, a region of interest in each image was identified as an area in which no Pencils of Wilson myelinated nerve bundles were present. A maximum intensity projection was generated for each region of interest z stack, and the image segmented using the Moments threshold. The area was measured and recorded.

Ex Vivo Fast-Scan Cyclic Voltammetry

Fast-scan cyclic voltammetry (FSCV) studies were performed by Dr. Suzanne Nolan as part of a collaboration with the laboratories of Drs. Erin Calipari and Cody Siciliano. FSCV was

used to characterize dopamine release and uptake in the dorsal striatum and the nucleus accumbens in CAPS1(G) and CAPS1(G) WT animals. Following rapid decapitation, a vibrating tissue slicer was used to prepare 300 µm thick coronal brain sections containing both the DS and the NAcc, and the slices were incubated for at least 45 minutes in room temperature oxygenated aCSF (in mM): 126 NaCl (126), 2.5 KCl (2.5), 1.2 NaH_2PO_4, 2.4 $CaCl_2$, 1.2 $MgCl_2$, 25 $NaHCO_3$, 11 glucose, 0.4 L-ascorbic acid, pH = 7.4]. Following the incubation period, the slice was transferred to the testing chamber, which contained oxygenated aCSF at 32°C, flowing at approximately 1mL per minute. A carbon fiber microelectrode (100–200 µm length, 7 µm diameter) and bipolar stimulating electrode were placed into the region of interest in close proximity. Baseline evoked dopamine release was measured in the DS following a single electrical pulse (250 – 350 µA, 4ms, monophasic) applied to the tissue every 3 minutes. The extracellular dopamine level was recorded via application of a triangular waveform (−0.4 to +1.2 to −0.4 V vs Ag/AgCl, 400 V/s). Once the peak of evoked dopamine release was stabilized (3 collections with <10% variability, not trending in the same direction), the amount of evoked dopamine release and release kinetics (such as τ and maximal rate of uptake [V_{max}]) were assessed in three concurrent collections and averaged for each animal.

The electrodes were then moved to the NAcc and the baseline collection procedure was repeated. Following stabilization and baseline assessments as described above, multiple-pulse stimulations were applied to slices, to determine the responsivity of NAcc terminals to stimulations encompassing tonic and phasic firing frequencies of dopamine neurons (5 pulses at 5, 10, 20, 60 and 100 Hz, delivered in ascending order). Further, to test the relationship between stimulus intensity and dopamine output, intensity of a single pulse stimulation was varied stepwise from 5 – 1000 µA every 60 seconds and evoked dopamine release was measured. Finally, paired pulse ratios were also collected in triplicate at varying interpulse intervals (10ms, 50ms, 100ms, 500ms). Paired pulse collections were ordered pseudo randomly, and each was referenced to a preceding single pulse collection for subsequent analyses. Following the conclusion of experiments,

electrodes were calibrated by recording responses to a known concentration (3 μM) of dopamine using a flow injection system and a calibration constant was determined for each electrode to convert electrical current to measured dopamine concentration as previously described (Siciliano, Calipari, Ferris, & Jones, 2014).

Voltametric Data Analysis

Demon voltammetry and analysis software was used for all analysis of FSCV data (Jordan T Yorgason, España, & Jones, 2011) . Baseline data were analyzed first by determining the peak height and latency to return to baseline (tau). Data were modeled either using Michaelis–Menten kinetics to determine modeled dopamine release and V_{max}, with *Km* fixed at 160 nM and all other parameters assumed to be floating to ensure best fitting line as described previously (Calipari et al., 2017). Paired pulse recordings were analyzed using a subtraction method wherein the amplitude of the preceding single pulse collection was subtracted from amplitude of the paired pulse collection to isolate the signal from the additional second pulse, similar to previous studies (Siciliano et al., 2014).

Monoamine Content Analysis

Tissue samples were obtained as described above. Protein quantification and monoamine concentrations were determined by the Vanderbilt Neurochemistry Core using a trichloroacetic acid-based sample extraction and HPLC-ECD for monoamine detection. Dopamine (DA), norepinephrine (NE), 3,4-dihydroxyphenylacetic acid (DOPAC), homovanillic acid (HVA), 3-methoxytyramine (3-MT), serotonin (5-HT), and 5-hydroxyindoleacetic acid (5-HIAA) values were reported for each tissue sample, normalized to total protein content.

Mouse Behavioral Assays

All behavioral assays, except for the sucrose positive reinforcement test, were performed in the Vanderbilt Neurobehavioral core facility. Animals were transferred to the facility at least 2 weeks prior to starting experiments. Animals were group housed with a mix of WT and CAPS1(G) genotypes, unless otherwise noted, in groupings of 2-5 per cage. All assays were performed

between 08:00 and 17:00, and time of day was controlled in each specific assay. Cages were moved into testing rooms for at least 30 minutes prior to beginning the experiment to allow animals to acclimate to the novel environment.

Home Cage Scan: Male mice, 11-16 weeks old, were housed individually for at least a week prior to starting the experiment. On the day of the experiment, home cages containing individually housed animals, with visual obstructions such as nests and huts removed, were placed in an incubator that was equipped with home cage monitoring hardware between 17:00 and 18:00 hours. The cage parameters were loaded into the software (HomeCageScan, CleverSys) and animal activity was monitored for 24 hours. Using infrared detection of animal movements, the Home Cage Scan system records distance traveled, and the frequency and time spent engaging in 20+ behaviors. Data was extracted in 1-hour bins and distanced traveled was plotted over time. For analysis of “repetitive behaviors”, those previously identified in literature including rearing, grooming, jumping, hanging, twitching, and digging were included in analysis. The total time spent engaged in each behavior during the 24-hour monitoring period was analyzed.

Open Field Test: Male and female mice, age 9-22 weeks old, were used for the test. Animals were individually placed in a 27 x 27 cm, sound attenuated open field chamber (Med Associates) and x, y beam breaks were recorded for 30 minutes to measure the distance traveled. Z beam break data was recorded simultaneously to measure rearing frequency. The assay was repeated on the following day.

Forepaw Grip Strength: Male and female mice, age 14-26 weeks old, were held by the tail and permitted to grip a wire attached to a force meter with their front paws only. Animals were slowly pulled by the base of the tail until they released the wire and the force generated was recorded. A total of 5 trials per animal were completed, with >10 minutes of rest time in between each trial.

Inverted Screen: Male and female mice, age 14-26 weeks old, were placed on a wire mesh grid and the grid was then slowly rotated 180 degrees such that the animals were hanging upside down. The amount of time the animal remained on the screen before falling to a cage below filled with soft bedding was recorded, with a maximum trial time of 60 seconds. A total of 3 trials per animal were completed with >10 minutes of rest time in between each trial.

Balance beam: Male and female mice,13-18 weeks old, were trained over two days to walk across 1 m long, 6mm and 12mm wide square beams from a platform at one end to an enclosed box with bedding at the other end. On the third day, each animal was placed on the platform and videotaped as it traversed the beam, with each beam size tested twice with >2-minute rest periods between each trial. The time to traverse the beam was recorded and videotapes analyzed to count the number of paw slips, which were scored as any paw placement not on the top of the beam.

Accelerating rotarod: Male mice,14-19 weeks old, and female mice,16-28 weeks old, were placed on a rotating cylinder, approximately 3 cm in diameter which rotated at a speed of 4 to 40 rpm, with speed increasing over 4 minutes. Each trial ends when the mouse falls off the rod, with a maximum trial time of 5 minutes. An additional criterion set to end a trial was rotation of the animal around the rod for three full revolutions without taking steps. Mice are tested in three trials per day across three consecutive days, with ample >10 minutes of rest between trials.

3-chamber test: Male mice, 12-14 weeks old, were placed into the center chamber of a 3-chamber cage separated with 2 plexiglass dividers and allowed to acclimate to the chamber for 5 minutes. Next, the plexiglass dividers were removed, and mice were allowed to freely explore the entire cage for 10 minutes. In the test phase, a novel mouse (age & sex matched C57Bl/6N) was placed under a wire cup in one chamber and a novel object (empty wire cup) was placed in the opposite chamber. The test subject was videotaped as it freely explored the chambers for 10 minutes. AnyMaze software was used to track the animal's movements in each chamber, and time spent with the novel mouse versus novel object was analyzed.

Tube Test: Male mice, 14-16 weeks old, were trained to run through a clear 20 cm long tube during two runs through the tube alone. The following day, a test subject animal is placed into one end of the tube, and a control subject animal (sex & age matched C57Bl/6N) is placed into the other end of the tube such that the animals face each other. The “winner” of a trial is the animal that proceeds to the opposite end of the tube, and therefore pushes the other animal out of the tube. Each test subject was tested twice against the same control subject, with the starting side of the tube varied between trials to balance an effect of tube side.

Cocaine-induced conditioned place preference: Male mice, 8 weeks old, were placed in a two-chamber box that had striped walls and a perforated floor on one side and clear walls with barred floor on the other side. Animals could freely explore the box for 20 minutes, and x y beam breaks were used to track the location of the animal. On the following day, a door separating the two chambers was closed and the animals were injected I.P. with normal saline (10uL/ gram body weight) and immediately placed into the preferred chamber, which was defined as the side the animal spent the most time in on the pre-test day, for 20 minutes. The next day, animals were dosed with 10 mg/kg cocaine (prepared fresh daily, 10uL/ gram body weight) and placed in the non-preferred chamber for 20 minutes. Saline and cocaine injections and box placement alternated daily for 8 training days. On the test day, the door separating the chambers was opened and animals were placed in the box and allowed to freely explore for 20 minutes. The amount of time spent in each chamber was analyzed.

Sucrose-mediated positive reinforcement: After arriving at the animal facility, animals were weighed for starting weight (ranging between 25 and 36g) and food restricted to 2.5 g per day per mouse in the cage (typically 3-4). After weights stabilized (between 23 and 34 g), the mice were trained in individual Med Associates operant conditioning chambers (St Albans, VT) fitted with two nose pokes (one active and one inactive), one delivery port and two cue lights. Responses on the active pole resulted in the delivery of a sucrose reinforcer while responses on the inactive operanda had no programmed consequence. The side of the active poke/cue light was

counterbalanced across the group. On the first day of the experiment, the animals were briefly magazine trained to encourage reinforcer collection, and both the active and inactive nose pokes were baited to encourage exploration. Each session consisted of a one-hour session, with white noise on for the duration of the session. The structure of the session was trial based, with a discriminative stimulus signaling the beginning of the trial wherein active responses were reinforced with a 10 uL delivery of the reinforcer (10% sucrose solution). If an active response was triggered during the discriminative stimulus, the reinforcer would be delivered, and a light turned on over the port to signal availability of the reinforcer. The port light was extinguished following the collection of the reinforcer (a triggered head entry). Failure to collect the reinforcer resulted in subsequent responses on the active poke to be recorded, but not reinforced, until the reinforcer had been collected. If an active response was initiated during the intertrial interval (VI-30s), the animal entered a time-out period wherein the house light was turned on for 30 seconds and any responding was recorded but did not result in reinforcer delivery. Following the cessation of the 30 second time out, the intertrial interval period was resumed. Following the session, the animals were weighed and fed.

Results

Characterization of CAPS1 expression and editing levels in dopaminergic brain regions

To better understand how *Cadps* editing impacts dopamine release, we began by characterizing the level of *Cadps* editing in the main dopaminergic neuron nuclei, the SN and VTA, in WT animals. In VTA-enriched brain sections 19.5± 2.1% (n=3) of *Cadps* transcripts are edited whereas as in the SN 11.3± 1.7% (n=5 animals) of transcripts are edited (Figure 13A). Prior studies, including those presented in Chapter II, indicated that *Cadps* editing levels are subject to modulation by neuronal activity. A previous study has also shown that ADAR2

expression and GluA2 Q/R site editing levels change in the NAcc shell following abstinence from cocaine self-administration (Schmidt et al., 2015), suggesting that cocaine may impact editing levels in the striatum. As we planned to use cocaine during select neurobehavioral assays, we sought to investigate the effect of cocaine administration on *Cadps* editing levels in the VTA and NAcc. Wild-type C57Bl/6N male mice were dosed for 4 consecutive days with 10 mg/kg cocaine or vehicle, and brain tissue was collected 48 hours after the last injection. Analysis of *Cadps* editing in saline (vehicle) treated animals in VTA-enriched tissue found ~20% of transcripts are edited, in line with our previous results (Figure 13A), whereas about 25% of transcripts are edited in the NAcc. Interestingly, cocaine treatment did not change the level of *Cadps* editing in either brain region tested (Figure 13B). This observation suggests that MSNs in the NAcc and dopamine neurons in the VTA do not alter *Cadps* editing levels in response to cocaine-induced increases in dopamine signaling and should not impact future behavioral analysis using wild-type animals as controls.

Next, we sought to evaluate CAPS1 protein expression in the SN in CAPS1(G) and CAPS1(G) WT animals. Using western blot analysis of SN tissue punches, CAPS1 expression was confirmed in the SN and did not vary based upon genotype (Figure 13C, D). To investigate whether CAPS1 is expressed specifically in dopaminergic neurons located in the SN and VTA, we turned to immunohistochemical analysis to assess co-localization of CAPS1 and tyrosine hydroxylase (TH), a marker for dopaminergic neurons. In both the SN and VTA, TH distinctly localizes to cell bodies and fibers, which are likely dopaminergic axons (Figure 14). CAPS1 is broadly expressed in both the SN and VTA, diffusely labeling cell bodies and the surrounding neuropil. Most TH+ cell bodies contain co-localizing CAPS1, indicating that CAPS1 may be expressed in dopaminergic cells. It should be noted that due to lack of availability of CAPS1 null animals, we are unable to optimize this method to eliminate non-specific background staining with the CAPS1 antibody. However, the absence of CAPS1 staining in some cell nuclei and distinct cell borders are indications that the staining shown is specific signal above background. In

summary, our data suggests CAPS1 is expressed in dopamine neurons in the VTA and SN and that *Cadps* transcripts are edited to a low level in both regions.

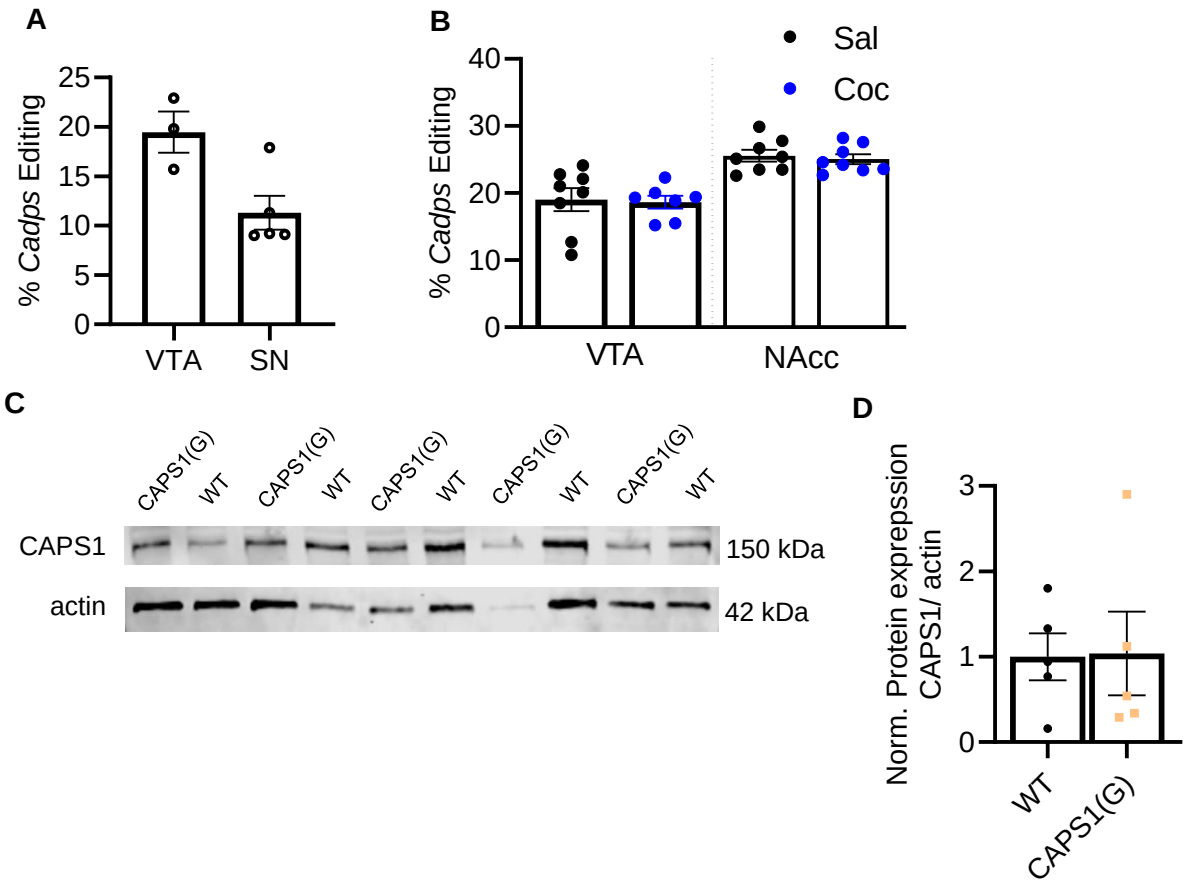

Figure 13. CAPS1 expression and editing levels in dopaminergic brain regions. (**A**) Quantification of *Cadps* editing levels in VTA and SN-enriched tissue sections from CAPS1(G) WT mice. (**B**) Quantification of *Cadps* editing levels in VTA enriched tissue sections and NAcc tissue punches from WT mice treated with saline (Sal) or 10 mg/kg cocaine (Coc) for 5 days, n=8 mice/treatment, Mann-Whitney tests, p>0.05. (**C**) Western blot analysis of CAPS1 and β-actin protein expression in the substantia nigra (SN) of CAPS1(G) and CAPS1(G) WT mice. (**D**) Quantification of CAPS1 protein expression, from the Western blot shown in B, is presented; n=5 animals/ genotype, Mann-Whitney test, p>0.05.

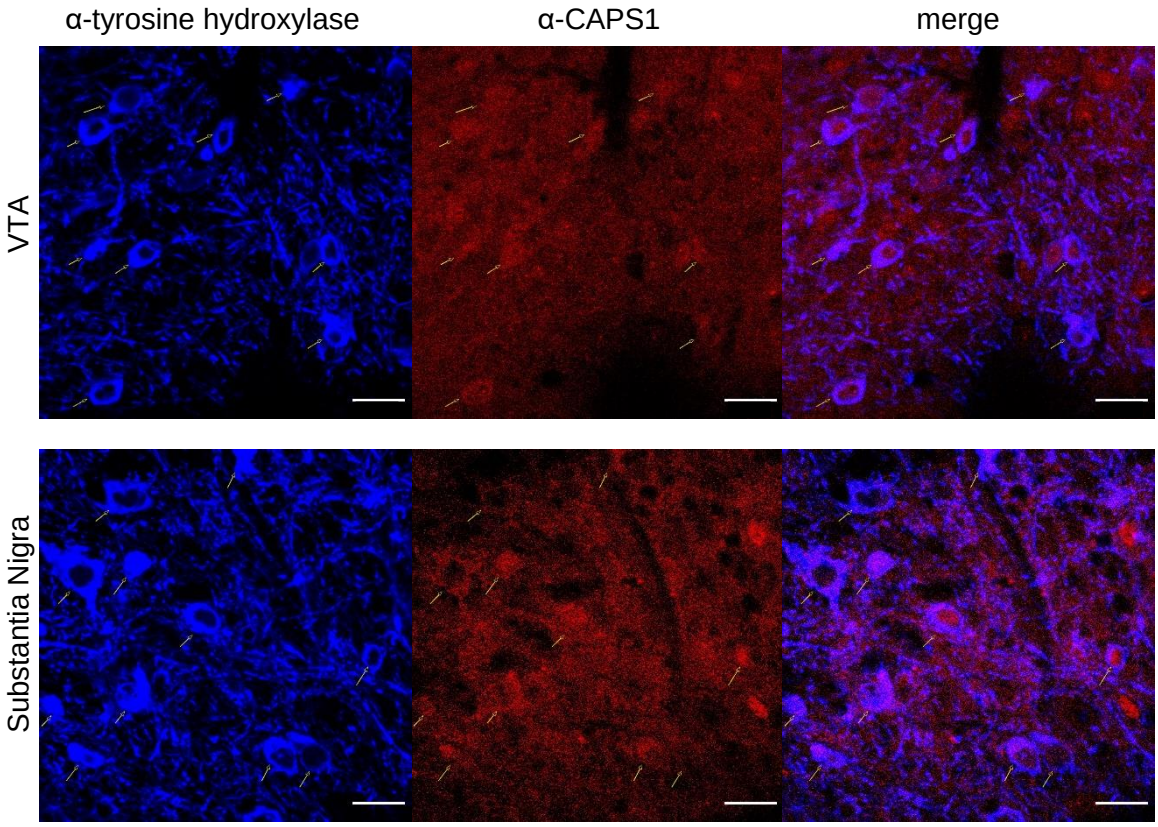

Figure 14. Immunohistochemical analysis of CAPS1 expression in dopaminergic neurons in the ventral tegmental area (VTA) and Substantia Nigra. A dopaminergic cell marker, tyrosine hydroxylase (TH, blue), and CAPS1 (red) co-localize in cell bodies located in the ventral tegmental area (top panel) and the substantia nigra (bottom panel). Arrows indicate TH+ cell bodies, scale bar= 20μm.

Investigation of the effect of Cadps editing on dopamine release

It has been reported previously that striatal synaptosomes prepared from CAPS1(G) mice have increased evoked dopamine release when compared to WT synaptosomes (Miyake et al., 2016). While this result suggests that *Cadps* editing enhances dopamine release, we sought to confirm this finding using intact tissue. We turned to fast scan cyclic voltammetry in *ex vivo* striatal slices from CAPS1(G) and CAPS1(G) WT mice to study evoked dopamine release in greater detail. Probes were placed in the dorsal striatum, and neurotransmitter release was elicited with an electrical stimulation (Figure 15A). As cyclic voltammetry detects changes in current across a range of voltages, it is possible to identify which species is neurotransmitter is likely being released based peak oxidation and reduction profiles of the transmitter. For example, dopamine is rapidly oxidized at +0.6 V and reduced at -0.1 V under typical FSCV recording conditions. Representative voltammograms from FSCV recording in the striatum of CAPS1(G) and CAPS1(G) WT animals show significant changes in current at +0.6V, confirming that dopamine is being measured (Figure 15B). Dopamine release, as measured by the peak height in a current over time plot, is increased in the dorsal striatum of CAPS1(G) animals compared to WT (Figure 15C, D). Dopamine re-uptake, as estimated by the decay constant, τ, from the current over time plot, is not changed in CAPS1(G) animals in the dorsal striatum (Figure 15E). To investigate dopamine release in greater detail, a modeling approach was used to estimate the amount of dopamine released per pulse, which accounts for dopamine diffusion and re-uptake during release. In CAPS1(G) mice, there is greater dopamine released per pulse, consistent with the increased release in dopamine based on peak height (Figure 15F). Finally, the maximal rate of dopamine re-uptake was modeled and CAPS1(G) mice were found to have a significantly greater V_{max} than CAPS1(G) WT animals (Figure 15G). The modeled parameter V_{max} is a measure of DAT function in re-uptake, which suggests that CAPS1(G) animals have increased DAT surface

expression or function. Therefore CAPS1(G) animals have increased dopamine release and increased DAT-mediated dopamine reuptake in the dorsal striatum.

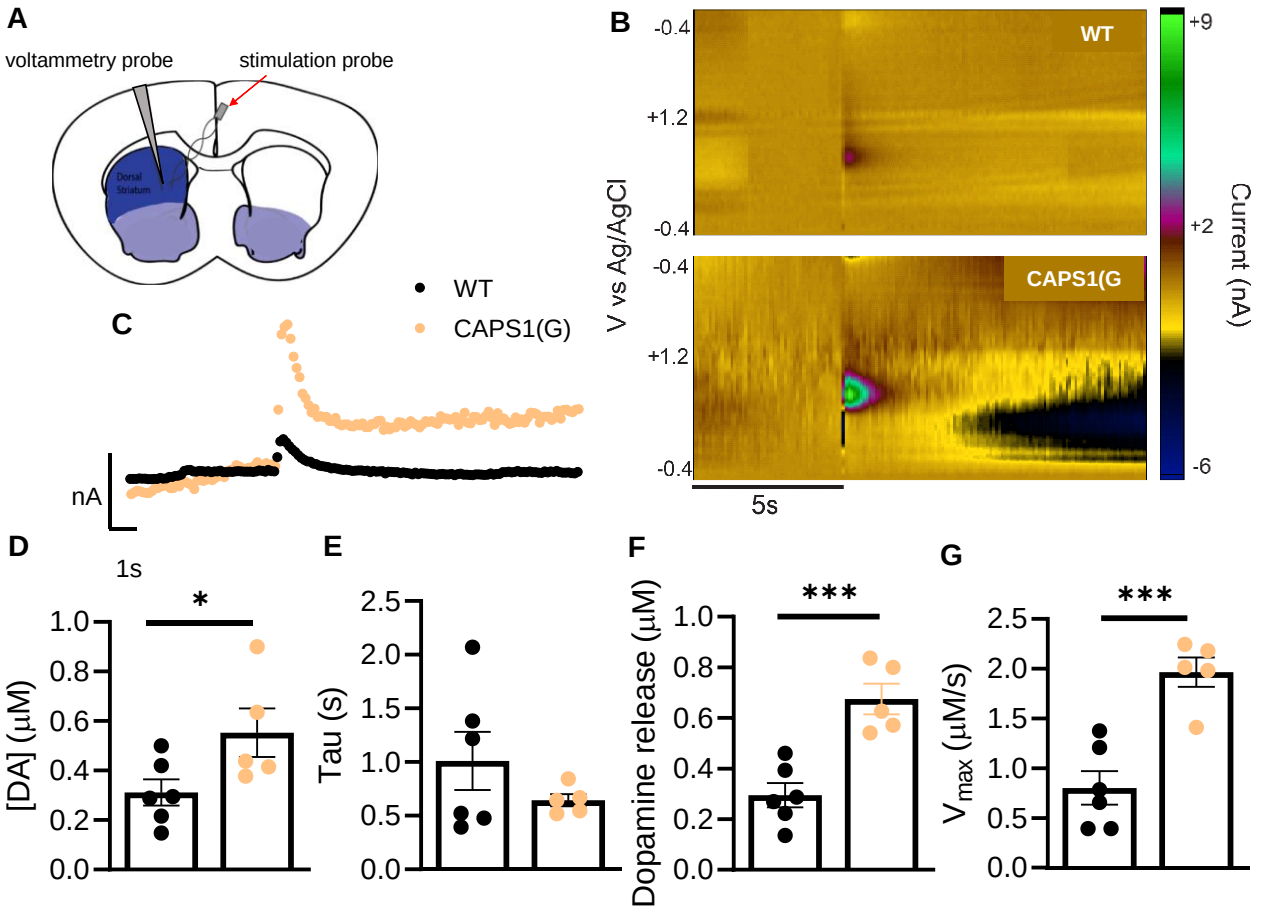

Figure 15. Dopamine release and re-uptake in the dorsal striatum of CAPS1(G) mice. (**A**) Schematic illustrating FSCV probe placement in the dorsal striatum of a coronal brain section. (**B**) Representative color plots of FSCV recordings from CAPS1(G) and CAPS1(G) WT mice. (**C**) Representative traces of the current measured at +0.6 V over time from CAPS1(G) and CAPS1(G) WT mice. (**D**) Evoked dopamine release, as measured by peak height with probe calibration; n=5-6 animals/genotype, Unpaired t-test, *p<0.05. (**E**) Dopamine clearance, estimated by calculation of the decay constant tau **(τ)**, n=5-6 animals/genotype, Unpaired t-test, p>0.05. (**F**) Modeled dopamine concentration per pulse; n=5-6 animals/genotype, Unpaired t-test, ***p<0.001. (**G**) Modeled maximal uptake rate; n=5-6 animals/genotype, unpaired t-test, ***p<0.001.

We next investigated the same dopamine release and re-uptake parameters in the NAcc core, a region of the ventral striatum. Given that the NAcc receives dopamine innervation largely from VTA neurons, not SN neurons, it is possible that *Cadps* editing could have a differential effect in this brain region. When dopamine release was measured in the NAcc core of CAPS1(G) animals, no changes were found compared to WT animals (Figure 16C, D). No differences in dopamine re-uptake, as measured by τ, were noted in CAPS1(G) animals (Figure 16E). Consistent with these results, there also were no changes in modeled dopamine release per pulse or V_{max} in CAPS1(G) animals (Figure 16F, G). In summary, CAPS1(G) animals have unaltered dopamine release and re-uptake in the nucleus accumbens core.

Given the similar CAPS1 expression profiles in dopamine neurons in the SN and VTA (Figure 14), the lack of change in dopamine release in the NAcc was unexpected. Therefore, we investigated NAcc core release in greater detail. First, a 5-pulse stimulation paradigm was used to assess phasic dopamine release. Across a range of different stimulation frequencies, from 5-100 Hz, no change in phasic dopamine release was noted in the NAcc core of CAPS1(G) animals (Figure 17A). To assess short-term synaptic plasticity, a paired-pulse ratio (PPR) was calculated for 2 stimuli delivered at varying frequencies and CAPS1(G) animals were found to have no change in PPR compared to CAPS1(G) WT animals (Figure 17B). Finally, an input-output curve was generated to measure dopamine release at submaximal stimulation intensities, and interestingly CAPS1(G) animals were found to release more dopamine in response to low stimulation intensities than CAPS1(G) WT animals (Figure 17C). These results depict a more nuanced level of dopamine release regulation in the NAcc core by *Cadps* editing.

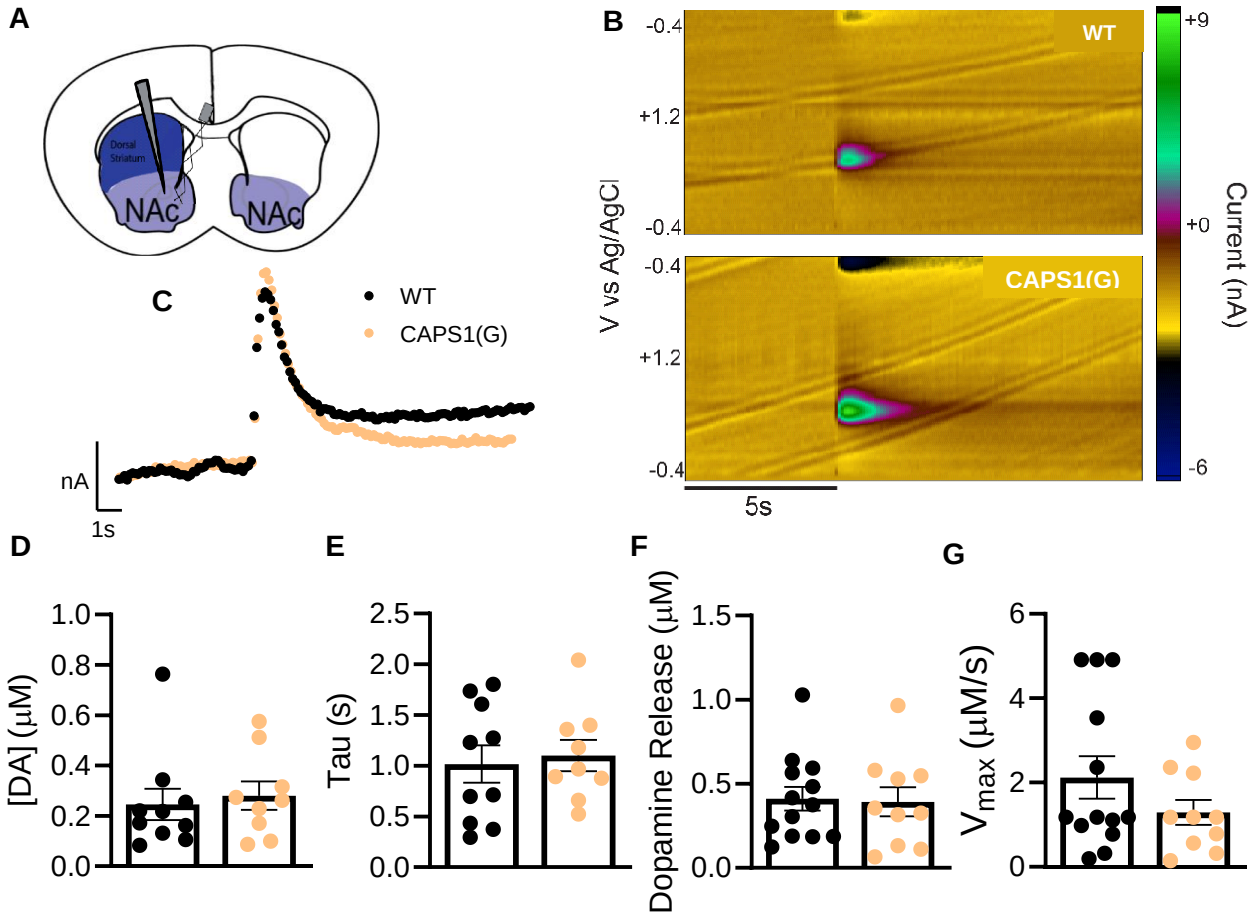

Figure 16. Dopamine release and re-uptake in the Nucleus Accumbens Core of CAPS1(G) mice. (**A**) Schematic illustrating FSCV probe placement in the NAcc of a coronal brain section. (**B**) Representative color plots of FSCV recordings from CAPS1(G) and CAPS1(G) WT mice. (**C**) Representative traces of the current measured at +0.6 V over time from CAPS1(G) and CAPS1(G) WT mice. (**D**) Evoked dopamine release, as measured by peak height with probe calibration; n=9-10 animals/genotype, Unpaired t-test, $p>0.05$. (**E**) Dopamine clearance, estimated by calculation of the decay constant τ (tau), n=9-10 animals/genotype, Unpaired t-test, $p>0.05$. (**F**) Modeled dopamine concentration per pulse; n=9-10 animals/genotype, Unpaired t-test, $p>0.05$. (**G**) Modeled maximal uptake rate; n=9-10 animals/genotype, Unpaired t-test, $p>0.05$.

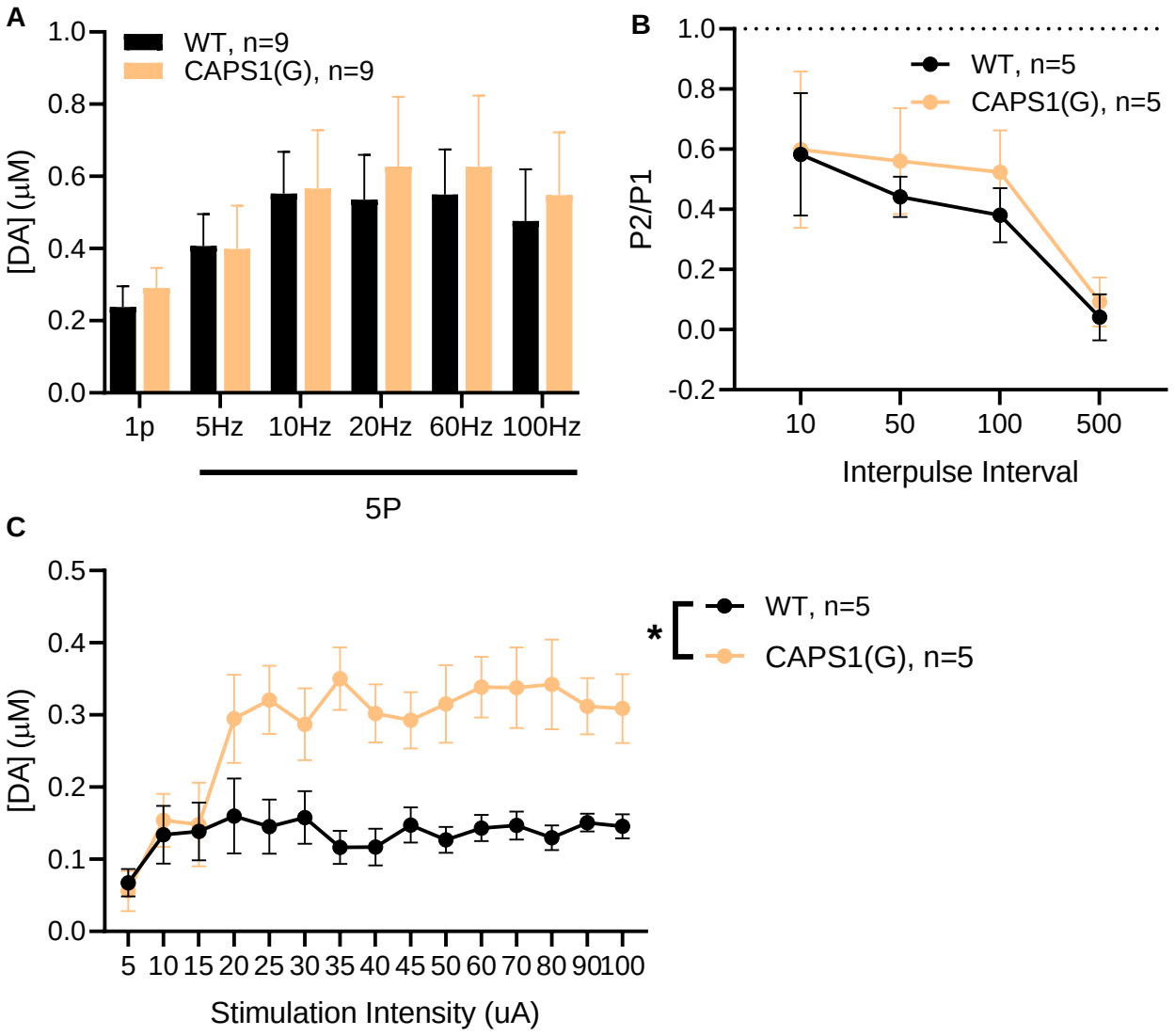

Figure 17. Extended analysis of dopamine release in the Nucleus Accumbens Core of CAPS1(G) mice. (**A**) Dopamine released in response to 1 pulse (1p) or 5 pulses (5p) given across a range of frequencies; 2-way RM-ANOVA, genotype effect F (1, 16) = 0.07, p = 0.78. (**B**) Paired pulse ratio of dopamine release from pulse 2/pulse 1, with pulses delivered across a range of frequencies; 2-way RM-ANOVA, genotype effect F (1, 8) = 0.23, p=0.64. (**C**) Input-output curve of dopamine release elicited using different stimulation intensities; 2-way RM-ANOVA, genotype effect F (1, 8) = 10.86, *p=0.0109.

Evaluation of Dopamine Axon Density & Synthesis and Metabolism in the Striatum

We have shown that CAPS1(G) animals have some level of altered dopamine release in both the dorsal and ventral striatum, which we would hypothesize is due to the role of CAPS1 in vesicle priming. However, alterations in other cellular processes linked to release could also be implicated. First, increased dopamine release could be due to increased dopamine neuron axon density in the striatum. While CAPS1 has not been linked directly to regulation of neuron development and synapse maturation, the genetic model used for experiments, CAPS1(G) animals, express the edited CAPS1 isoform in all tissues throughout development, which leaves open the possibility that CAPS1(G) animals may have altered dopamine neuron innervation in the striatum. To test this hypothesis, an immunohistochemistry approach was used to quantify the density of dopamine neuron innervation in the dorsal and ventral striatum of CAPS1(G) and CAPS1(G) WT animals. Coronal sections containing the striatum were labeled with an antibody targeting tyrosine hydroxylase (TH), an enzyme essential for the conversion of tyrosine to dopamine. The area of TH labeling in regions of interest in the dorsal and ventral striatum did not differ between CAPS1(G) and CAPS1(G) WT animals (Figure 18), suggesting that *Cadps* editing does not impact the development and maintenance of dopamine projections in these brain regions.

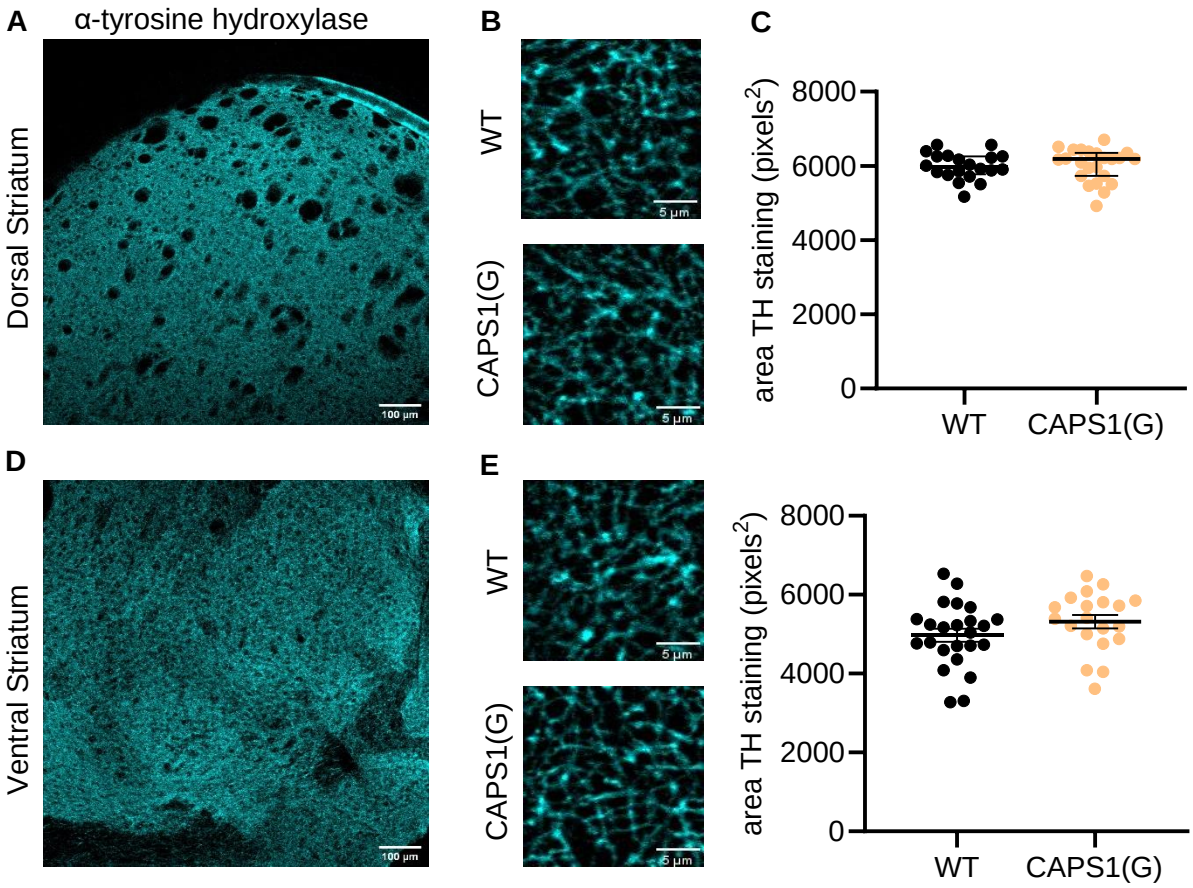

Figure 18. Dopamine axon density in the striatum of CAPS1(G) mice. (**A,D**) Representative images from dorsal (**A**) and ventral striatum (**D**) sections from CAPS1(G) WT mice labeled with an antibody to a dopamine cell marker, tyrosine hydroxylase (cyan); scale bar= 100µm. (**B,E**) High magnification representative images of CAPS1(G) and CAPS1(G) WT brain sections from the dorsal (**B**) and ventral (**E**) striatum, labeled as in A and D; scale bar = 5µm. (**C,F**) Quantification of the area of TH staining from regions of interest as shown in B and E; n=20-23 regions of interest, 1 ROI per image, 2-3 images per section, 2 sections per animal, 4 animals per genotype; unpaired t-test, p>0.05.

Another possible explanation for increased dopamine release is that dopamine synthesis is enhanced, or dopamine metabolism is impaired in CAPS1(G) animals, leading to increased intracellular concentrations of dopamine. Frequently animal models with disrupted DA signaling have altered tissue levels of DA and metabolites, including DAT KO mice (Jones et al., 1998), DAT T356M mutant mice (DiCarlo et al., 2019), and D2 autoreceptor KO mice (Anzalone et al., 2012). For the next set of experiments, we analyzed the levels of neurotransmitters and their metabolites in dopamine projection brain regions, including the dorsal striatum, NAcc, and pre-frontal cortex (PFC). Brain punches were taken from CAPS1(G) and CAPS1(G) WT animals that contained each region of interest, and tissue monoamine content was analyzed by HPLC with electrochemical detection. As expected, the highest concentrations of dopamine were found in the dorsal striatum and NAcc, with low levels of dopamine detected in the PFC (Figure 19A, C, E). No genotype differences were found in dopamine levels measured in any brain region. As monoamine content analyzed from tissue punches largely reflects intracellular levels of these chemicals, this result suggests there is no change in dopamine synthesis in CAPS1(G) animals. Levels of dopamine metabolites, DOPAC, 3-MT, and HVA, were also not changed in CAPS1(G) animals in any region analyzed (Figure 19A, C, E), suggesting there were no changes in dopamine metabolism in this animal model. Together these results indicate the CAPS1(G) animals have normal dopamine synthesis and metabolism, making it unlikely that altered intracellular dopamine concentration plays a role in the enhanced dopamine release phenotype.

While our focus was on quantification of dopamine and its metabolites, the analysis method employed allowed for simultaneous measurement of norepinephrine, 5-HT, and 5-HT metabolites. Given the broad expression pattern of CAPS1, we analyzed levels of these transmitters and metabolites as a pilot investigation for possible future studies. However, no changes in NE, 5-HT, or 5-HIAA levels were found in any tissue analyzed in CAPS1(G) animals (Figure 19B, D, F). Overall, this indicates that *Cadps* editing does not impact monoamine neurotransmitter synthesis or metabolism in the dorsal striatum, NAcc, or PFC.

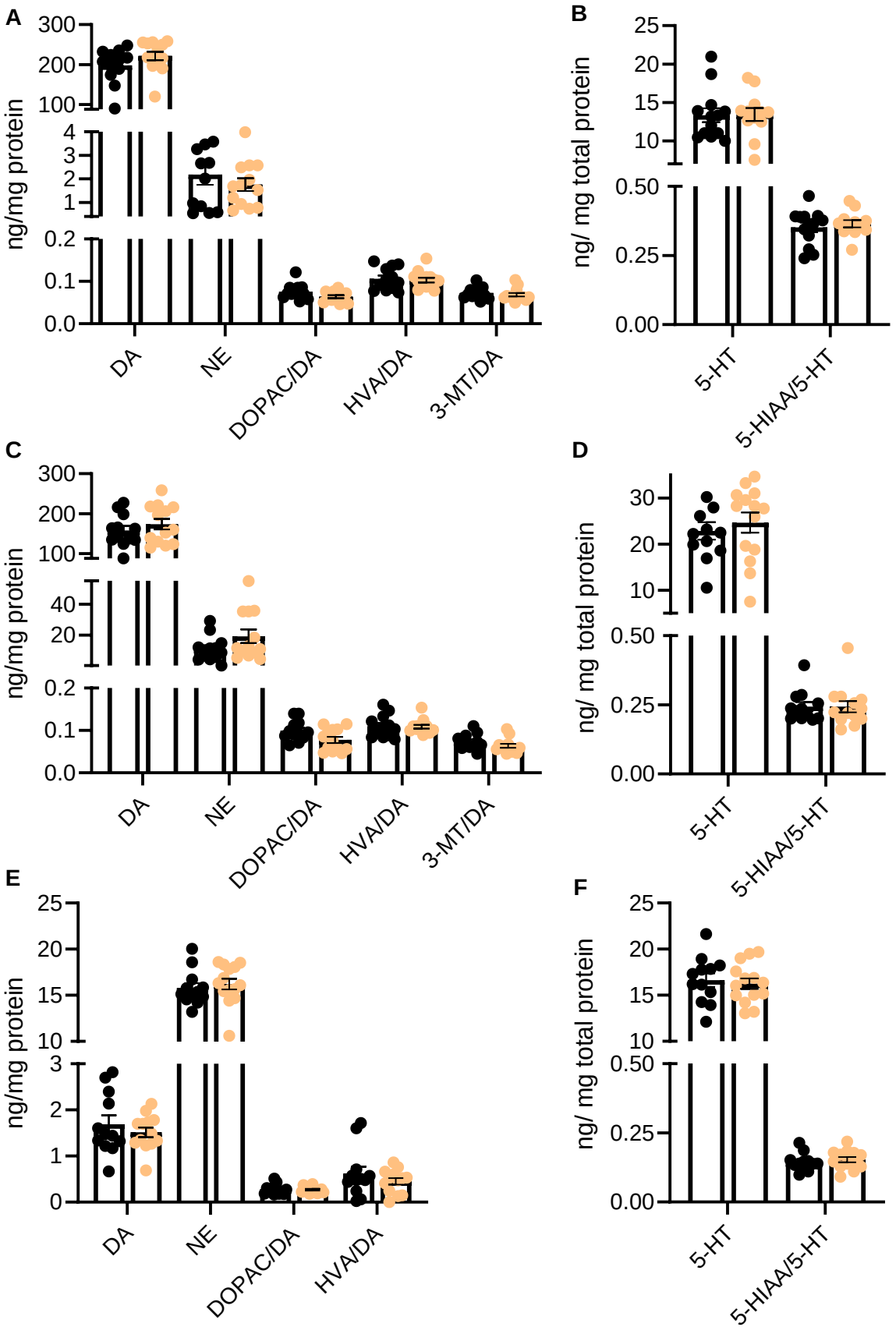
A
ng/mg protein
300
200
100
4
3
2
1
0.2
0.1
0.0
DA
NE
DOPAC/DA
HVA/DA
3-MT/DA
B
ng/ mg total protein
25
20
15
10
0.50
0.25
0.00
5-HT
5-HIAA/5-HT
C
ng/mg protein
300
200
100
40
20
0.2
0.1
0.0
DA
NE
DOPAC/DA
HVA/DA
3-MT/DA
D
ng/ mg total protein
30
20
10
0.50
0.25
0.00
5-HT
5-HIAA/5-HT
E
ng/mg protein
25
20
15
10
3
2
1
0
DA
NE
DOPAC/DA
HVA/DA
F
ng/ mg total protein
25
20
15
10
0.50
0.25
0.00
5-HT
5-HIAA/5-HT

Figure 19. Monoamine and metabolite analysis from dopamine projection brain regions of CAPS1(G) and CAPS1(G) WT animals. (**A, C, E**) Quantification of dopamine (DA), norepinephrine (NE), and their metabolites, HVA, 3-MT, and COMT, normalized to DA concentration found in the dorsal striatum (**A**), NAcc (**C**), and PFC (**E**); n= 12-13 animals/genotype, Multiple Mann-Whitney tests with FDR correction, p>0.05. (**B, D, F**) Quantification of serotonin (5-HT) and its metabolite, 5-HIAA, normalized to 5-HT concentration found in the dorsal striatum (**B**), NAcc (**D**), and PFC (**F**); n= 12-13 animals/genotype, Multiple Mann-Whitney tests with FDR correction, p>0.05.

Dopamine-associated animal behaviors: Locomotor Activity

Once our cellular experiments confirmed that *Cadps* editing increases dopamine release in the striatum, we began investigating dopamine-associated animal behaviors to understand the physiological outcomes of this effect. It has been reported that CAPS1(G) animals are hyperactive, and that their activity can be modulated with haloperidol, a D2 receptor antagonist (Miyake et al., 2016). We sought to replicate these findings in our laboratory, and to characterize other dopamine-associated behaviors in CAPS1(G) animals.

We first assessed locomotor activity in CAPS1(G) animals using an open field test and home cage monitoring. In both experimental paradigms CAPS1(G) animals display increased locomotor activity when compared to WT littermates (Figure 20A-D). As hyperactivity is noted in both assays, the effect is not solely a novelty induced phenotype, as is reported in other models of dysregulated dopamine systems (Anzalone et al., 2012). Also, CAPS1(G) animals acclimate to the novel environment of an open field chamber at the same rate as WT littermates, indicating normal habituation behavior. Diurnal analysis of home cage monitoring data demonstrates that CAPS1(G) animals are primarily hyperactive during the dark phase, with no change in locomotor activity levels during the light phase, which suggests that CAPS1(G) animals likely have normal sleep-wake cycles (Figure 20B).

To test whether hyperactivity in CAPS1(G) animals is due to enhanced dopamine signaling, animals were dosed with a dopamine releaser, cocaine, and a D2R antagonist, haloperidol. In response to a low dose of cocaine that does not impact WT animals, CAPS1(G) mice display increased locomotor activity (Figure 20E). Conversely, CAPS1(G) animals dosed with haloperidol have a significant decrease in locomotor activity compared to vehicle treated littermates (Figure 20F). Haloperidol-treated CAPS1(G) WT animals did not exhibit a significant decrease in locomotor activity when compared to the vehicle treated group. Given that CAPS1(G) animals are hypersensitive to activating and blocking dopamine signaling, we conclude that hyperactivity in CAPS1(G) animals is likely driven by hyperdopaminergia. In summary, we were

able to successfully reproduce the findings of Miyake and colleagues that CAPS1(G) mice are hyperactive, likely due to increased dopamine signaling.

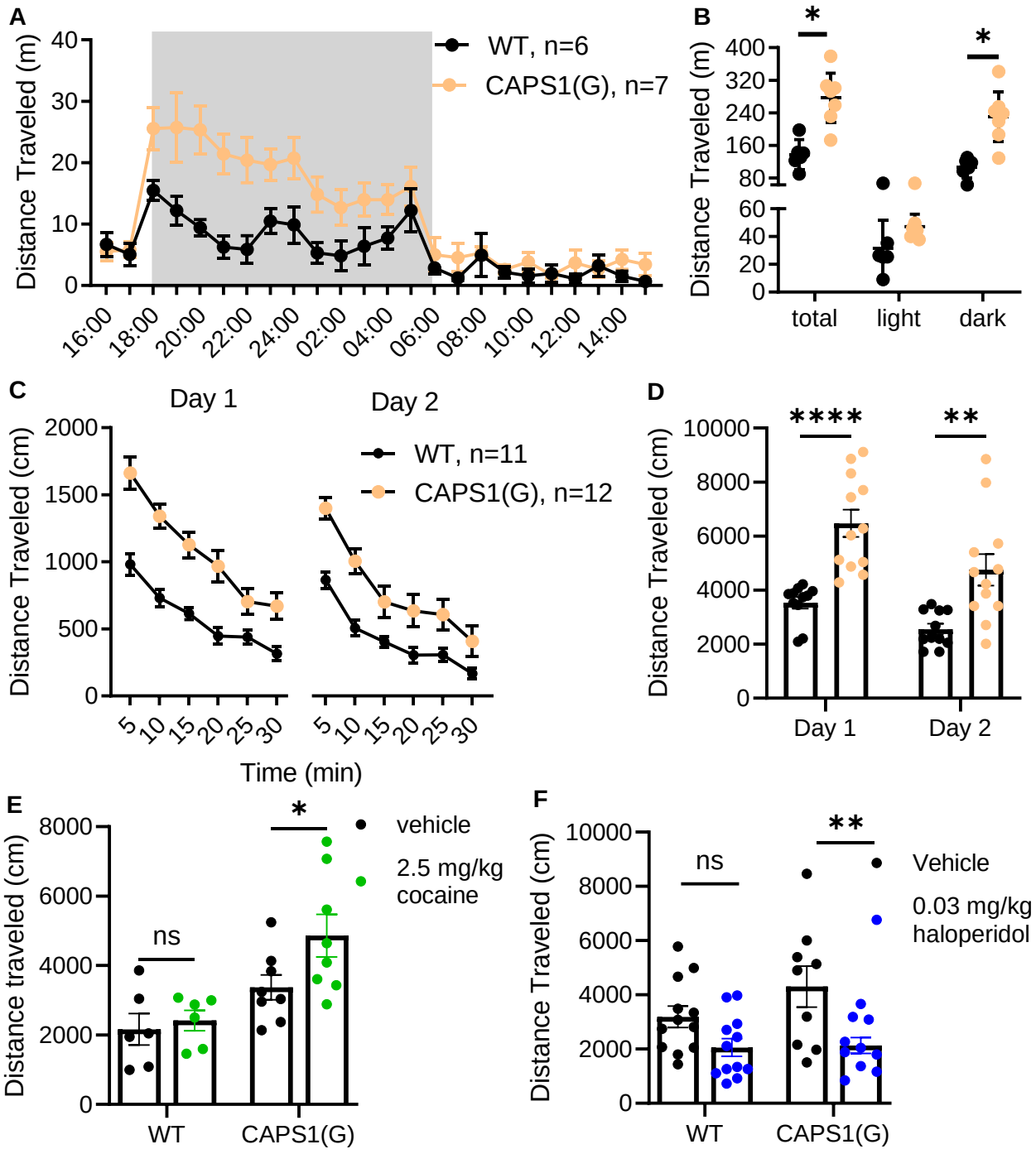

Figure 20. Evaluation of locomotor activity in CAPS1(G) animals. (**A**) Distance traveled over 24 hours in the home cage and (**B**) a summary of the total distance traveled during total, light, and dark time periods; n=6-7 male mice/ genotype, Multiple Mann-Whitney tests with post-hoc correction for multiple comparisons, *p<0.05. (**C**) Distance traveled over 30 minutes in an open field test across two days and (**D**) Quantification of the total distance traveled by day; n=11-12 male and female mice/genotype, 2-way ANOVA with Sidak's multiple comparison test, **p<0.01, ****p<0.0001. (**E**) Quantification of the distance traveled for 20 minutes after vehicle or 2.5 mg/kg cocaine injection; n=6-8 female mice/genotype, 2-way ANOVA with Sidak's multiple comparison test, *p<0.05. (**F**) Quantification of the distance traveled for 1 hour after vehicle or 0.03 mg/kg haloperidol injection; n=9-12 male mice/genotype, 2-way ANOVA with Sidak's multiple comparison test, **p<0.01.

Dopamine-associated animal behaviors: Strength and motor coordination

As CAPS1(G) animals have increased striatal dopamine release and are hyperactive, we hypothesized that these mice may display alterations in motor coordination, in a manner like the dyskinesia noted in Parkinson's patients treated with dopamine enhancing drugs. Therefore, we sought to characterize other motor-related behavioral phenotypes in this mutant mouse line. First, the forepaw grip strength of CAPS1(G) animals was measured, and while a significant effect of sex was noted, there was no effect of genotype (Figure 21A). These results rule out insufficient muscle tone as a variable that could confound the interpretation of assays that depend on the animal's ability to maintain a grip on a piece of equipment. Next, a panel of assays were used to assess motor coordination, including the inverted cage hang, the balance beam, and the accelerating rotarod assays. In the inverted screen test, there was a significant effect of genotype and sex on the amount of time spent on the screen, with CAPS1(G) animals remaining on the inverted cage for less time than WT littermate control animals, though post-hoc analysis of the data did not detect a significant pairwise effect (Figure 21B). CAPS1(G) animals performed equally well as WT littermates on the balance beam assay, requiring a similar amount of time to cross and experiencing the same number of paw slips. In the accelerating rotarod assay, CAPS1(G) animals outperformed WT littermate controls with significant differences noted on day 2 of the assay in male mice. In summary, though CAPS1(G) animals perform worse on the inverted screen, their performance across the panel of assays is consistent with normal motor coordination. Interestingly, CAPS1(G) animals may exhibit enhanced motor learning, as demonstrated by the rotarod assay, though additional assays should be performed to support this conclusion.

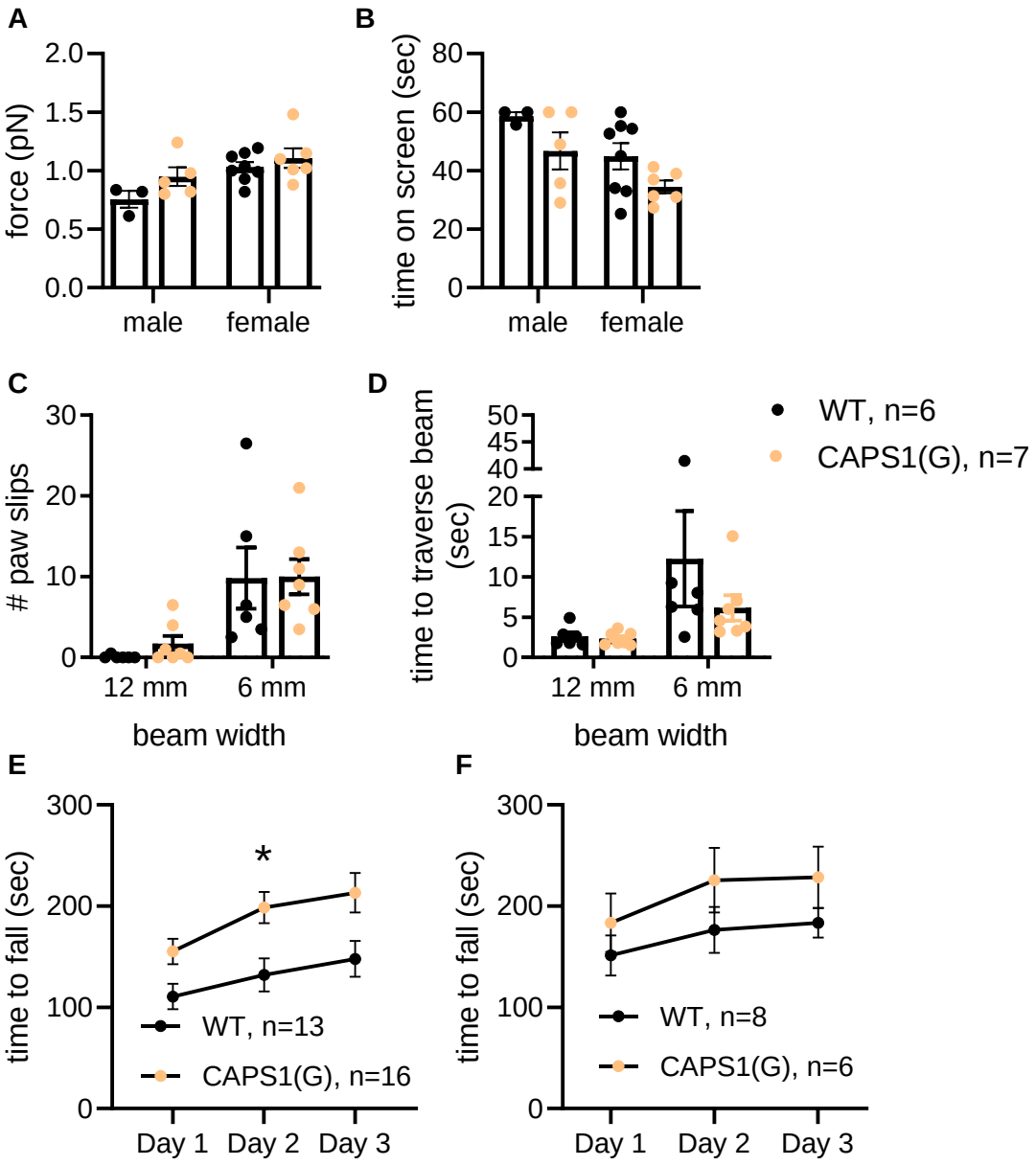

Figure 21. Evaluation of strength and motor coordination in CAPS1(G) animals. (**A**) Forepaw grip strength of male and female mice; n=3-8 mice/sex/genotype, 2-way ANOVA, sex effect F (1,18) = 8.675, p=0.008, genotype effect F (1,18) = 3.321, p>0.05. (**B**) Time spent hanging on an inverted screen for male and female animals; n=3-8 mice/sex/genotype, 2-way ANOVA, sex effect F 1,18) = 7.013, p=0.0164, genotype effect F (1,18) =5.206, p=0.0349, Sidak's multiple comparison tests CAPS1(G) v. WT, p>0.05. (**C**) The number of paw slips experienced while crossing a 12 or 6mm beam and (**D**) Time spent crossing the beam for male and female animals; n=6-7 male and female mice/genotype, 2-way repeated measures ANOVA for C, beam width effect F (1,11)= 20.65, p=0.0008, genotype effect F (1,11)= 0.1455, p=0.7101; 2-way RM-ANOVA for D, beam width effect F (1,11)= 6.70, p=0.0252, genotype effect F (1,11)=1.048 , p=0.3279. (**E, F**) Time spent on an accelerating rotarod across three days for male (**E**) and female (**F**) animals; 2-way RM ANOVA for E, genotype effect F (1,27) =9.155, p=0.0054, Sidak's multiple comparison test, Day 2 *p<0.05. 2-way RM ANOVA for F, genotype effect F (1,12) = 1.765, p=0.2087.

Dopamine-associated animal behaviors: Sociability and Social Dominance

It has been reported recently that excessive dopamine signaling in the dorsal striatum triggers autistic-like behaviors in mice, including impaired sociability, impaired preference for social novelty, and enhanced repetitive behaviors (Lee et al., 2018). Additionally, similar behaviors have been characterized in genetic models of enhanced dopamine release by independent research groups (DiCarlo et al., 2019) and mutations in the human DAT that cause anomalous dopamine efflux have been linked to autism (Bhat, El-Kasaby, Freissmuth, & Sucic, 2020). Furthermore, a recent GWAS study identified SNPs in human *CADPS* that are associated with an increased risk for developing autism (Grove et al., 2019), lending further support to the notion that altered CAPS1 function may be involved in the molecular underpinnings of autistic-like behaviors. Therefore, we hypothesized that CAPS1(G) animals would display autism-associated behaviors. Analysis of these behaviors in CAPS1(G) animals was performed using a panel of assays including repetitive behavior analysis, sociability, and social dominance assays.

First, we assessed repetitive behaviors using data from the open field test and home cage scan systems. Analysis of rearing, grooming, hanging, twitching, digging, and jumping in the home cage found no changes in the amount of time CAPS1(G) animals engaged in these behaviors when compared to WT littermate animals (Figure 22A). Of note, hanging and jumping behaviors trend toward increased in CAPS1(G) animals, suggesting that analysis of additional subjects may be warranted. I also have observed CAPS1(G) animals performing repetitive loops of jumping to the wire cage lid, climbing back and forth, and then repeating the loop when viewing home cage video recordings and during normal husbandry. In a separate experiment, the frequency of rearing behavior in CAPS1(G) animals was quantified in an open field test over 2 days. On the first day there were no differences in rearing frequency, but on the second day female CAPS1(G) mice displayed increased rearing frequency compared to WT littermates (Figure 22B). Together these results suggest CAPS1(G) animals may have a tendency towards performing behaviors such as jumping, hanging, and rearing repetitively.

Next, we sought to characterize social behaviors in CAPS1(G) animals and used a three-chamber test to study sociability. In this assay animals are tested for their preference of spending time with a novel mouse or a novel object. This assay was created to mimic a playground setting in which children typically play together, instead of alone. It is often noted that children with autism will prefer to play alone in this setting, and as such this sociability assay is one of several that are used to screen mice for autistic-like behaviors (Crawley, 2007). When tested in the three-chamber assay, CAPS1(G) animals spent more time with the novel mouse than the novel object, similarly to WT animals (Figure 22C), indicating that CAPS1(G) animals have no impairments in sociability.

Finally, another social behavior, social dominance, was assessed in CAPS1(G) animals using a tube test. In this assay, CAPS1(G) and WT littermates were faced off against a novel mouse in a confined cylinder to see which animal would back out of the cylinder, indicating a lack of social dominance. CAPS1(G) animals only won 3 of 26 matchups, a frequency significantly less than would be expected by random chance (13 out of 26 or 50% chance) (Figure 22D). WT littermate animals won at a frequency that was no different than chance. These results indicate that CAPS1(G) animals are not socially dominant. Taken together, these experiments suggest that CAPS1(G) animals may exhibit repetitive behaviors and have some social deficits like those observed in autism, which could be explored in future investigations.

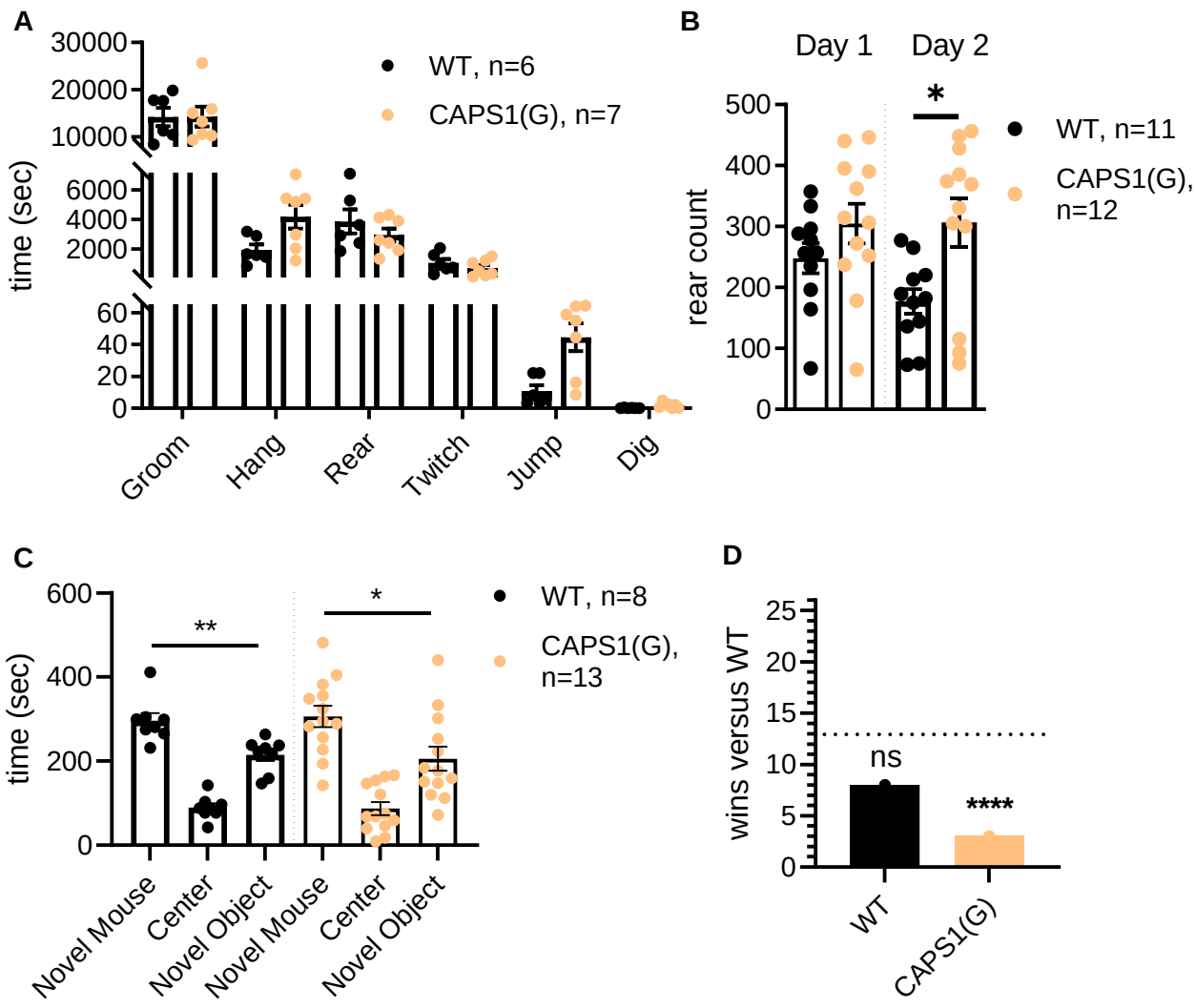

Figure 22. Evaluation of repetitive and social behaviors in CAPS1(G) animals. (**A**) Quantification of time spent engaged in various behaviors over 24 hours in the home cage for male animals; Multiple Mann-Whitney tests with post-hoc correction, p>0.05 for all. (**B**) Rearing frequency over 30 minutes in an open field test for male and female animals across two days; 2-way RM ANOVA, genotype effect F (1,21) = 5.092, p=0.0348, Sidak's multiple comparison test, Day 1 p>0.05, Day 2 **p<0.01. (**C**) The amount of time spent in a novel mouse, empty (center), or novel object chamber during a 3-chamber test for male mice; Mann-Whitney test mouse v. object, **p<0.01 WT, *p<0.05 CAPS1(G). (**D**) The number of wins experienced in a tube test when facing an unknown WT mouse for male animals; n=13 mice/genotype, 2 trials/mice, two-tailed binomial test, p>0.05 WT, ****p<0.0001 CAPS1(G).

Dopamine-associated animal behaviors: Reward and positive reinforcement behaviors

Dopamine signaling in the NAcc is associated with reward-driven behavior, and a standard rodent assay used to assess reward is the conditioned place preference assay. As CAPS1(G) animals have increased dopamine release in the NAcc during sub-maximal stimulation, we sought to test whether this change in release was physiologically relevant. To address this question, animals are trained to associate one side of a chamber with a rewarding stimulus, cocaine, and to associate the other side with saline by giving daily injections of either substance and restricting the animal's movements to the respective chamber side. The time animals spend in the cocaine paired chamber is measured before and after conditioning. As expected, both CAPS1(G) and WT animals spent more time in the cocaine-paired chamber on the post-test day than on the pre-test day (Figure 23A). When the difference in time spent on the cocaine-paired chamber was compared across genotypes, no effect was noted, indicating that CAPS1(G) animals respond to 10 mg/kg cocaine similarly to WT animals (Figure 23B).

Other types of behaviors frequently associated with dopamine signaling in the NAcc are motivated behaviors. To investigate the effect of *Cadps* editing on motivated behaviors, a sucrose-mediated positive reinforcement assay was performed. Briefly, animals underwent slight calorie restriction and were taught to level press to receive a sucrose reward. Animals were tested over several sessions and the number of sucrose reinforcers earned was analyzed. Using this method, CAPS1(G) animals were no different from WT littermate animals in the number of reinforcers earned (Figure 23C). This indicates that CAPS1(G) animals exhibit normal sucrose-motivated behavior.

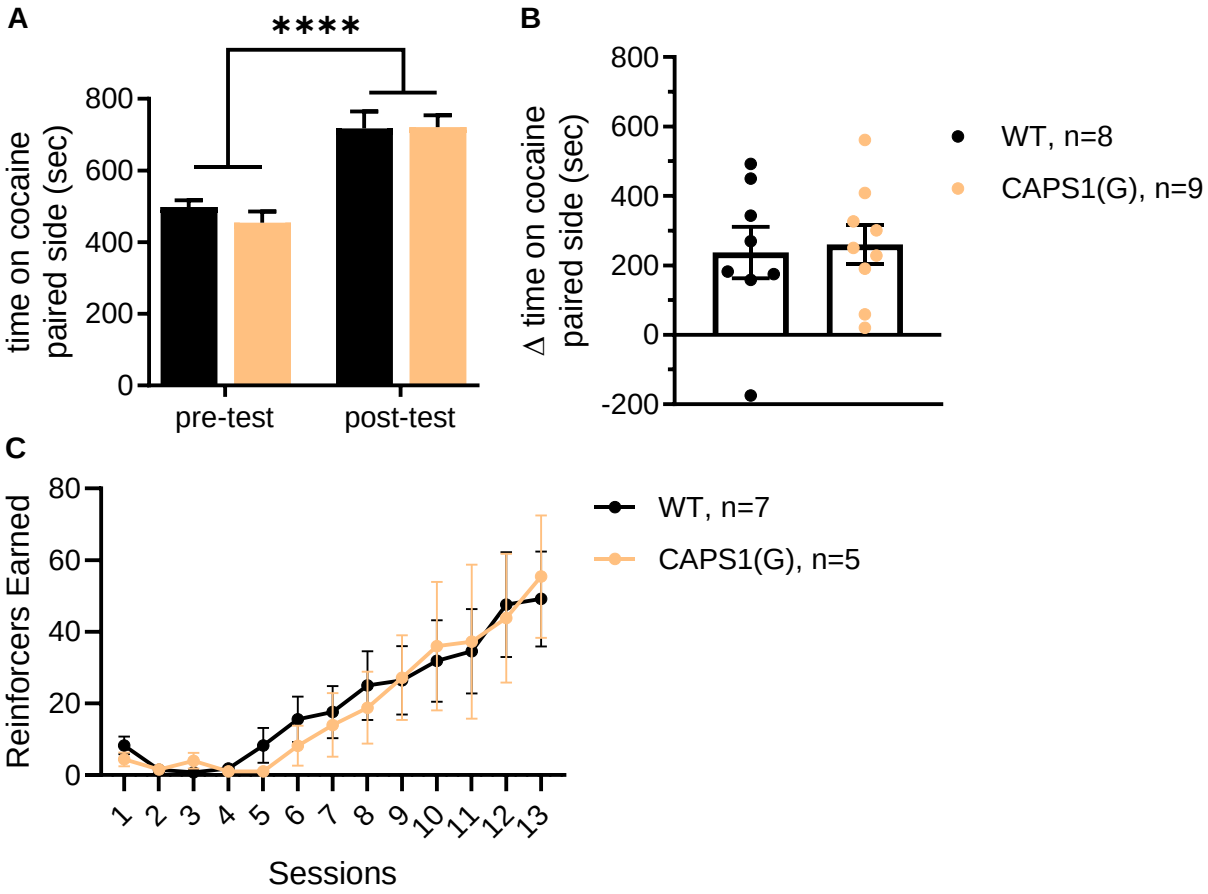

Figure 23. Evaluation of reward and motivated behaviors in CAPS1(G) animals. (**A**) Analysis of cocaine induced conditioned place preference, time spent on the cocaine paired side was measured before and after conditioning; Two-way ANOVA, conditioning effect F (1, 15) = 29.86, ****p<0.0001, genotype effect F (1,15) = 0.039, p>0.05. (**B**) Quantification of the change in time spent on the cocaine paired side from pre to post-test; Mann-Whitney, p>0.05. (**C**) Sucrose-mediated positive reinforcement task; Two-way ANOVA, genotype effect F (1, 120) = 1.208, p>0.05.

Discussion

In this chapter, I have investigated the role of *Cadps* editing in regulating release of the neuromodulatory transmitter, dopamine. Building upon the preliminary findings by Miyake and colleagues that *Cadps* editing enhances dopamine release in striatal synaptosomes and leads to hyperactivity in CAPS1(G) mice, we were able to further characterize this effect and independently reproduce select datasets (Miyake et al., 2016). Our studies provide key insights into CAPS1 expression in dopamine neurons, *Cadps* editing-dependent regulation of dopamine release in sub-regions of the striatum, and the physiologic outcomes associated with altered dopamine release.

In our first set of studies, we sought to characterize *Cadps* editing levels and CAPS1 expression in dopamine centers in the brain. We found ~10% of *Cadps* transcripts are edited in the SN and ~20% are edited in the VTA. It should be noted that these values reflect the average tissue level of *Cadps* editing and are not specific to dopamine neurons alone. Future studies using single cell RNA sequencing technology may provide a more granular view of the distribution of editing frequency among various cell types contained within a tissue punch. Tissue-level *Cadps* editing percentage analysis does support the selection of CAPS1(G) animals as a preferred model system to study the effect of *Cadps* editing on dopamine release, as these mice should reflect an ~80-90% change in the level of *Cadps* editing when compared to wild-type littermates. In our next set of studies, we also found CAPS1 protein expression in tissue punches of SN that did not vary based on genotype, indicating that changes identified in CAPS1(G) animals are independent of altered CAPS1 expression.

When investigating CAPS1 expression in dopamine neurons using immunohistochemistry, we identified CAPS1 expression in TH-positive neurons in both the VTA and SN, which contradicts a previous report (Sadakata et al., 2006). Future studies using RNAscope to verify *Cadps* expression in *Th*-positive neurons will be helpful to validate our IHC study. Given that enhanced synaptic localization of CAPS1(G) was reported in glutamatergic and

GABAergic synapses (Chapter 2), we were interested in assessing CAPS1 localization in dopamine terminals of the striatum. However, technical limitations related to antibody avidity and the lack of CAPS1-null animals prevented us from generating reliable data. Future assessment of CAPS1(E) and CAPS1(G) synaptic localization in dopamine neurons will be important to understand whether the mechanism(s) underlying enhanced exocytosis are the same in fast and neuromodulatory transmission. Thus, our studies in this chapter rely on the assumption that CAPS1 expression in cell bodies is indicative of CAPS1 expression and function in dopamine terminals. In summary, we detected low levels of *Cadps* editing in the SN and VTA and found expression of CAPS1 in dopamine neurons in both brain regions.

In the next set of experiments, we investigated the role of *Cadps* editing in regulating dopamine release from the dorsal and ventral striatum using FSCV. These studies indicate that CAPS1(G) enhances dopamine release and increases DAT expression or function in the dorsal striatum. The effect of CAPS1(G) on dopamine release is consistent with previous reports using an alternative analysis method to evaluate dopamine release and is consistent with reports of enhanced transmitter release from other cell types as well, including adrenal chromaffin cells (Miyake et al., 2016). A limitation of this study is that we cannot conclude that *Cadps* editing directly augments dopamine release, given the possibility of a cholinergic effect. The limited temporal resolution of the FSCV assay leaves open the possibility that the effect is not directly due to enhanced release of dopamine but could be attributed to indirect effects of other neurotransmitter systems acting on dopaminergic terminals. For example, it is well established that release of acetylcholine in the striatum triggers dopamine release through activation of pre-synaptic nicotinic receptors on dopamine terminals (Threlfell et al., 2012; Zhang & Sulzer, 2004; F. M. Zhou, Liang, & Dani, 2001). In a mouse model with cholinergic channel-rhodopsin expression, the timeframe for dopamine release in the putamen, as measured using FSCV, is practically identical regardless of whether release is triggered by electrical stimulation or by laser-dependent activation of cholinergic terminals (Threlfell et al., 2012). Thus, it remains possible that

increased dopamine release is triggered through an indirect mechanism, such as enhanced release of acetylcholine, and is not the sole result of edited CAPS1 acting in dopaminergic terminals. Future studies utilizing NAchR antagonists while measuring electrically stimulated dopamine release from the dorsal striatum in CAPS1(G) and WT animals could be performed to address this limitation. In summary, CAPS1(G) robustly enhances dopamine release in intact tissue in the dorsal striatum.

The finding that CAPS1(G) animals have increased V_{max} indicates that an increase of DAT surface expression or function is likely. While it is possible this effect is due to increased DAT surface expression, our data using cocaine to elicit a behavioral effect suggests this is not the case. We found that CAPS1(G) animals are hypersensitive to a low dose of cocaine (a DAT blocker), which suggests that DAT surface expression is not increased, as this would be expected to cause CAPS1(G) animals to require a higher dose of cocaine than WT to elicit a behavioral effect. A more likely possibility is that increased signaling through D2 autoreceptors increases DAT function in CAPS1(G) animals, as it has been shown that signaling through this population of D2Rs positively modulates DAT activity (Anzalone et al., 2012; Dickinson et al., 1999; Gowrishankar et al., 2018). Therefore, I predict that CAPS1(G) animals have increased DAT function. It is well established that DAT activity is regulated through phosphorylation, including ERK-dependent phosphorylation at DAT T53, which increases DAT surface expression and transport capacity (Bolan et al., 2007; Foster et al., 2012; Ramamoorthy, Shippenberg, & Jayanthi, 2011). Future studies analyzing DAT expression and phospho-DAT levels in membrane preparations from the dorsal striatum of CAPS1(G) animals could be used address these hypotheses.

After analyzing dopamine release in the dorsal striatum, probes were moved to the ventral striatum to assess release in the NAcc core. While these regions are innervated by different neurons, our CAPS1 expression data would suggest that similar effects would be found in both regions of the striatum. However, no effects of *Cadps* editing on baseline evoked release or re-

uptake were identified in the NAcc. A more thorough investigation of release in the NAcc core identified alterations in dopamine release at sub-maximal stimulation intensities, indicating enhanced excitability of dopamine terminals in the NAcc core of CAPS1(G) animals. It is possible that CAPS1(G) increases the initial release probability in the NAcc such that terminals not normally responsive to mild stimulation are triggered to release in CAPS1(G) animals. Indeed, we noted an increase in the release probability in GABAergic terminals in CAPS1(G) neurons in Chapter II by measurement of paired-pulse ratios, though no change in the paired-pulse ratio was noted in FSCV NAcc recordings. A second possibility is that enhanced excitability is due to a change in Ca^{2+} sensitivity, perhaps through alterations to Ca^{2+} channels or Ca^{2+} sensors. Interestingly, CAPS1 directly interacts with the calcium-sensing protein NCS-1 (Haynes et al., 2006), and NCS-1 knockout decreases release probability in NAcc DA terminals (Ng et al., 2016). While the functional effect of a CAPS1-NCS-1 interaction is unknown, it is intriguing to consider enhanced interactions between edited CAPS1 and NCS-1 could play a role in increased release probability and/or calcium-sensing in the NAcc. While the underlying mechanisms presented are speculative, it is clear that *Cadps* editing has a very modest impact on NAcc dopamine release.

Prior studies of regional differences in the regulation of dopamine release and CAPS1 dopamine receptor interactions offer additional insight to develop hypotheses explaining the region-specific effect of *Cadps* editing on striatal dopamine release. The family of D2R-like receptors have differential expression patterns across the striatum, with D2Rs expressed broadly throughout the tissue while D3Rs are only expressed in the NAcc (Le Moine & Bloch, 1996; Levesque et al., 1992). CAPS1 interacts with D2Rs, but not D3Rs, and this interaction was shown to selectively enhance release of dopamine, but not norepinephrine or BDNF, from PC12 cells (Binda, Kabbani, & Levenson, 2005). Given this data, one hypothesis to explain the region-specific effects of *Cadps* editing on striatal dopamine release is that in the dorsal striatum, D2R autoreceptor signaling is influenced by CAPS1, while in the ventral striatum D3R autoreceptor signaling is independent of CAPS1. In this way, CAPS1(G) can act in multiple capacities in the

dorsal striatum, potentially through enhanced vesicle priming and enhanced signaling through D2Rs, to increase dopamine release. The underlying mechanism(s) dictating the region-specific effects of *Cadps* editing remain to be elucidated, however our data clearly demonstrates a more significant effect in the dorsal than ventral striatum on enhancing dopamine release and re-uptake.

In the next set of experiments, the effect of *Cadps* editing on dopamine-associated animal behaviors was investigated using CAPS1(G) and CAPS1(G) WT animals as a model system. In agreement with previous reports, we found significant increases in locomotor activity in CAPS1(G) mice (Miyake et al., 2016). Furthermore, locomotor activity was bidirectionally modulated by pharmacologic manipulation of dopamine signaling, and CAPS1(G) animals were sensitive to lower doses of the drugs than WT animals, indicating that enhanced dopamine signaling underlies hyperactivity in CAPS1(G) animals. As other genetic mouse models of altered dopamine signaling experience motor coordination deficits, we analyzed these behaviors using a collection of assays and found no conclusive impairment in CAPS1(G) animals. In fact, a trend towards enhanced performance on the accelerating rotarod assay was found, which is a phenotype noted in another model of enhanced dopamine release, DAT T356M knock-in mice (DiCarlo et al., 2019). Performance on the rotarod assay has been used as a measure of motor learning (Shiotsuki et al., 2010), and is shown to be dependent on nigrostriatal dopamine signaling (Ogura et al., 2005; Shiotsuki et al., 2010). In this regard, our data suggest CAPS1(G) animals may have an enhanced motor learning phenotype, yet further behavioral characterization with additional assays will be necessary to confirm this finding.

Next, we characterized autism-associated behaviors as they have been strongly linked to aberrant dopaminergic signaling in the dorsal striatum (DiCarlo et al., 2019; Fuccillo, 2016; Lee et al., 2018). We were also particularly interested in these behaviors as *Cadps* editing levels are decreased in the brains of FMR1 knockout mice (Filippini et al., 2017), a model of the most common type of autism, Fragile X syndrome. Patients with Fragile X syndrome have also been

found to have altered *Cadps* editing patterns (Tran et al., 2019). Our pilot studies revealed no changes in home cage repetitive behaviors in CAPS1(G) animals, though a more thorough investigation may be warranted given the trend towards increased hanging and jumping. Increased rearing in CAPS1(G) was seen in the open field test, but only during day two of the assay, suggesting a mild phenotype. CAPS1(G) animals displayed normal sociability, with a preference for interacting with novel mice over novel objects but displayed a significant reduction in social dominance behavior. These results suggest CAPS1(G) animals may have impairment in specific types of social interactions, and further testing of reciprocal social interactions may provide additional insight into these phenotypes. Overall, CAPS1(G) mice appear to display some behaviors, including increased rearing and impaired social dominance, that are representative of autistic-like behaviors. Further testing using a full panel of autism-associated behavioral assays (Crawley, 2007), including vocalization and reversal learning, could be employed to delineate the precise phenotypes expressed by CAPS1(G) animals. Additionally, it would be interesting to further investigate the association between *Cadps* editing and FMR1 function.

In a final set of behavioral assays, we characterized rewarding and motivated behaviors as these are commonly associated with altered dopamine signaling in the ventral striatum. No changes in CAPS1(G) animal behavior were found in either a cocaine-induced CPP assay or sucrose-mediated positive reinforcement task. These results are consistent with the subtle effect of *Cadps* editing on dopamine release in the NAcc and suggest that CAPS1(G) animals have no changes in behaviors associated with ventral striatum dopamine signaling.

In conclusion, *Cadps* editing increases tonic dopamine release and re-uptake in the dorsal striatum and increases terminal excitability in the NAcc core in a manner that is independent of dopamine synthesis and metabolism and dopamine axon density. Further experiments will be required to understand the region specificity of these effects. Additionally, CAPS1(G) animals display behavioral phenotypes, such as hyperactivity, that are associated with increased dorsal striatal dopamine signaling and have no changes in behavioral outcomes mediated by ventral

striatal dopamine signaling. Collectively these data suggest *Cadps* editing has a more profound effect on dopamine signaling in the dorsal striatum. Furthermore, our data implicates CAPS1 as a modulator of dopamine release, adding to the list of active zone proteins that act in both fast and neuromodulatory transmission. In the future it will be interesting to see if CAPS1 functions in the same capacity in both types of synapses, or differentially, as has been described for other active zone proteins like RIMS and ELKS.

CHAPTER 4

Functional Effects of *Cadps* Editing on Hormone Release

Introduction

The work described in this chapter stems from the central hypothesis that *Cadps* editing globally enhances release of neurotransmitters and peptide hormones. As such, mice solely expressing fully edited or non-edited CAPS1 may have altered physiologic outcomes due to dysregulated hormone release. In 2016, Miyake and colleagues described the effect of *Cadps* editing on release of neurotransmitters from various model systems, including release of norepinephrine from PC12 cells and primary adrenal chromaffin cells. As these model systems included endocrine cells of the adrenal gland, we hypothesized that *Cadps* RNA editing would affect exocytosis in any cells which CAPS1 was expressed. Therefore, three endocrine systems were selected to study the effect of *Cadps* editing on hormone release and to evaluate the physiologic outcome(s) associated with altered hormone release.

The first system selected was the neural and peripheral circuitry involved in energy homeostasis, including regulation of feeding and energy expenditure. This system was selected for evaluation based on the findings by Miyake and colleagues that CAPS1(G) animals are hyperactive and have increased energy expenditure (Miyake et al., 2016). Rodent energy homeostasis is a complex subject that involves the coordination of both peripherally and centrally released hormones and neuropeptides. Pro-opiomelanocortin/ cocaine and amphetamine regulated transcript (POMC/CART) and neuropeptide Y/ agouti-related peptide (NPY/AgRP) neurons located in the arcuate nucleus of the hypothalamus and POMC/CART neurons in the nucleus tractus solitarius of the brainstem are the primary neurons that integrate signals from these hormones and neuropeptides to control energy homeostasis (Cone, 2005). Broadly

speaking, NPY/AgRP neurons signal to increase food intake and decrease energy expenditure, while POMC neurons act in an opposing manner. Various peripherally released peptide hormones, including leptin, ghrelin, cholecystokinin (CCK), peptide YY (PP Y) 3-36, glucagon-like peptide (GLP) 1, oxyntomodulin (OXM), pancreatic polypeptide (PP), and insulin exert their actions on NPY/AgRP and POMC/CART neurons in both excitatory and inhibitory fashions. Central regulation of the arcuate neurons includes NPY/AgRP neuron signaling to POMC/CART neurons in the hypothalamus through release of GABA, NPY, and AgRP, and α-adrenergic and serotonergic inputs to POMC/CART neurons (Cone, 2005). Decades of studies have explored the role that each of these peripherally released hormones and centrally released neuropeptides and neurotransmitters play in regulating energy homeostasis. I hypothesize that dysregulation of release of these factors in mouse models of *Cadps* editing leads to the altered energy homeostasis noted in CAPS1(G) animals.

To understand the role of CAPS1 in this system, it is important to highlight what is known about CAPS1 expression. In the central nervous system, CAPS1 is highly expressed in the arcuate nucleus of the hypothalamus in E16 mice (Sadakata et al., 2006), but expression in the brainstem is uncharacterized. In the periphery, CAPS1 is expressed deep in the gastric glands in non-chief cells of the stomach while expression was barely detected in the jejunum, ileum, and ascending colon (Sadakata, Washida, Morita, & Furuichi, 2007). While the specifics of CAPS1 expression in specialized enteroendocrine and hypothalamic CNS neurons remains unknown, there is evidence to suggest that CAPS1 is expressed in at least a portion of these cells, therefore *Cadps* editing could impact energy homeostasis. Very recently, a role for CAPS2, a CAPS1 paralog, in modulating release of POMC-derived peptides from the intermediate pituitary was described, lending further credence to the hypothesis that CAPS1 may modulate release of hormones or neuropeptides that regulate energy homeostasis (Fujima, Amemiya, Arima, Sano, & Furuichi, 2020). This hypothesis has not been explored, likely due in part to the perinatal lethality caused by global CAPS1 knockout. Therefore, we sought to use CAPS1(E) and CAPS1(G)

mouse models to investigate the possible role of *Cadps* editing in modulating energy homeostasis.

The next system selected for study was pancreatic islet-mediated glucose homeostasis. The islets of Langerhans, consisting of both alpha and beta cells, are collections of specialized endocrine cells in the pancreas that function to modulate blood glucose levels. CAPS1 RNA and protein expression is detected in the pancreas (Sadakata, Washida, Morita, et al., 2007), and immunohistochemical analysis identified CAPS1 expression in both insulin producing β-cells and glucagon secreting α-cells (Speidel et al., 2008; Wassenberg & Martin, 2002), with staining absent in acinar cells that surround islets. CAPS2 is also expressed in both cell types. β cells sense and respond to elevated extracellular glucose via intracellular signaling mechanisms that culminate in release of insulin granules through regulated exocytosis. There is a well-established role of CAPS1 in regulating insulin release from β-cells. Using pancreatic islets isolated from heterozygous CAPS1-null mice on a CAPS2-null background (CAPS1 +/-, CAPS2 -/-), Speidel and colleagues found a decrease in glucose stimulated insulin release and no changes in basal or high potassium evoked insulin release in mutant islets compared to WT or CAPS2 -/- islets. The changes in release were concurrent with decreased islet insulin content yet without changes in proinsulin content. Electron micrographs from islets of CAPS1 +/-, CAPS2 -/- mice showed a significant decrease in the number of docked insulin granules (0-0.2 µm of the plasma membrane) and a significant decrease in granule density compared to CAPS2 -/- islets (Speidel et al., 2008). Decreased insulin content and granule density was attributed to an increase in lysosomal degradation, as the cellular density of lysosomes and activity of the lysosomal proteinase cathepsin D was greater in CAPS1 +/-, CAPS2 -/- islets than in CAPS2 -/- or WT islets. Assessment of *in vivo* glucose tolerance and insulin secretion found slight alterations in glucose and insulin levels at time points corresponding to phase two of insulin release in CAPS1 -/+, CAPS2 -/- mice when compared to CAPS2-/- mice and no changes in fasted blood glucose levels (Speidel et al., 2008). Collectively these studies support a role for CAPS1 in maintaining insulin

granule stability and in regulating the degree of glucose stimulated release of insulin granules. In separate study, ADAR2 knockdown in primary beta cells and INS-1 cells, a rat insulinoma cell line, found decreased glucose-stimulated and high potassium-evoked insulin release. There was also a decrease in the number of membrane proximal granules in the INS-1 ADAR2 knockdown cells (L. Yang et al., 2010). These results suggest that regulation of RNA editing impacts GSIS, though the specific RNA targets that mediate this effect have not been determined. As CAPS1 is known to be a target of ADAR2, I hypothesize that *Cadps* editing will enhance glucose-stimulated insulin release and could improve glucose clearance in CAPS1(G) animals.

The hypothalamic-pituitary axes were the final system in which we sought to investigate the role of CAPS1 editing in hormone release. Neurons in the hypothalamus release hormones into the hypophyseal duct system where they are sensed by endocrine cells in the anterior pituitary gland to stimulate or inhibit production and release of systemic hormones. For example, thyrotropin releasing hormone (TRH) neurons, originating in the paraventricular nucleus, send projections to the median eminence where they release TRH. Thyrotropes, specialized endocrine cells in the anterior pituitary, contain TRH receptors that signal to increase expression and release of thyroid stimulating hormone (TSH) into the systemic circulation. Other axes with similar circuitry include corticotropin releasing hormone (CRH) neurons which signal from the PVN to corticotropes in the anterior pituitary to release adrenocorticotropin hormone (ACTH), and growth hormone releasing hormone (GHRH) neurons projecting from the arcuate nucleus to signal to pituitary somatotrophs to release growth hormone (GH). The last studied axis is the prolactin axis, in which dopamine neurons from the arcuate nucleus inhibit expression and release of prolactin from lactotrophs of the anterior pituitary while PVN neuron-derived TRH stimulates release of prolactin. The systemic hormones released from the anterior pituitary signal in their target organs to produce downstream effects, generally including release of additional hormones including T3/T4 from the thyroid, glucocorticoids from the adrenal gland, and insulin-like growth factor 1

(IGF-1) from the liver. The hypothalamic-anterior pituitary signaling axes have broad physiologic effects, making them an ideal system to study the effect of *Cadps* editing on hormone release.

CAPS1 is expressed in the hypothalamus, with high levels of protein expression noted in the arcuate nucleus (Sadakata et al., 2006), and also is expressed in the pituitary gland though there are conflicting reports of the level of expression in the anterior pituitary based on immunohistochemical analysis with different antibodies (Wassenberg & Martin, 2002) (Sadakata et al., 2006). CAPS1 function in hypothalamic and anterior pituitary hormone release has not been studied. However, regulation of fast release of LDCVs from isolated melanotrophs is CAPS-dependent and a portion of LDCVs in the melanotrophs were found to co-localize with CAPS (Rupnik et al., 2000), though it should be noted that at the time of this publication it was not appreciated that two CAPS family members exist. Therefore, while it is not possible to determine if the effect of CAPS in melanotrophs is mediated by CAPS1, CAPS2, or both, it is clear that the CAPS-family of proteins regulate release of DCVs from cells that are functionally similar to somatropes, lactotropes, and corticotropes of the anterior pituitary. As such, we sought to investigate the role of *Cadps* editing in the release and regulation of key hypothalamic-pituitary-target organ axes.

While decades of studies have been dedicated to understanding the precise mechanisms governing neurotransmission, far fewer have investigated regulated exocytosis in endocrine cells including the anterior pituitary cells, pancreatic beta cells, and enteroendocrine cells that will be the focus of this chapter. Many of the same properties of regulated exocytosis apply to endocrine cells, including a Ca^{2+}-driven process that requires SNARE proteins (Gaisano, 2017; Thorn, Zorec, Rettig, & Keating, 2016). However, there are several differences in exocytosis to note. First, studies using capacitance recordings to measure exocytosis events triggered by flash photolysis-induced release of caged calcium have demonstrated that exocytosis occurs more slowly (at least 10 fold) in endocrine cells, including melanotrophs and beta cells, than in neurons (Barg et al., 2001; Kreft, Krizaj, Grilc, & Zorec, 2003; Kreft, Kuster, et al., 2003; Rupnik et al.,

2000; Thomas, Wong, Lee, & Almers, 1993). Thus, differences in calcium triggered membrane fusion machinery or in the kinetics of delivery of vesicles to sites of release, processes that may be impacted by CAPS1, may exist in endocrine cells (Thorn et al., 2016). Another distinct property of endocrine cell exocytosis is enhanced calcium sensitivity, such that lower levels of calcium influx mediate release compared to the change in calcium concentration required to trigger release in neurons (Kreft, Kuster, et al., 2003). Beyond these two principles that apply to endocrine cells at large, cell-type specific principles of exocytosis in beta cells also have been identified. Beta cell-mediated insulin release is different from neuronal exocytosis in that it occurs in two phases, with the first phase of release mediated by pre-docked, readily releasable granules and the second phase release mediated by “newcomer” or reserve pool granules. V-SNARE composition appears to determine if a granule is pre-docked or part of the reserve pool and SNAREs and accessory proteins that mediate insulin granule release differ between the two phases (Gaisano, 2017). This is in line with a report that CAPS1 functions primarily in phase two of GSIS (Speidel et al., 2008). In summary, compared to fast and neuromodulatory transmission, much less is known about the regulation of hormone exocytosis. While general principles of regulated exocytosis apply, the molecular mechanisms governing hormone release remain to be elucidated, particularly in enteroendocrine and pituitary cells. The work in this chapter may help identify whether CAPS1 plays a significant role in the regulation of release of hormones from the endocrine systems studied.

Materials and Methods

Body Composition and Indirect Calorimetry Analysis

Singly housed, 14-week-old male mice, maintained on standard chow were transferred to the Mouse Metabolic Phenotyping Core for all procedures, and allowed to acclimate to the new housing room for at least one week prior to study initiation. Body composition was analyzed by NMR analysis (Bruker Minispec) before and after indirect calorimetry. Data is presented from

“before” analysis. For indirect calorimetry studies, individual animals were placed in metabolic cages containing a weighted food hopper, drink dispenser, running wheel, and normal bedding for at least 72 hours and up to 120 hours. A Promethion system (Sable Systems) was used to record gas exchange, locomotor activity, and food and water intake data, which was split into 12-hour light and dark cycles and averaged over at least 72 hours.

Pancreatic Beta Cell Isolation

In collaboration with the laboratory of Dr. Maureen Gannon, beta cells were isolated from 4–14-week-old male mIns1-H2B-mCherry mice, which are on a C57Bl/6N background. The mouse insulin promotor, ins, drives transcription of mCherry selectively in beta cells. Islets were isolated by the Vanderbilt Islet Procurement and Analysis Core and were dissociated before FACS sorting for mCherry positive cells. The cells were sorted into Trizol and stored at -20°C until use for RNA extraction.

Glucose Tolerance Test

Singly housed, 8–10-week-old male mice, were transferred to clean cages with Alpha Dri Plus bedding and fasted for 16 hours. Mice were weighed, anesthetized with isoflurane, and injected IP with 20% dextrose solution at 2 mg / gram body weight. Blood glucose measurements were taken directly before injection and 15, 30, 60, 90, and 120 minutes after glucose administration. Tail blood samples were immediately assayed using Accu-Chek Aviva blood glucose test strips in an Accu-Chek Aviva device (Roche).

Islet isolation, perfusion, and glucose stimulated insulin release assay

Male mice, 8-10 weeks old, were transferred to the Vanderbilt Islet Procurement and Analysis Core for all procedures. Briefly, mouse islets were isolated by collagenase digestion. Collagenase P in HBS was directly infused into the pancreas through the bile duct and groups of two pancreata were digested in 6.7 mL collagenase P for 6-8 min at 37°C using a wrist-action shaker. Islets were handpicked under microscopic guidance and cultured in RPMI-1640 media with 5mM glucose at 37°C. Fifty islet equivalents were loaded into a perifusion chamber and islets

were perfused with normal media (RPMI-1640 with 5 mM glucose) for 10 minutes. Perfusate flowed at 1 mL / minute and fractions of perfusate were collected every 3 minutes. Fractions were assayed for insulin content using a radioimmunoassay. Total insulin content was measured by radioimmunoassay.

Hormone Assays

Male and female mice, 12 weeks of age, were euthanized with isoflurane and blood was immediately drawn by cardiac puncture. Blood from each animal was split into two samples to be processed for serum and plasma samples. Plasma samples were generated by allowing blood to clot at room temperature for 1 hour followed by centrifugation at 1,500 x g for 15 minutes, and supernatant collection. Serum samples were generated by placing blood in EDTA containing tubes on ice for followed by centrifugation at 1,500 x g for 15 minutes, and supernatant collection. Serum and plasma samples were stored at -80°C. Plasma samples were submitted to the Hormone Assay and Analytical Services core for multiplex analysis of TSH, GH, and ACTH using a mouse pituitary Luminex panel (Millipore Sigma). Plasma samples were also assayed by the Hormone Assay and Analytical Services core for total T4 content using an in-house radioimmunoassay. Plasma samples from female mice were analyzed for IGF-1 content using a commercially available sandwich ELISA kit (RAB0229-1KT, Sigma-Aldrich). Serum samples from male mice were analyzed for prolactin content using a commercially available sandwich ELISA kit (Thermo Fisher, cat. EMPRL).

Quantification of RNA expression by qRT-PCR

Female mice, n=5-6/ genotype, were euthanized by isoflurane overdose and decapitated. The pituitary gland was rapidly dissected, and flash frozen in liquid N_2. RNA was extracted from the whole pituitary gland in 1 mL Trizol Reagent and samples were treated with Turbo DNase (Ambion) to eliminate genomic DNA contamination, as some Taqman probes used did not span exons. RNA was quantified and diluted to 2 µg/10 µL for cDNA synthesis using the High-Capacity cDNA Reverse Transcription Kit with random primers (ABI Technologies). qPCR reactions were

prepared with TaqMan Gene Expression Mastermix (ABI Technologies) and Taqman Probes (Mm00433590_g1 G*h,* Mm03990915_g1 *Tshb*, Mm00599949_m1 P*rl,* Mm00435874_m1 P*omc,* 4352341E mouse *actb*) (Thermo Scientific). Expression of a gene of interest and a housekeeping gene were assessed in every reaction for normalization of the data. Relative gene expression was calculated using the ΔΔCT method previously described (Livak & Schmittgen, 2001).

Results

Growth Curve and Body Composition Characterization of CAPS1(E) and CAPS1(G) mice

CAPS1(E) animals are viable with no gross anatomical abnormalities, and pups born from heterozygous breeding show no deviation from the expected Mendelian distribution (Table 2). Male homozygous CAPS1(E) mice are fertile, while female homozygous CAPS1(E) mice are fertile and have no apparent pup rearing deficiencies. Male and female mice have normal growth curves from week 3-12 after birth, and male mice have no difference in total body mass, fat mass, or lean mass compared to CAPS1(E) WT littermates when assessed at 14 weeks of age (Figure 24).

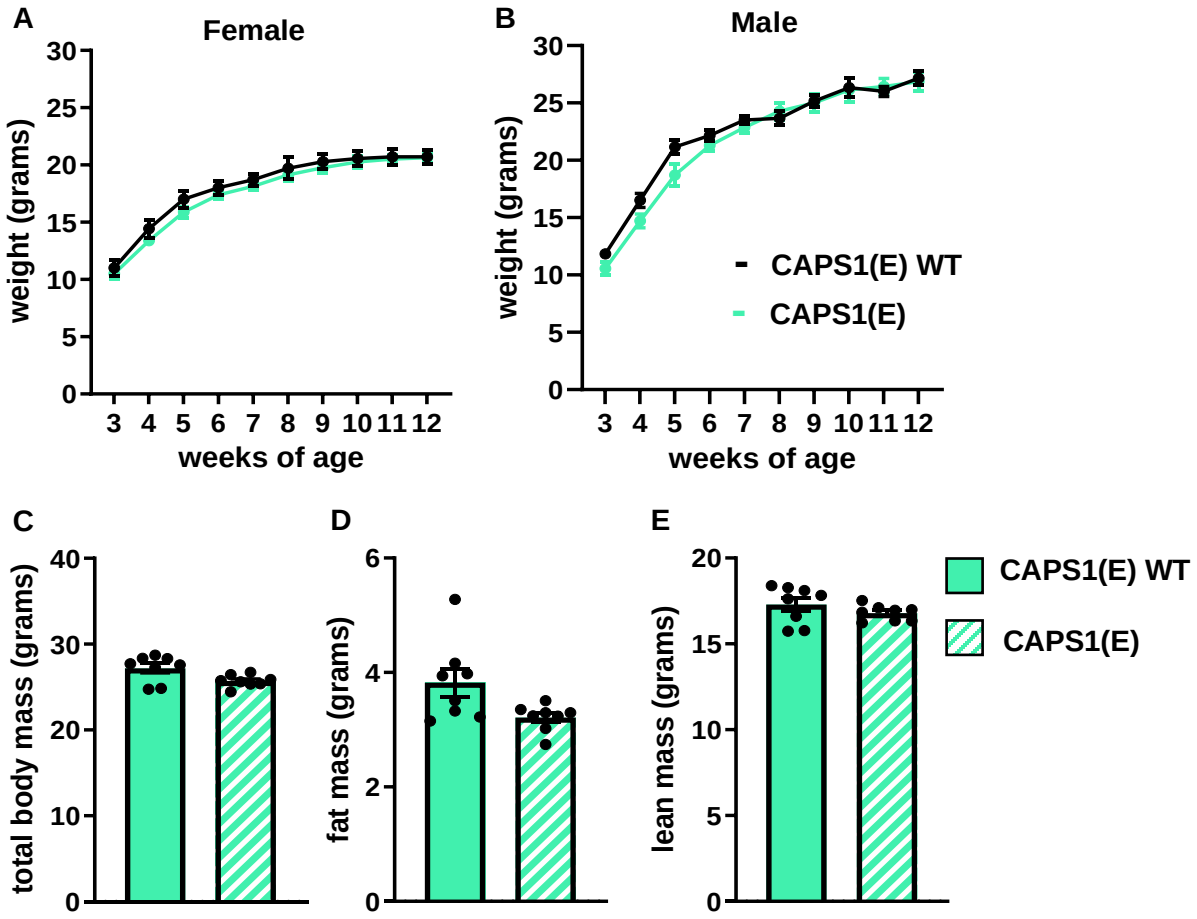

Figure 24. CAPS1(E) mice exhibit normal growth and body composition. (A, B) Growth curves for female (**A**) and male (**B**) CAPS1(E) WT and CAPS1(E) mutant mice from 3 to 12 weeks of age; n= 6-8 mice/genotype. (**C-E**) Body composition of 14-week-old male CAPS1(E) WT and CAPS1(E) mutant mice as measured by total body mass (**C**), fat mass (**D**), and lean mass (**E**) is presented; n=8 mice/genotype, mean ± SEM.

CAPS1(G) animals also exhibited no overt breeding phenotypes, and offspring of heterozygous matings conformed to the expected Mendelian distribution (Table 3). Male and female mice had normal growth curves from three to twelve weeks of age. Male mice did exhibit a trend towards lower body mass in the 8–12-week region of the growth curve, and when analyzed at 14 weeks of age were found to be underweight, with decreased fat and lean mass compared to CAPS1(G) WT littermate animals (Figure 25). This body composition data is in line with previous reports of a decreased body mass in male CAPS1(G) mice (Miyake et al., 2016), however we identified a decrease in lean mass that was not previously reported. Different methodologies used to analyze lean mass may explain the divergence in outcomes. Miyake and colleagues used mass measurements from dissected organs while we used NMR-based body composition analysis to generate a total lean mass measurement. Our data demonstrate male CAPS1(G) mice are overall smaller than their wildtype counterparts, as they have decreases in both fat and lean mass.

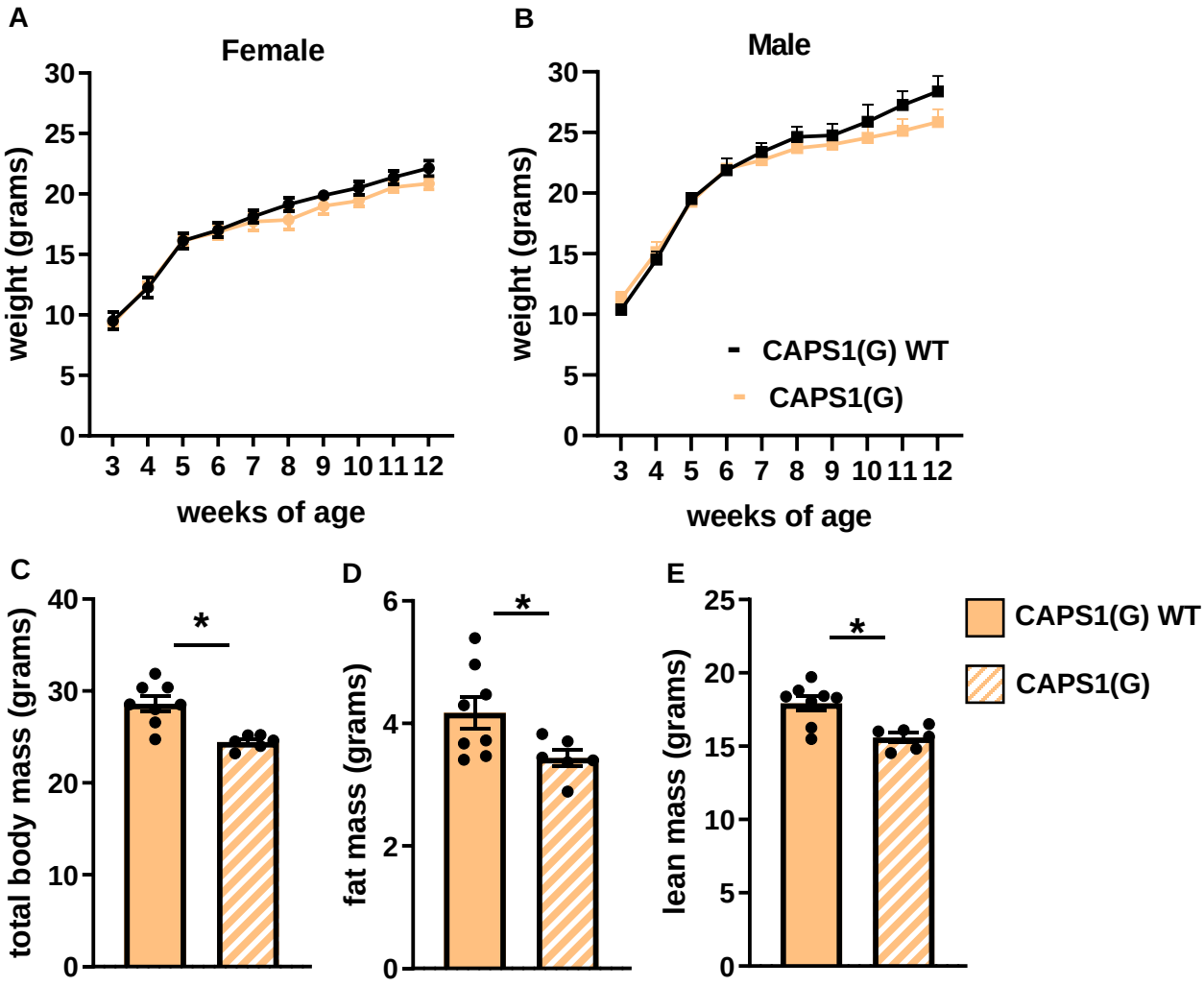

Figure 25. CAPS1(G) mice exhibit normal growth but altered body composition. (A, B) Growth curves for female (**A**) and male (**B**) CAPS1(G) WT and CAPS1(G) mutant mice from 3 to 12 weeks of age; n= 7-8 mice/genotype. (**C-E**) Body composition of 14-week-old male CAPS1(G) WT and CAPS1(G) mice as measured by total body mass (**C**), fat mass (D), and lean mass (**E**) is presented; n=6-8 mice/genotype, mean ± SEM (* p<0.05, Mann-Whitney test).

Non-Edited: CAPS1(E)/+ x CAPS1(E)/+

	Male	Female
genotype	Obs (Exp)	Obs (Exp)
Wildtype +/+	18 (27.5)	23 (27.5)
Heterozygous CAPS1(E)/ +	64 (55)	63 (55)
Homozygous CAPS1(E)/ CAPS1(E)	28 (27.5)	24 (27.5)
total	110	110
p-value	p=0.0924	p=0.3095

Table 2. Mendelian distribution of CAPS1(E) offspring, with Chi square analysis.

Edited: CAPS1(G)/+ x CAPS1(G)/+

	Male	Female
genotype	Obs (Exp)	Obs (Exp)
Wildtype +/+	55 (55.25)	75 (66)
Heterozygous CAPS1(G)/ +	117 (110.5)	122 (132)
Homozygous CAPS1(G)/ CAPS1(G)	49 (55.25)	67 (66)
total	221	264
p-value	p=0.5797	p=0.3679

Table 3. Mendelian distribution of CAPS1(G) offspring, with Chi square analysis.

Energy Homeostasis

As it has been previously reported that CAPS1(G) mice have increased energy expenditure (Miyake et al., 2016), we collaborated with the Mouse Metabolic Phenotyping Center at Vanderbilt to perform metabolic analysis of the CAPS1(E) and CAPS1(G) mouse lines. Fourteen-week-old male animals were monitored for 72-96 hours in metabolic cages equipped with indirect calorimetry monitoring software. The data reported here cover the twelve-hour dark phase only, as ~70% of mouse activity occurs during this time. However, similar data trends are seen in light phase analyses.

In agreement with previous reports, CAPS1(G) mice exhibit increased energy expenditure during the dark phase when regressed by body mass to account for the dependency of metabolic demand on fat mass (Figure 26A). CAPS1(G) mice have no changes in dark phase respiratory quotient, a ratio of oxygen consumption over carbon dioxide consumption (Figure 26B). This indicates there is no change in the type of macromolecule being metabolized (i.e., carbohydrates versus protein) compared to wild-type littermates. Simultaneous locomotor activity measurements were recorded and show that CAPS1(G) mice are hyperactive, in agreement with previous reports (Figure 26C, Chapter III and (Miyake et al., 2016)).

As CAPS1(G) mice have increased energy expenditure, we hypothesized CAPS1(E) mice would have decreased energy expenditure. However, analyses in metabolic cages revealed no changes in energy expenditure, or respiratory quotient in CAPS1(E) mice (Figure 26D, E). Simultaneous locomotor recordings also found no changes in CAPS1(E) mouse activity levels in the dark phase of the light cycle (Figure 26F). Given the profound hyperactivity noted in CAPS1(G) mice (~2 fold greater than WT littermates), we sought to further characterize CAPS1(E) mouse locomotor activity. Open field and home cage scan systems were used to monitor activity in a novel environment and in the home cage setting, respectively. In an open field assay, no change in locomotor activity was identified in CAPS1(E) mice when compared to CAPS1(E) WT littermate animals (Figure 27A, B). The data presented include both male and female animals, as no sex

specific effects were identified. Monitoring in the home cage, to control for novelty-induced phenotypes, also found no change in CAPS1(E) mouse locomotor activity (Figure 27C, D). Significant sex differences in locomotor activity were identified in this assay, and only male data is reported, though no genotype-specific effects were noted in female mice either.

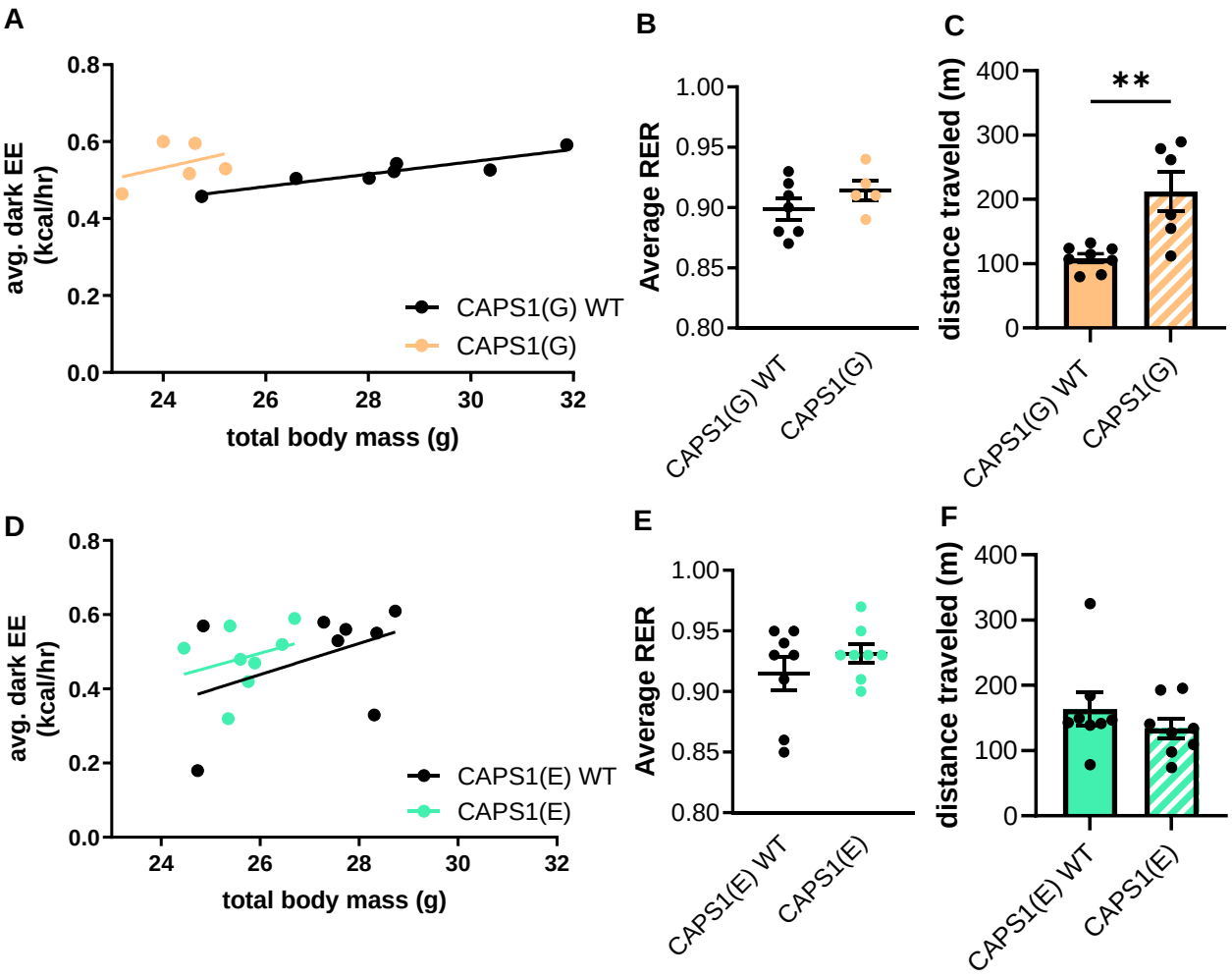

Figure 26. CAPS1(G) mice exhibit increased energy expenditure amidst increased locomotor activity. (A, D) Average energy expenditure plotted by total body mass with linear regression, (**B, E**) average respiratory quotient (RER), and (**C, F**) average pedestrian locomotion (speed >1 cm/second) during the dark phase for CAPS1(G) (**A-C**) and CAPS1(E) (**D-F**) 14-week-old male mice are shown; n=6-8 mice/genotype, mean ± SEM (** p<0.01, Mann-Whitney test).

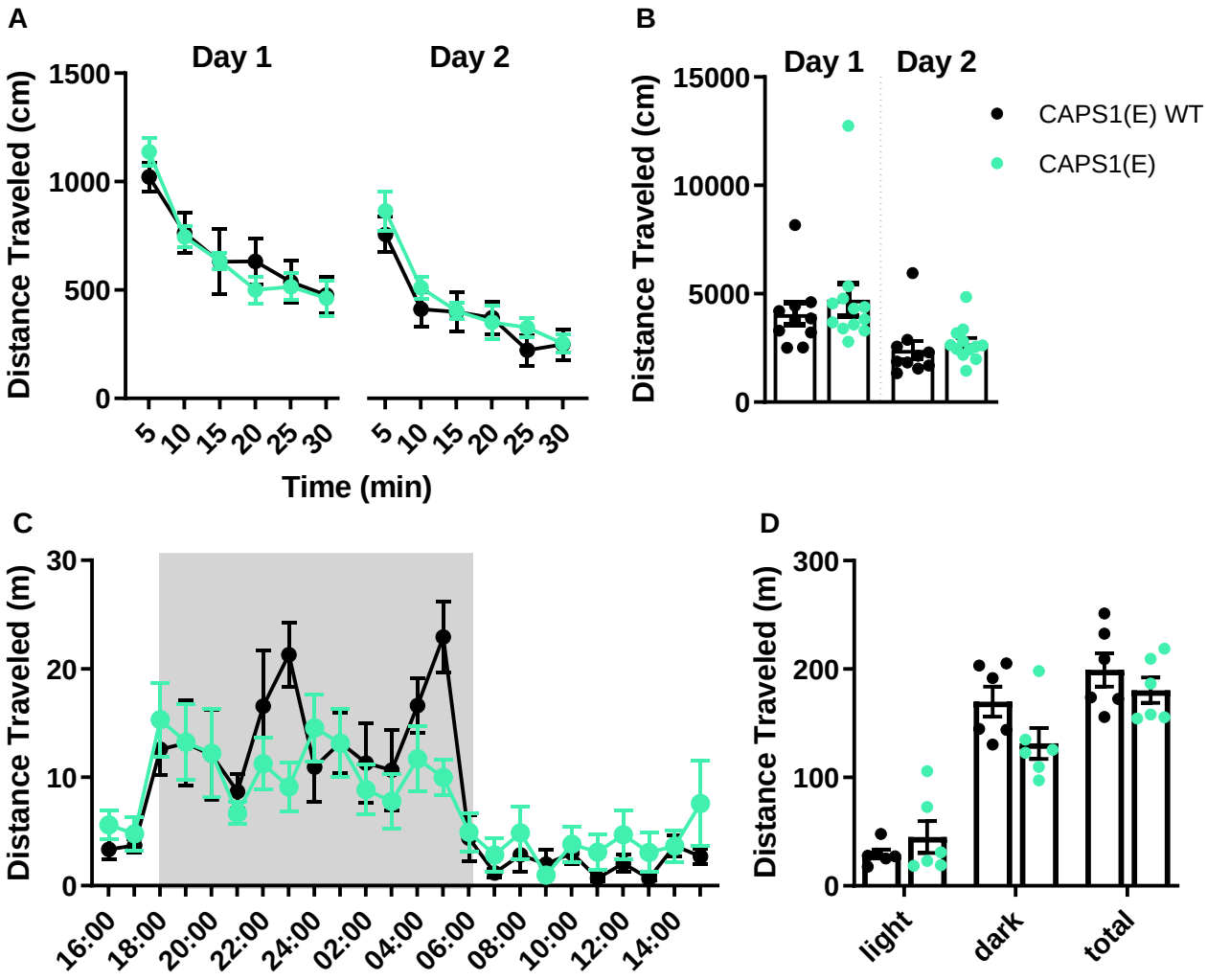

Figure 27. CAPS1(E) mice exhibit normal locomotor activity. (A) Distance traveled in an open field test for 30 minutes across two consecutive days and (**B**) total distance traveled each day are shown; n=10-11 mice/genotype, mixed sex. (**C**) Distance traveled in the home cage over 24 hours, with dark phase indicated by shaded area, and (**D**) total distance traveled for light, dark, and total phases are presented.; n=6 male mice/genotype, mean ± SEM.

Given that CAPS1(G) animals have increased locomotor activity and energy expenditure, we assessed food intake to determine whether the animals exhibit normal energy homeostasis. There were neither changes in food and water intake in CAPS1(G) mice during the dark phase (Figure 28A, B), nor changes in total 24-hour food and water intake (*data not shown*). Surprisingly, CAPS1(G) mice have altered meal patterning, consuming smaller meals more frequently, resulting in no net change in total calories consumed over a 12 or 24-hour period (Figure 28C-E). No changes in water intake patterning were identified (*data not shown*). The same assessment was performed in CAPS1(E) animals showing normal 12-hour total food and water intake, and meal and water intake patterns (Figure 28F-J). Together, this data demonstrates that CAPS1(G) animals have an energy imbalance, reflected by increased locomotor activity and energy expenditure without commensurate increases in food intake. The identified alterations in meal patterning may provide insight into the systems disrupted in CAPS1(G) mice that play a role in maintaining energy homeostasis. CAPS1(E) mice have normal energy homeostasis and are not impacted by changes in *Cadps* RNA editing.

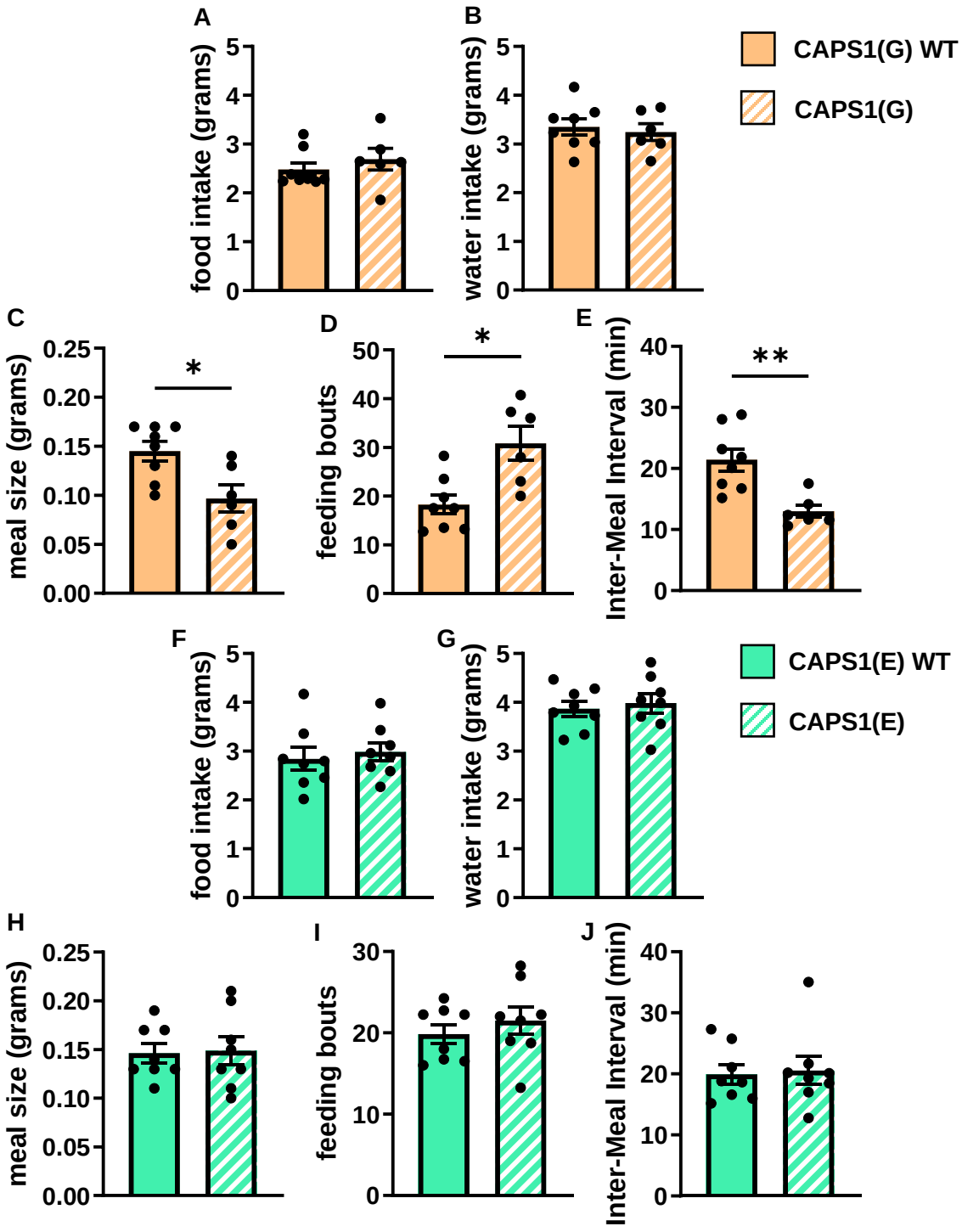

Figure 28. CAPS1(G) mice exhibit altered meal patterning. (**A, F**) Average total 12-hour food intake and (**B, G**) average total 12-hour water intake in CAPS1(E) (**A, B**) and CAPS1(G) (**F, G**) male mice are shown. Meal pattern analysis including (**C, H**) average meal size, (**D, I**) average number of meals and (**E, J**) average time between meals in CAPS1(G) (**C-E**) and CAPS1(E) (H-J) male mice are presented; n= 6-8 mice/genotype; mean ± SEM, (*p<0.05, **p<0.01, Mann-Whitney Test).

We have shown male CAPS1(G) mice have increased energy expenditure and decreased body mass when fed a normal chow diet. Both parameters suggest that CAPS1(G) mice could be impervious to high fat diet-induced weight gain. To test this hypothesis, female CAPS1(G) and wildtype littermate animals were placed on high fat diet (HFD) or a low fat, ingredient matched control diet for ten weeks. As expected, WT mice experience enhanced weight gain on HFD, with significant differences apparent after 3 weeks of food manipulation (Figure 29). CAPS1(G) mice also gain more weight on a HFD than control diet, with significant differences appearing after 4.5 weeks on diet (Figure 29). When comparing CAPS1(G) to WT mice on HFD, there were no significant differences in weight across the experiment. This data suggests that *Cadps* editing delays HFD-induced weight gain by 1.5 weeks in female mice but ultimately CAPS1(G) mice are as susceptible as WT mice to HFD-induced weight gain.

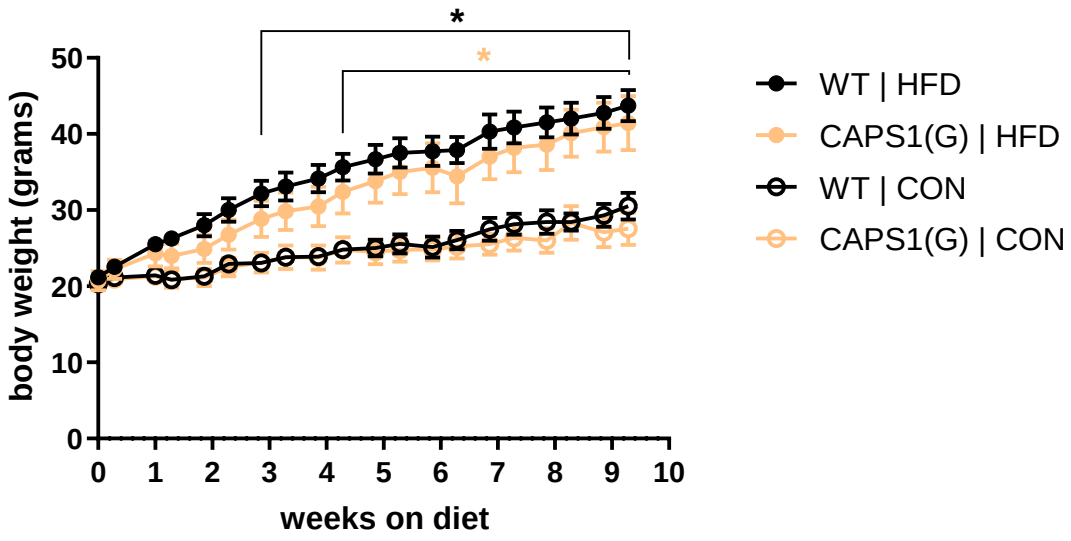

Figure 29. CAPS1(G) mice are susceptible to High Fat Diet-Induced weight gain. Growth curve of 8-week-old CAPS1(G) female mice and wildtype littermates fed HFD or control diet for 10 weeks are presented; n= 4-6 mice/genotype/diet; mean ± SEM, (* $p<0.05$ WT HFD vs. WT CON, * $p<0.05$ CAPS1(G) HFD vs. CAPS1(G) CON, Tukey's Multiple Comparison Test).

Glucose Homeostasis

As CAPS1 is expressed in pancreatic beta cells and the CAPS family proteins play a role in regulated exocytosis of insulin granules, we elected to study glucose homeostasis in CAPS1(E) and CAPS1(G) mice. CAPS1 expression was confirmed in isolated pancreatic islets and in sorted beta cells from WT mice by RT-PCR (*data not shown*). In wildtype pancreatic islets, 20.0± 0.6% (n=2 islet preparations) of CAPS1 transcripts were edited, while in beta cells 14.7± 1.8% (n=3 beta cell preparations) of CAPS1 transcripts were edited. Thus, altering the ratio of edited *Cadps* transcripts, using CAPS1(E) and CAPS1 (G) mice, could impact CAPS1 function in mediating glucose homeostasis.

To assess *in vivo* glucose tolerance, mice were subjected to a 16 hour fast and blood glucose levels were measured. There were no significant differences in fasted blood glucose between CAPS1(E) and CAPS1 (G) mice and wildtype littermates (Figure 30A, B). To monitor glucose clearance, a proxy measure of insulin release *in vivo,* an I.P. injection of glucose was administered, and blood glucose levels were monitored for 120 minutes. There were no differences in blood glucose values at any time point tested or in total area under the curve in either CAPS1(E) or CAPS1 (G) mice (Figure 30C, D). As noted previously, CAPS1 is thought to be most important for phase two of insulin release, which occurs at least 15 minutes after glucose bolus injection *in vivo*. While the data is not significant, we note a trend toward increased clearance of glucose during phase two insulin release in CAPS1(G) mice as shown by the increased slope of the glucose clearance curve compared to WT littermates.

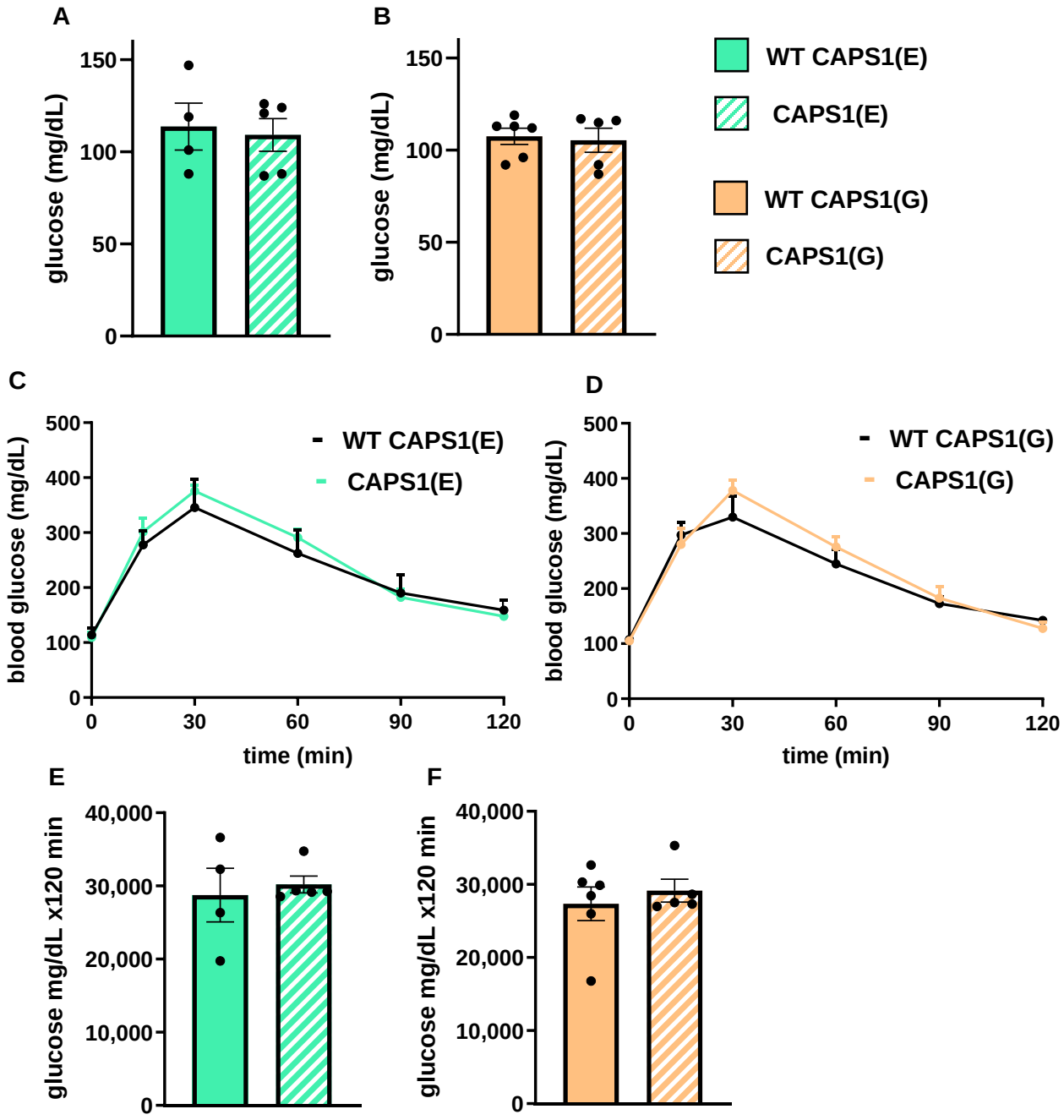

Figure 30. ***In vivo*** **glucose homeostasis is not altered in CAPS1(E) and CAPS1(G) mutant mice. (A, B**) Fasted blood glucose measurements and (**C, D**) Blood glucose measurements over time following i.e., injection of dextrose solution (2 mg/g body weight) are shown. (**E, F**) Area under the curve analysis of blood glucose measurements over time. n=4-6 mice/genotype, mean ± SEM.

To study insulin release directly, we moved to an *in vitro* system where isolated pancreatic islets were perfused with glucose and secreted insulin was measured. We collaborated with the Vanderbilt Islet Procurement and Analysis core to perform glucose stimulated insulin secretion (GSIS) assays on islets isolated from CAPS1(G) mice and WT littermates. Islets were perfused with 5.6 mM glucose to generate a baseline response for 9 minutes, and then 16.7 mM glucose was perfused for 30 minutes to evoke GSIS. Perfusion was returned to baseline glucose (5.6 mM) for 24 minutes before a high potassium stimulation (20 mM KCl) was given to stimulate release of all vesicles. The insulin content of perfusate samples collected throughout the protocol was measured to test for differences in basal or evoked released. No differences in basal insulin release, glucose stimulated insulin release phase one or two, or high potassium triggered insulin release were found (Figure 31A-E). Additionally, the total islet insulin content did not differ between genotypes (Figure 31F). This data suggests that *Cadps* editing does not impact insulin granule maturation or storage, as total islet insulin content was identical. These data also further indicate that *Cadps* editing does not impact glucose stimulated or total evoked insulin release from isolated pancreatic islets.

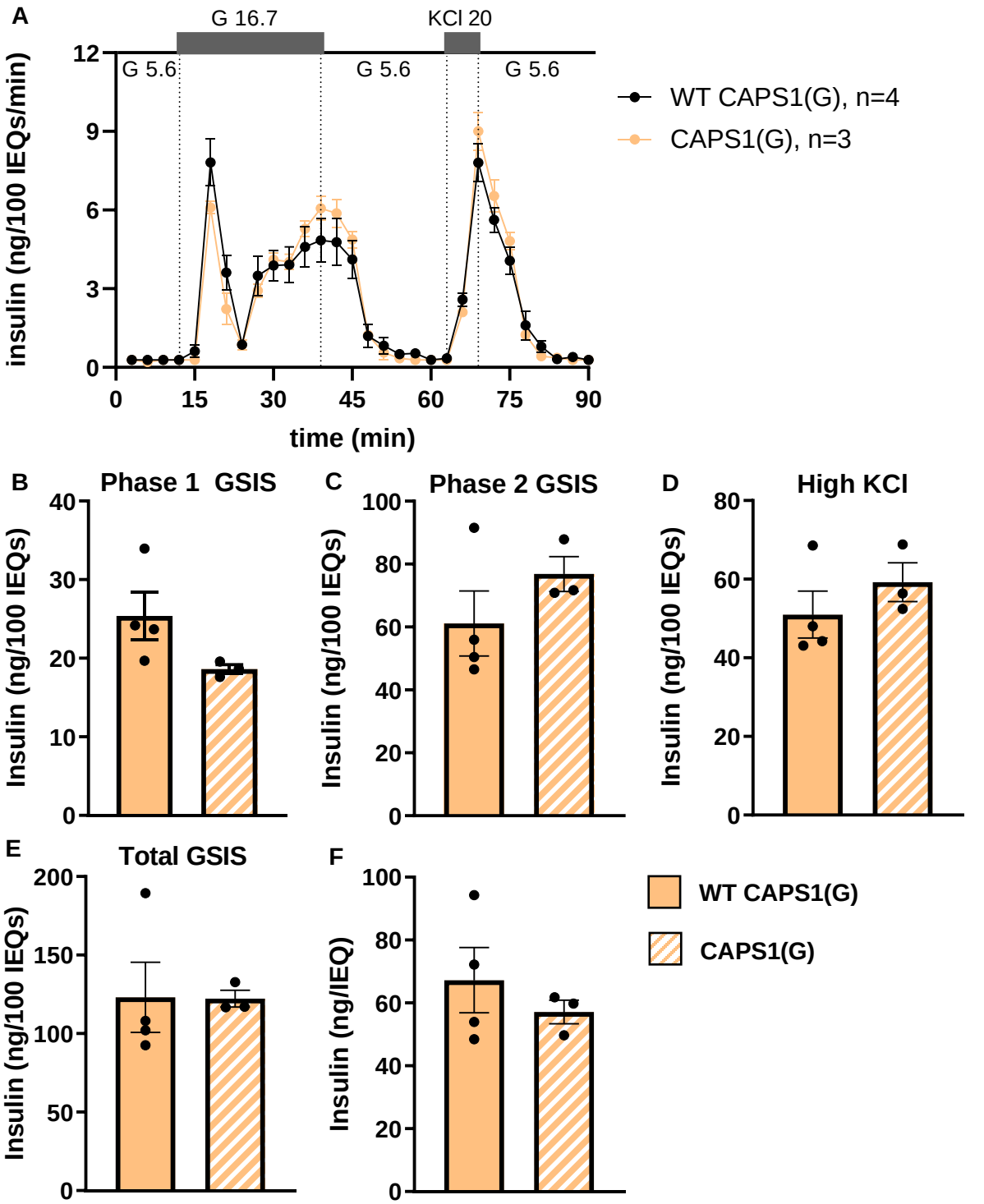

Figure 31. *In vitro* insulin release from pancreatic islets is not altered by CAPS1 RNA editing. (**A**) Insulin release over time from islets perfused with glucose, high glucose, and KCl is shown; numbers over plot represent concentration (mM). (**B-E**) Area under the curve analysis of phase-1 insulin release (9-24 minutes), (**B**), phase-2 insulin release (24-60 minutes), (**C**), KCl-stimulated insulin release (60-84 minutes), (**D**) and total GSIS (9-60 minutes), (**E**) are presented. (**F**) Total islet insulin content. n= 3-4 mice/genotype for islet harvest, mean ± SEM.

Involvement of CAPS1 RNA Editing in the Hypothalamic-Pituitary Axis

In a final set of studies, we investigated the role of *Cadps* editing in several hypothalamic-pituitary axes, including the thyrotroph, somatotroph, corticotroph, and lactotroph axes from the anterior pituitary gland. CAPS1 expression in the hypothalamus and pituitary gland of WT mice was confirmed by western blot (Figure 32A). In the hypothalamus 43.5 ± 0.4% of CAPS1 transcripts were edited while in the pituitary gland 12.9 ± 0.2% of transcripts were edited (n=2) (Figure 32B, C).

As an orthogonal approach to quantify levels of releasing factors secreted from the hypothalamus, RNA expression of downstream effectors of releasing factor signaling were analyzed, i.e., peptide hormone transcript levels in the pituitary gland. Releasing factors, such as corticotropin releasing hormone, drive expression of cognate pituitary hormone transcripts, such as ACTH; therefore, increased hypothalamic pituitary signaling would result in increased expression of RNAs encoding pituitary hormones. No differences in gene expression of adrenocorticotropin (*Acth*), growth hormone (G*h*), or thyroid stimulating hormone (T*shb*) were found for CAPS1 (E) or CAPS1(G) mice compared to wild-type littermates (Figure 33), suggesting normal hypothalamic to pituitary signaling in CAPS1(E) and CAPS1(G) mice.

To study the effect of *Cadps* editing on release of hormones from the pituitary gland, we collaborated with the Vanderbilt Hormone Assay and Analytical Services Core to directly measure hormone levels from plasma samples. Hormone levels were assessed in male and female mice and sex-dependent effects were noted in TSH and ACTH levels (Figure 34B-D). However, there are no differences in plasma levels of ACTH or TSH based on genotype (Figure 34A-D). An increase in GH levels was noted in CAPS1(G) females but not males, and no differences in GH levels were found in CAPS1(E) mice (Figure 34E, F). We assessed circulating levels of prolactin in male mice, as prolactin levels in females vary with phase of estrous cycle, a factor not controlled for in our experimental design. A commercial ELISA was used to quantify prolactin levels, and no differences were found CAPS1(E) or CAPS1(G) male mice (Figure 34G).

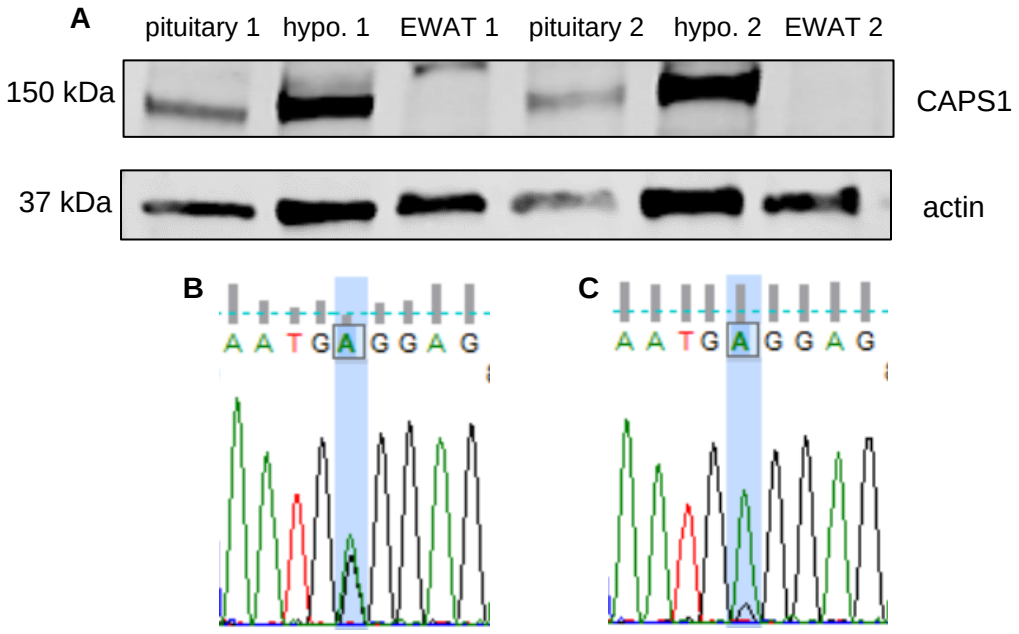

Figure 32. CAPS1 protein expression and RNA editing levels in the hypothalamus and pituitary gland. (A) Western blotting analysis of CAPS1 and β-actin protein expression in whole cell lysates isolated from the pituitary, hypothalamus and epididymal white adipose tissue (EWAT) pooled from two wild-type mice each. (**B, C**) Electropherogram traces of RT-PCR amplicons generated from *Cadps* transcripts isolated from the hypothalamus (**B**) and pituitary gland (**C**) of wild-type mice. The highlighted position represents the CAPS1 E/G editing site, illustrating tissue-specific levels of adenosine (green) and guanosine (black) resulting from *Cadps* RNA editing.

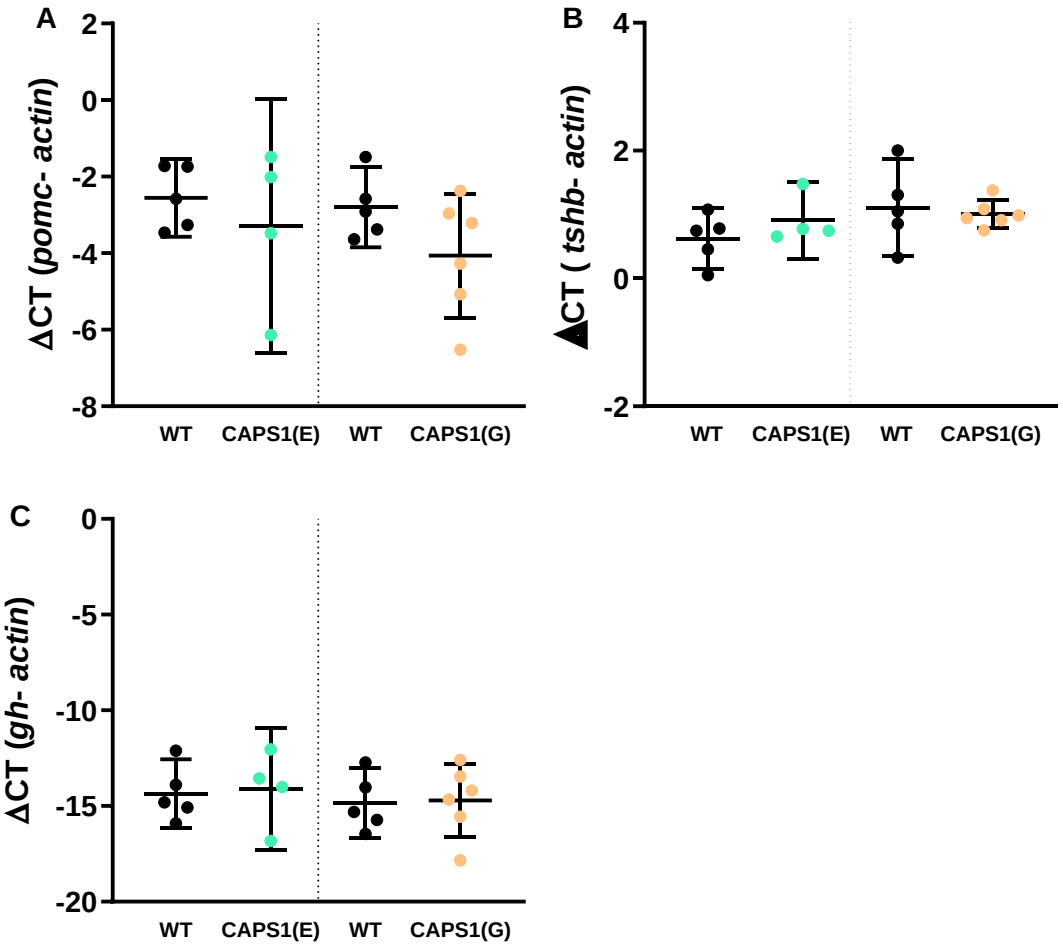

Figure 33. Expression of pituitary hormone RNA transcripts is unchanged in CAPS1(E) and CAPS1(G) mice. qRT-PCR analysis of *Pomc* (**A**), *Tshb* (**B**), and *Gh* (**C**) gene expression revealed no changes in pituitary gene expression in CAPS1(E) or CAPS1(G) mice when compared to wild-type littermate controls; (n=4-6 female mice /genotype, mean ± 95% CI.

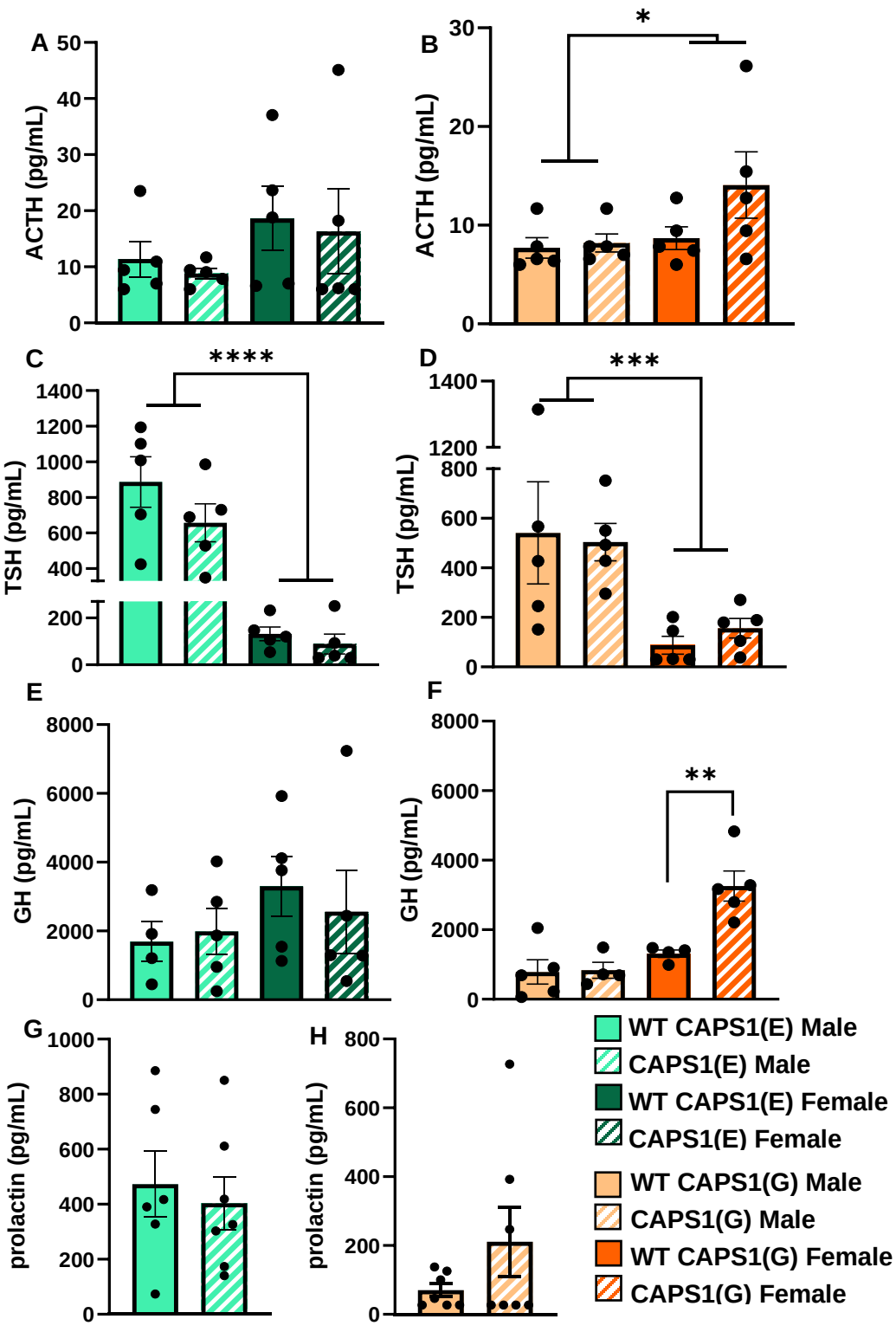

Figure 34. Circulating pituitary hormone levels are normal in CAPS1(E) and CAPS1(G) male and female mice. Quantitative analysis of ACTH (A-B), TSH (C-D), and GH (E-F) in male and female CAPS1(E) and CAPS1(G) mice from plasma samples and measurement of prolactin (G-H) in male CAPS1(E) and CAPS1(G) mice; n= 5-7 mice/genotype and gender, mean ± SEM (*p<0.05, Dunn's Multiple Comparison Test).

As a final assessment of the effect of *Cadps* editing on the hypothalamic-pituitary hormone axes, we measured the amount of hormones released from target organs, including the liver and thyroid. The Vanderbilt Hormone Assay and Analytical Services Core analyzed serum samples for total T4 content and found no effect of genotype on T4 levels (Figure 35A, B). Circulating levels of IGF-1, a hormone released from the liver in response to GH signaling, were quantified using a commercially available ELISA and no differences were detected between CAPS1(E), CAPS1(G), and wild-type littermates (Figure 35C, D). In summary, no impact of *Cadps* editing was identified on the hypothalamic-pituitary axes including the complete liver and thyroid axes, and portions of the lactotroph and corticotroph axes.

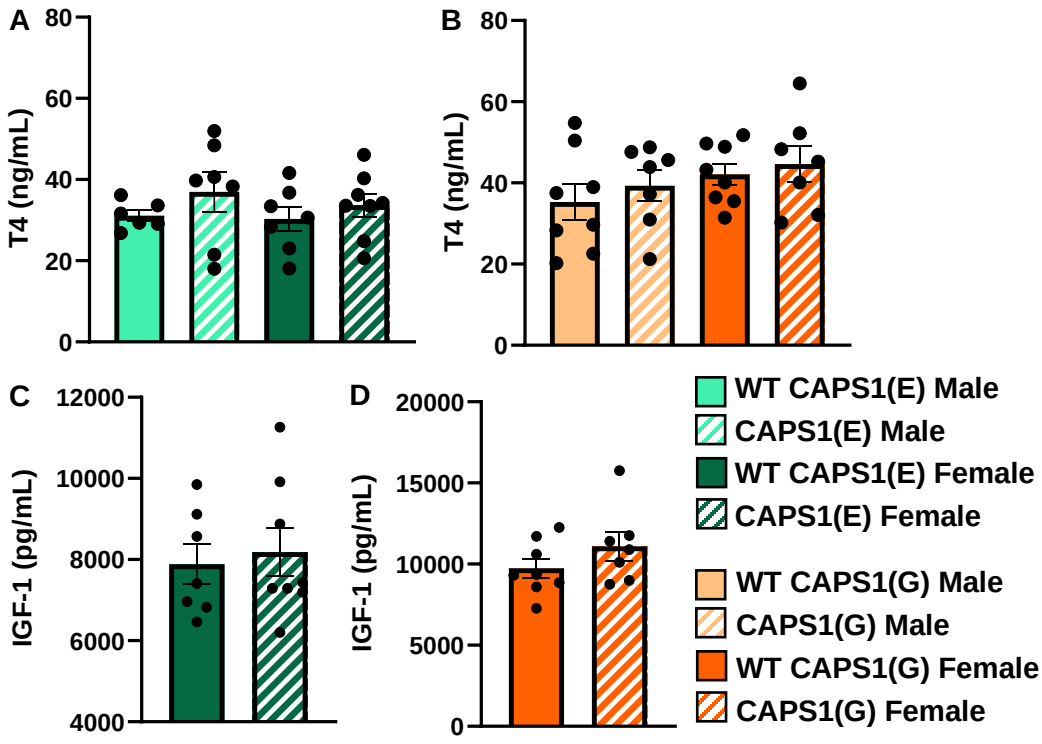

Figure 35. Circulating T4 and IGF-1 levels are normal in CAPS1(E) and CAPS1(G) mice. Quantitative analysis of plasma levels for total T4 (**A-B**) in male and female CAPS1(E) and CAPS1(G) mice and IGF-1 (**C-D**) in female mice are shown; n=5-7 mice/genotype and gender, mean ± SEM.

CAPS1 RNA Editing regulation of plasma cholesterol levels

A previous study characterizing CAPS1(G) mice found increased circulating cholesterol levels (Miyake et al., 2016). We sought to independently validate this finding in the CAPS1(G) mice and hypothesized that CAPS1(E) mice would conversely have decreased circulating cholesterol levels. In collaboration with the Vanderbilt University Medical Center Lipid Core, cholesterol levels were quantified in plasma samples collected from male and female CAPS1(E) and CAPS1(G) mice along with WT littermates. Analysis of cholesterol levels revealed no changes in CAPS1(E) or CAPS1(G), male or female mice (

Figure 36).

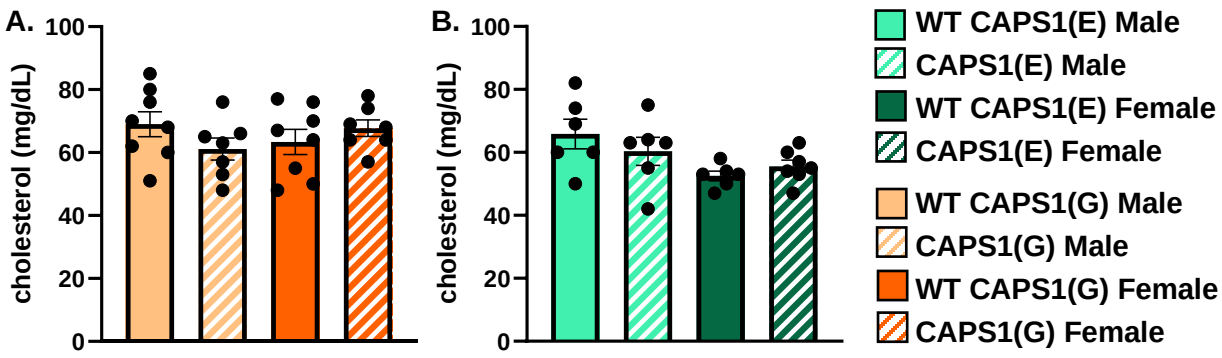

Figure 36.Plasma total cholesterol levels are normal in fed CAPS1(E) and CAPS1(G) mice. Quantitative analysis of plasma levels for total cholesterol (**A, B**) in male and female CAPS1(E) and CAPS1(G) mice are shown; n=6-8 mice/genotype and gender, mean ± SEM.

Discussion

In this series of experiments, I have investigated the effect of *Cadps* RNA editing on the release of hormones, such as insulin, ACTH, TSH, GH, and prolactin, and have explored the associated physiological outcomes using CAPS1(E) and CAPS(G) mouse models. Overall, the effect of *Cadps* editing in the selected endocrine systems appears to be minimal, though the results suggest that a more detailed investigation of energy homeostasis may reveal *Cadps* editing-dependent effects on this system.

In our first studies, we largely confirmed the findings of Miyake and colleagues by showing that male CAPS1(G) mice have decreased fat and lean mass at 14 weeks of age and are hyperactive with increased energy expenditure. Given the energy expenditure findings, we would expect CAPS1(G) mice to have increased food intake to compensate for their increased energy output. Several lines of evidence indicate that mice maintain energy homeostasis by changing food intake to match metabolic demands. For example, mice selectively bred as “high-wheel running” will increase their food intake to compensate for increased motor activity, resulting in no net change in body mass (Swallow, Koteja, Carter, & Garland, 2001). The same principle applies to other types of metabolic demand, including cold exposure-induced increases in thermogenesis, which also increases the metabolic demand in mice. Animals exposed to intermittent cold temperatures consume more food to offset energy expenditure and maintain a normal body mass (Ravussin, Xiao, Gavrilova, & Reitman, 2014). Therefore, the lack of increased food intake in CAPS1(G) mice suggests dysfunction in a system controlling energy homeostasis. These results also suggest that CAPS1(G) mice may be underweight due to perpetual caloric imbalance.

Rodent energy homeostasis is a complex subject that involves the coordination of both peripherally and centrally released hormones and neuropeptides. Central to energy homeostasis are the POMC/CART and NPY/AgRP neurons located in the arcuate nucleus of the hypothalamus. Broadly speaking, NPY/AgRP neurons signal to increase food intake and decrease energy expenditure, while POMC neurons act in an opposing manner. Therefore, our

data is consistent with decreased activity of orexigenic NPY/AgRP neuron signaling or increased anorexigenic POMC/CART neuron signaling. Various peripherally released peptides, including leptin, ghrelin, cholecystokinin (CCK), peptide YY (PP Y) 3-36, glucagon-like peptide (GLP) 1, oxyntomodulin (OXM), pancreatic polypeptide (PP), and insulin exert their actions on NPY/AgRP and POMC/CART neurons in both excitatory and inhibitory fashions. Adding to the complexity, NPY/AgRP neurons have been shown to inhibit POMC/CART neurons through GABA signaling, and AgRP is an antagonist of receptors targeted by peptides released from POMC/CART neurons, melanocortin 3 and 4 receptors. Unraveling the precise peptide(s) and signaling pathway(s) that are dysregulated in CAPS1(G) animals would require extensive investigation of these systems. However, results from additional metabolic studies and endocrine system investigations have provided some insight.

As part of our evaluation of energy expenditure we also were able to investigate meal patterning and found significant changes in CAPS1(G) animals. CAPS1(G) mice maintain normal 12 and 24-hour total food intake compared to wild-type animals but consume smaller meals more frequently. This suggests CAPS1(G) mice may have increased signaling of satiation factors, which are released during feeding to indicate that a “full” state has been reached to end food intake (Benelam, 2009). Alternatively, CAPS1(G) mice may have decreased signaling of satiety factors, which are released during fasting to prevent additional food intake (Benelam, 2009). As our studies have shown that CAPS1(G) broadly enhances release of neurotransmitters, I hypothesize that the effect of *Cadps* editing on meal patterning also will be due to an increase in release of a hormone or neurotransmitter, therefore narrowing the field of potential signaling molecules that are dysregulated. As release of GLP-1, OXM, PP Y (3-36), and PP are all known to increase satiety (Benelam, 2009), it is less likely that altered signaling originating from enhanced release of these molecules would account for altered meal patterning in CAPS1(G) mice.

A major satiation factor is cholecystokinin (CCK), which is released from endocrine L cells located in the jejunum and duodenum and signals through receptors on the vagal nerve to the hypothalamus to end food intake. Administering exogenous CCK to rats reduces subsequent meal size in a dose-dependent manner (West, Fey, & Woods, 1984) and interestingly, CCK_1 receptor knockout mice consume fewer, but larger meals than wild-type animals with no change in total daily food intake or body weight (Donovan, Paulino, & Raybould, 2007). As the phenotypes of CCK_1 receptor knockout mice are opposite to those identified in CAPS1(G) animals, it is possible that increased CCK signaling could drive altered meal patterning in CAPS1(G) mice. Future studies should investigate expression of CAPS1 in L cells and use CCK receptor antagonists and vagotomies to study the role of *Cadps* editing in meal patterning.

A satiety signal of potential interest is ghrelin, a hormone released from the stomach and intestine that signals hunger (Benelam, 2009). Notably, ghrelin receptor knockout mice eat fewer, larger meals with no change in total food intake or body mass (Lin et al., 2014). Therefore, it is possible that increased ghrelin release in CAPS1(G) animals could account for altered meal patterning, and future studies using ghrelin receptor antagonists would help elucidate the role of this signaling molecule in altered meal patterning in CAPS1(G) animals.

The remaining peripherally released hormones that impact energy homeostasis are insulin and leptin, both of which are unlikely to contribute to the phenotype of CAPS1(G) animals. First, we have directly investigated the effect of *Cadps* editing on release of insulin and found no apparent changes, indicating that altered insulin release is unlikely to account for the energy homeostasis phenotype of CAPS1(G) animals (Figure 31). Next, CAPS1 is not expressed in white adipose tissue (Figure 32), which is the largest source of leptin-producing cells in the mammal, suggesting CAPS1 does not regulate the release of leptin from fat. Additionally, leptin levels are known to closely reflect fat mass, and CAPS1(G) animals have lower fat mass than wild-type animals which suggest decreased circulating leptin levels would be anticipated. However, as leptin is an anorexigenic peptide, decreased circulating leptin levels would be expected to reduce

signaling of POMC/CART neurons leading to increased food intake and decreased energy expenditure. As these outcomes are opposite of what is observed in CAPS1(G) animals, dysregulation of leptin release appears unlikely to be the cause of altered energy homeostasis.

While CCK and ghrelin are the most promising candidates for peripherally released hormones whose enhanced release in CAPS1(G) animals could underlie the observed meal patterning phenotypes, there are also a multitude of signaling pathways that originate in the arcuate nucleus that may contribute to the phenotypes. As previously stated, it would be hypothesized broadly that either increased NPY/AgRP neuron signaling or increased POMC/CART neuron signaling could play a role. Future studies could include assessing activation of POMC and NPY neurons in fasted and fed states in CAPS1(G) mice compared to wild-type mice to help identify which group of neurons is most affected. Additionally, investigation of circulating corticosterone and leptin levels, and analysis of the RNA expression levels of key hypothalamic neuropeptides, including *Npy, Pomc, Crh, Agrp, Mch*, and *Trh,* may provide additional insight into this complex system. Detailed analysis of CAPS1 expression in enteroendocrine cells in the digestive tract and in hypothalamic neurons may also provide insight into which systems are dysregulated in CAPS1(G) animals. The results from these studies could reveal pathways that are regulated by *Cadps* editing and provide additional insight into the regulation of energy homeostasis.

Understanding the mechanisms that dictate food intake and energy expenditure is a subject area that has garnered much interest due to the obesity epidemic, which is largely driven by increased caloric consumption of a high-fat diet. To investigate whether the effects of *Cadps* editing on energy homeostasis could modulate high-fat diet induced weight gain, we provided high-fat and control diets to CAPS1(G) and wild-type littermate mice for 10 weeks and monitored body mass over the course of the experiment. Interestingly, while HFD-fed CAPS1(G) animals never differed in body mass compared to HFD- fed wild-type littermates, we found that CAPS1(G) mice take 1.5 weeks longer than wild-type animals to differ in body mass size between control

and HFD-fed animals. It has been shown that increased locomotor activity alone will not prevent HFD-induced weight gain, as wheel running mice gain the same amount of weight as non-wheel running animals on a HFD (Jung & Luthin, 2010). These results suggest that alterations in energy homeostasis systems, irrespective of hyperactivity, may contribute to the delayed onset of HFD-induced weight gain in CAPS1(G) mice. Once the systems that are dysregulated in CAPS1(G) animals are identified, this information can be integrated with the broad literature on HFD-induced weight gain in mice to further understand how *Cadps* editing could impact obesity.

In the context of pancreatic beta cells, *Cadps* editing does not appear to have an impact on glucose-stimulated or high potassium stimulated insulin release. As the level of *Cadps* editing in beta cells is relatively low in wild-type animals, the difference in editing between CAPS1(G) WT and CAPS1(G) animals (~80%) would be anticipated to be large enough to detect any potential editing-dependent effect. One caveat is the relatively small number of islet preparations tested in the islet perfusion experiment (n= 3-4 preparations/ genotype). It remains possible that a small effect in phase two insulin release may be detected when using a sufficient sample size to detect small changes. We also did not find any physiologic changes in CAPS1(G) animals subjected to a glucose tolerance test. Our studies to date suggest that *Cadps* editing does not impact insulin release to an extent that alters systemic glucose clearance.

In a final set of experiments, the effect of *Cadps* editing on several hypothalamic-pituitary axes was examined. Using qRT-PCR to quantify gene expression, no significant changes in *Pomc, Tshb, Gh,* or *Prl* RNA were identified in CAPS1(E) or CAPS1(G) animals when compared to wild-type littermates. These results suggest release of Corticotropin Releasing Hormone (CRH), Thyrotropin Releasing Hormone (TRH), and Growth Hormone Releasing Hormone (GHRH) is not impacted by *Cadps* editing, as these “releasing” factors drive increased gene expression of their downstream targets, *Pomc, Tshb,* and *Gh*, respectively. Expression of *Fsh* and *Lh,* genes whose expression is driven by release of gonadotropin releasing hormone (GnRH) from the hypothalamus, were not investigated. Female animals were used for this study and the

stage of the estrous cycle, which dictates GnRH release, was not determined prior to sacrifice. Interestingly, there is much greater variability in *Pomc* expression levels in CAPS1(E) and CAPS1(G) animals compared to WT littermates. While this data did not clearly indicate editing-dependent changes in CRH release, the level of variability in mutant animals suggests there may be dysregulation of *Pomc* expression. Expression of *Pomc* is promoted by CRH signaling yet inhibited by corticosterone signaling through feedback inhibition. Future studies investigating the role of CAPS1 editing in stress-mediated responses may uncover novel phenotypes that help explain the large variability in pituitary *Pomc* gene expression in CAPS1(E) and CAPS1(G) animals.

Evaluation of circulating plasma levels of ACTH, TSH-β, and GH was used to assess CAPS1 editing-dependent effects on anterior pituitary hormone release. While there was no effect of genotype on ACTH levels, there was a significant effect of sex in the CAPS1(G) mouse line, with female animals having higher levels of ACTH than males. This finding agrees with previously identified sex-specific differences in the HPA axis, including increased CRH expression in the hypothalamus and increased circulating corticosterone levels in female mice compared to males (Bangasser & Wiersielis, 2018). While no effect of genotype was identified in plasma TSH levels, a sex-dependent effect was noted in both mutant mouse lines, with female animals having significantly lower levels of circulating TSH compared to male animals, once again in agreement with previously published studies (McLachlan, Hamidi, Aliesky, Williams, & Rapoport, 2014). When assessing the growth hormone axis, there is a significant increase in circulating levels of GH in CAPS1(G) female animals compared to CAPS1(G) WT female animals. No effect is found in CAPS1(G) male animals nor in CAPS1(E) female or male animals. It will be interesting for future studies to determine if increased GH release causes physiologically relevant changes in CAPS1(G) female mice, including enhanced long bone growth and production of IGF-1, as well as additional metabolic effects.

In an additional investigation of hormone release from the anterior pituitary, circulating levels of prolactin were studied in male mice. This pathway was of particular interest as release of prolactin is known to be negatively regulated by dopamine signaling through the tuberoinfundibular pathway. Given that we identified increased dopamine release in the dorsal striatum of CAPS1(G) animals (Chapter III), we hypothesized that circulating prolactin levels may be decreased in CAPS1(G) mice due to tonic inhibition by increased dopamine signaling. However, no changes in circulating prolactin levels were found. A possible explanation for this observation is that increased inhibition by dopamine signaling is balanced by enhanced release of vesicles containing prolactin from hypothalamic prolactin-expressing neurons. In this manner, neural circuits that rely on feed forward inhibition are less likely to be impacted by *Cadps* editing than those relying upon feed forward activation, where the effects of editing on the circuit output could be additive.

As a final means of investigating the effect of *Cadps* editing in hypothalamic-pituitary axes, the levels of target-organ-derived hormones T4 and IGF-1 were assessed. While T4 is release in a vesicle-independent manner, we hypothesized that *Cadps* editing could have an indirect effect to increase total T4 levels due to enhanced TSH signaling to the thyroid. In the liver, GH triggers vesicular release of IGF-1, therefore we hypothesized *Cadps* editing could have a direct effect on release of this hormone and a potential additive circuit effect from enhanced circulating GH levels. No significant effects of genotype were found for either analyte, indicating that editing does not directly or indirectly impact release of T4 or IGF-1 in male mice. It would be interesting to investigate circulating IGF-1 levels in female CAPS1(G) animals, as these mice exhibit increased GH blood levels.

In a final study of CAPS1 editing-dependent effects on hypothalamic-pituitary axes, I investigated a physiological outcome of dysregulated thyroid axis signaling, plasma cholesterol levels. It has been previously reported that CAPS1(G) male mice have decreased plasma cholesterol levels (Miyake et al., 2016). In our study, CAPS1(E) and CAPS1(G) male mice had

normal cholesterol levels, compared to wild-type littermate animals. However, in the Miyake study, fasted blood samples were used for cholesterol measurements, whereas our studies did not control for food intake, which is known to directly impact circulating cholesterol. Therefore, while no changes in fed-mouse cholesterol levels were identified, additional studies are needed to determine if the results presented by Miyake and colleagues are reproducible.

In conclusion, the effect of *Cadps* editing on hormone release from endocrine cells is minor and the impact(s) of these effects on whole animal physiology appear minimal. While a few significant effects are noted in specific studies, i.e., altered meal patterning in CAPS1(G) mice, increased circulating GH levels in CAPS1(G) female mice, the main conclusion is that *Cadps* editing does not meaningfully impact release of hormones in the endocrine systems examined. Robust feedback circuits that maintain homeostasis within living organisms may overcome any minor changes in hormone release in the systems we investigated, thus mitigating physiologically significant outcomes. To this end, future studies using system stressors that mimic human disease states, such as loss of functioning islets or diet manipulation, may uncover new roles for *Cadps* editing in modulating hormone release.

CHAPTER 5

Summary & Discussion

Summary of Findings

The focus of this dissertation work is centered on understanding the functional outcomes of *Cadps* A-to-I RNA editing at both the cellular and physiological levels. RNA editing of *Cadps* results in a glutamate to glycine substitution in the C-terminal domain of the protein thus providing increased diversity in the protein products generated from the *Cadps* gene. In all tissues studied, there are a mix of edited and non-edited *Cadps* transcripts. Therefore, mouse models that solely expressed either non-edited or edited CAPS1 were employed to address the research aims. From this work, we have gained further insight into the effect of *Cadps* editing in regulating the release of hormones and neuromodulatory and fast-acting neurotransmitters. Future studies focused on the molecular interactions that are impacted by *Cadps* editing may shed light on the mechanisms that underlie the findings presented in this dissertation.

In the first research chapter, I reported the effects of neuronal activity on *Cadps* editing levels and reported how CAPS1 synaptic localization and spontaneous and evoked neurotransmission are altered by sole expression of edited CAPS1. We employed primary hippocampal neurons cultured from CAPS1(E) and CAPS1(G) animals as a model system. From the data, we concluded that *Cadps* editing levels and ADAR2 expression are activity-dependent in cultures of WT neurons, with increased activity leading to increased editing and expression and decreased activity causing the opposite. Given the known role of the CAPS1 C-terminal domain in synaptic enrichment, synaptic localization of CAPS1 in cultures from CAPS1(E) and CAPS1(G) animals was investigated and it was shown that CAPS1(G) localizes to a greater proportion of both excitatory and inhibitory synapses. Interestingly, I also showed that CAPS1 localizes to far

greater (80-90%) of GABAergic terminals than to glutamatergic terminals (5-10%) in this model system. Finally, we evaluated spontaneous and evoked release using electrophysiology and found that edited CAPS1 enhances short-term depression at inhibitory synapses, likely through enhanced release probability. We also found an increase in the amplitude of mIPSC events in CAPS1(G) neurons, suggesting that edited CAPS1 increases GABA loading into synaptic vesicles. Together, these experiments describe the cellular effect of *Cadps* editing on fast-acting neurotransmission and demonstrate the potential for editing levels to change in response to environmental cues.

The second research chapter of this dissertation reports the functional outcomes of *Cadps* editing in regulating a neuromodulatory transmission system, the dopamine system. I primarily used the CAPS1(G) mouse line to study cellular release of dopamine and explored the physiologic outcomes using dopamine-associated neurobehavioral assays. From FSCV experiments, we concluded that *Cadps* editing enhances dopamine release and re-uptake, primarily in the dorsal and not the ventral striatum. Increased release in the striatum was found to be independent of changes in dopamine axon density and dopamine synthesis and metabolism, suggesting the outcome is due to enhanced CAPS1 synaptic function. CAPS1(G) animals were found to be hyperactive in both novel and familiar environments and this behavior is likely to be driven by enhanced dopamine signaling, as the CAPS1(G) animals were hypersensitive to both a dopamine releaser and a D2R antagonist. Characterization of other dopamine-associated behaviors found that CAPS1(G) animals have normal motor coordination, normal motivated and reward behaviors, and may display some autism-associated phenotypes including altered social behaviors and increased repetitive activities. In summary, these experiments report the cellular effect of *Cadps* editing on dopamine release and explore the associated physiological outcomes.

In the third research chapter, I report the cellular and physiological outcomes associated with *Cadps* editing in multiple endocrine systems, including those associated with energy homeostasis, glucose stimulated insulin secretion, and hypothalamic-pituitary pathways. First,

CAPS1(E) and CAPS1(G) animals were assessed for changes in metabolism, and CAPS1(G) animals were reported to have increased energy expenditure without an increase in food intake resulting in animals being underweight. From this data we concluded that CAPS1(G) animals have altered energy homeostasis, and we also identified altered meal patterning in these animals which provided additional insight into which pathways may be dysregulated in CAPS1(G) mice. CAPS1(E) animals were normal in all metabolic tests. Next, I used cellular and physiological assays to determine that CAPS1(G) animals have no changes in glucose-stimulated insulin release from pancreatic beta cells. Finally, I investigated the role of *Cadps* editing in several hypothalamic-pituitary axes and did not identify any profound changes in these systems in either CAPS1(E) or CAPS1(G), male or female mice. I noted an increase in circulating GH levels in CAPS1(G) female animals and large variability in pituitary *Acth* levels, both of which may point towards altered function if studied in greater detail. Overall, the effects of *Cadps* editing in the endocrine systems studied were minimal.

Cumulative Themes

Central themes in the functional effects of *Cadps* editing emerge when the research findings presented in each chapter are considered together. When surveying the results of cellular assays, if any effect is present, *Cadps* editing enhances release of neurotransmitters or hormones. This is demonstrated in GABAergic transmission during high frequency stimulation, in dopamine transmission within the dorsal striatum, and in growth hormone released from the anterior pituitary. While there are many instances where no effect of *Cadps* editing was identified in specific cells, such as in glutamatergic transmission and insulin release, we never identified a cellular response of decreased release of a transmitter or hormone in response to increased *Cadps* editing levels. Additionally, this conclusion is supported by the findings of Miyake and colleagues, who identified increases in exocytosis events in adrenal chromaffin cells, increased release of norepinephrine from PC12 cells, and increased release of dopamine from striatal

synaptosomes when edited CAPS1 was solely expressed (Miyake et al., 2016). Together, this body of work strongly supports the conclusion that *Cadps* editing enhances regulated exocytosis.

A second conclusion that is consistently shared across this body of work is that *Cadps* editing does not alter CAPS1 expression levels. I have demonstrated that there are no *Cadps* editing-dependent alterations in CAPS1 expression in whole brain protein extracts from CAPS1(E) animals (Chapter II) or in SN-containing brain punches from CAPS1(G) animals (Chapter III). This suggests that both isoforms of CAPS1 have similar protein stability, though this has not been directly tested. Other A-to-I editing events have dramatic effects on protein stability, such as the profound increase in 5-HT_{2C} receptor protein expression found in 5-HT_{2c} VGV animals, a model of the "fully edited" 5-HT_{2c} receptor (Morabito et al., 2010). However, CAPS1(E) and CAPS1(G) appear to have equal stability which allows us to draw conclusions about isoform-specific functions that are independent of changes in expression level. This is important as changes in CAPS1 protein expression alone can have significant effects on neurotransmission (Shaib et al., 2018).

A final observation noted throughout this work is that CAPS1 must play a dominant role in regulating exocytosis in a cell for an effect of *Cadps* editing to be realized. There are several instances in this dissertation where CAPS1 is clearly expressed in a tissue or cell type, yet no effect of *Cadps* editing were noted. No effect of *Cadps* editing was noted in glutamatergic transmission though 5-10% of these synapses contained CAPS1 (Chapter II). There was also no effect of *Cadps* editing on insulin release (Chapter IV), though CAPS1 expression in beta cells has been reported by multiple groups. Further, in both systems a role of CAPS1 in regulating exocytosis was previously reported. There are possible explanations for the experimental outcomes, including low CAPS1 expression levels in glutamate synapses and beta cells and the use of different model systems to investigate glutamate release, autaptic versus dissociated hippocampal cultures. However, these results collectively show that CAPS1 protein expression does not equate with significant protein function in regulating exocytosis, at least in the ways we

measured exocytosis, and illustrates how proteins traditionally thought to regulate exocytosis may have alternative functions in specific synapse/cell types.

Future Directions

An intriguing question that comes out of this body of work is whether edited CAPS1 acts as a hypermorph solely due to enhanced localization of the protein to sites of action. We have shown that edited CAPS1 traffics to more glutamatergic and GABAergic synapses than non-edited CAPS1 in hippocampal neurons, and have demonstrated that not all synapses contain CAPS1, non-edited or edited. Additionally, we have reported that edited CAPS1 enhances several functions associated with CAPS1, including enhanced exocytosis and enhanced loading of GABA-containing synaptic vesicles. Therefore, the result of editing-dependent enhanced synaptic localization could be that CAPS1 is now present at more sites of release and able to perform all its known regulatory functions. As such, one could hypothesize that edited and non-edited CAPS1 have equal functionality when equally expressed at sites of release. One way to test this hypothesis would be to assay CAPS1 functions using model systems in which the concentration of CAPS1 can be tightly controlled. For example, a liposome fusion assay could be used to assess the effect of *Cadps* editing on exocytosis by measuring lipid or content mixing in the presence of fixed concentrations of edited or non-edited CAPS1. Additionally, the effect of *Cadps* editing on vesicle loading could be assessed by evaluating the effect of a fixed concentration of edited or non-edited CAPS1 on vGlut1 or vMAT2-mediated loading of glutamate or catecholamines into vesicles. Each of these proposed experiments would require a source of purified CAPS1, either recombinantly expressed or isolated from CAPS1(G) and CAPS1(E) mouse brains, which proved to be a barrier that inhibited us from performing these experiments.

Alternatively, Miyake and colleagues reported edited CAPS1 has enhanced binding to syntaxin-1 when compared to non-edited CAPS1 and suggested this as a possible mechanistic explanation underlying enhanced exocytosis. Given the recent structure-based insights provided by Zhou and colleagues, we could predict that enhanced binding to syntaxin-1 would further

stabilize syntaxin-1/SNAP-25 SNARE complex intermediates thus promoting the formation of functional, zippered SNARE complexes to enhance exocytosis (H. Zhou et al., 2019). This is an intriguing hypothesis that explains how edited CAPS1 enhances exocytosis, but it does not address the extended role of edited CAPS1 enhancing GABA loading into synaptic vesicles. This would require an additional hypothesis that edited CAPS1 has enhanced interactions with other key proteins that regulate vesicle loading. It seems unlikely that the C-terminal domain of CAPS1 has meaningful interactions with several synaptic proteins to regulate multiple aspects of neurotransmission. It will be interesting for future studies to determine which molecular interactions are altered by *Cadps* editing as this will provide meaningful insight into the mechanism(s) linking changes in *Cadps* editing levels to altered CAPS1 cellular function.

Through our investigation of the effects of *Cadps* editing on regulated exocytosis we have gained new insight into how an RNA editing event can impact cellular and physiological functions. We have also shown dynamic modulation of *Cadps* RNA editing levels in response to neuronal activation which suggests the outcomes we identified in response to changes in editing may be reflected during certain physiological or pathophysiological states. Dysregulation of global RNA editing has been linked to several neurological disorders, including schizophrenia, Alzheimer's disease, and autism, and in various cancers (Breen et al., 2019; Khermesh et al., 2016; Tran et al., 2019; Xu, Wang, & Liang, 2018). As CAPS1 has a well-established role in regulating neurotransmission, it is interesting to speculate that altered *Cadps* editing may play a role in these disorders. Additionally, CAPS1 has recently emerged as an oncogene, as upregulation promotes epithelial to mesenchymal transition of cancer cells and is linked to metastasis in colorectal cancers (Wu et al., 2019; Zhao et al., 2019). Given the well-established link between increased RNA editing levels and cancer, future studies should consider that upregulation of *Cadps* editing may also play a role in colorectal cancer progression. In summary, the results presented in this dissertation may provide future insight into how changes in *Cadps* editing play a role in human disease.

REFERENCES

Acuna, C., Liu, X., & Sudhof, T. C. (2016). How to Make an Active Zone: Unexpected Universal Functional Redundancy between RIMs and RIM-BPs. *Neuron, 91*(4), 792-807. doi:10.1016/j.neuron.2016.07.042

Andrews-Zwilling, Y. S., Kawabe, H., Reim, K., Varoqueaux, F., & Brose, N. (2006). Binding to Rab3A-interacting molecule RIM regulates the presynaptic recruitment of Munc13-1 and ubMunc13-2. *J Biol Chem, 281*(28), 19720-19731. doi:10.1074/jbc.M601421200

Ann, K., Kowalchyk, J. A., Loyet, K. M., & Martin, T. F. (1997). Novel Ca2+-binding protein (CAPS) related to UNC-31 required for Ca2+-activated exocytosis. *J Biol Chem, 272*(32), 19637-19640.

Anzalone, A., Lizardi-Ortiz, J. E., Ramos, M., De Mei, C., Hopf, F. W., Iaccarino, C., . . . Borrelli, E. (2012). Dual control of dopamine synthesis and release by presynaptic and postsynaptic dopamine D2 receptors. *J Neurosci, 32*(26), 9023-9034. doi:10.1523/JNEUROSCI.0918-12.2012

Augustin, I., Rosenmund, C., Sudhof, T., & Brose, N. (1999). Munc13-1 is essential for fusion competence of glutamatergic synaptic vesicles. *Nature, 400*, 457-461.

Avery, L., Bargmann, C. I., & Horvitz, H. R. (1993). The Caenorhabditis elegans unc-31 gene affects multiple nervous system-controlled functions. *Genetics, 134*(2), 455-464.

Avery, M. C., & Krichmar, J. L. (2017). Neuromodulatory Systems and Their Interactions: A Review of Models, Theories, and Experiments. *Front Neural Circuits, 11*, 108. doi:10.3389/fncir.2017.00108

Bahn, J. H., Lee, J. H., Li, G., Greer, C., Peng, G., & Xiao, X. (2012). Accurate identification of A-to-I RNA editing in human by transcriptome sequencing. *Genome Res, 22*(1), 142-150. doi:10.1101/gr.124107.111

Balik, A., Penn, A. C., Nemoda, Z., & Greger, I. H. (2013). Activity-regulated RNA editing in select neuronal subfields in hippocampus. *Nucleic Acids Res, 41*(2), 1124-1134. doi:10.1093/nar/gks1045

Banerjee, A., Imig, C., Balakrishnan, K., Kershberg, L., Lipstein, N., Uronen, R.-L., . . . Kaeser, P. S. (2020). Molecular and functional architecture of striatal dopamine release sites. *bioRxiv*, 2020.2011.2025.398255. doi:10.1101/2020.11.25.398255

Bangasser, D. A., & Wiersielis, K. R. (2018). Sex differences in stress responses: a critical role for corticotropin-releasing factor. *Hormones (Athens), 17*(1), 5-13. doi:10.1007/s42000-018-0002-z

Barg, S., Ma, X., Eliasson, L., Galvanovskis, J., Gopel, S. O., Obermueller, S., . . . Rorsman, P. (2001). Fast Exocytosis with Few Ca2+ Channels in Insulin-Secreting Mouse Pancreatic B Cells. *Biophys J, 81*, 3308-3323.

Basilio, C., Wahba, A. J., Lengyel, P., Speyer, J. F., & Ochoa, S. (1962). Synthetic polynucleotides and the amino acid code, V. *Proc Natl Acad Sci U S A, 48*(4), 613-616.

Bassell, G. J., Zhang, H., L., B. A., Femino, A. M., Singer, H. S., Taneja, K. L., . . . Kosik, K. S. (1998). Sorting of beta-actin mRNA and protein to neurites and growth cones in culture. *J Neuro, 18*(1), 251-265.

Beites, C. L., Xie, H., Bowser, R., & Trimble, W. S. (1999). The septin CDCrel-1 binds syntaxin and inhibits exocytosis. *Nat Neurosci, 2*(5), 434-429.

Benelam, B. (2009). Satiation, satiety and their effects on eating behaviour. *Nutrition Bulletin, 34*(2), 126-173. doi:10.1111/j.1467-3010.2009.01753.x

Bergquist, F., Niazi, H. S., & Nissbrandt, H. (2002). Evidence for different exocytosis pathways in dendritic and terminal dopamine release in vivo. *Brain Research, 950*, 245-253.

Bhat, S., El-Kasaby, A., Freissmuth, M., & Sucic, S. (2020). Functional and Biochemical Consequences of Disease Variants in Neurotransmitter Transporters: A Special Emphasis on Folding and Trafficking Deficits. *Pharmacol Ther, 222*, 107785. doi:10.1016/j.pharmthera.2020.107785

Binda, A. V., Kabbani, N., & Levenson, R. (2005). Regulation of dense core vesicle release from PC12 cells by interaction between the D2 dopamine receptor and calcium-dependent activator protein for secretion (CAPS). *Biochem Pharmacol, 69*(10), 1451-1461. doi:10.1016/j.bcp.2005.02.015

Blesa, J., & Przedborski, S. (2014). Parkinson's disease: animal models and dopaminergic cell vulnerability. *Front Neuroanat, 8*, 155. doi:10.3389/fnana.2014.00155

Bolan, E. A., Kivell, B., Jaligam, V., Oz, M., Jayanthi, L. D., Han, Y., . . . Shippenberg, T. S. (2007). D2 receptors regulate dopamine transporter function via an extracellular signal-regulated kinases 1 and 2-dependent and phosphoinositide 3 kinase-independent mechanism. *Mol Pharmacol, 71*(5), 1222-1232. doi:10.1124/mol.106.027763

Bolte, S., & Cordelieres, F. P. (2006). A guided tour into subcellular colocalization analysis in light microscopy. *J Microsc, 224*(3).

Breen, M. S., Dobbyn, A., Li, Q., Roussos, P., Hoffman, G. E., Stahl, E., . . . CommonMind, C. (2019). Global landscape and genetic regulation of RNA editing in cortical samples from individuals with schizophrenia. *Nat Neurosci, 22*(9), 1402-1412. doi:10.1038/s41593-019-0463-7

Brenner, S. (1974). The genetics of Caenorhabditis elegans. *Genetics, 77*(1), 71-94.

Brimblecombe, K. R., Gracie, C. J., Platt, N. J., & Cragg, S. J. (2015). Gating of dopamine transmission by calcium and axonal N-, Q-, T- and L-type voltage-gated calcium channels differs between striatal domains. *J Physiol, 593*(4), 929-946. doi:10.1113/jphysiol.2014.285890

Brunk, I., Blex, C., Speidel, D., Brose, N., & Ahnert-Hilger, G. (2009). Ca2+-dependent activator proteins of secretion promote vesicular monoamine uptake. *J Biol Chem, 284*(2), 1050-1056. doi:10.1074/jbc.M805328200

Brussa, R., Zimmermann, F., Koh, D.-S., Feldmeyer, D., Gass, P., Seeburg, P. H., & Sprengel, R. (1995). Early-Onset Epilepsy and Postnatal Lethality Associated with an Editing-Deficient GluR-B Allele in Mice. *Science, 270*(5242), 1677-1680.

Caille, I., Dumartin, B., & Bloch, B. (1996). Ultrastructural localization of D1 dopamine receptor immunoreactivity in rat striatonigral regions and its relation with dopaminergic innervation. *Brain Research, 730*, 17-31.

Calipari, E. S., Juarez, B., Morel, C., Walker, D. M., Cahill, M. E., Ribeiro, E., . . . Nestler, E. J. (2017). Dopaminergic dynamics underlying sex-specific cocaine reward. *Nat. Commun., 8*, 13877. doi:10.1038/ncomms13877

Charlie, N. K., Schade, M. A., Thomure, A. M., & Miller, K. G. (2006). Presynaptic UNC-31 (CAPS) is required to activate the G alpha(s) pathway of the Caenorhabditis elegans synaptic signaling network. *Genetics, 172*(2), 943-961. doi:10.1534/genetics.105.049577

Chen, C., Cho, D. S., Wang, Q., Lai, F., Carter, K. C., & Nishikura, K. (2000). A third member of the RNA-specific adenosine deaminase gene family, ADAR3, contains both single- and double-stranded RNA binding domains. *RNA, 6*, 755-767.

Cijsouw, T., Weber, J. P., Broeke, J. H., Broek, J. A., Schut, D., Kroon, T., . . . Toonen, R. F. (2014). Munc18-1 redistributes in nerve terminals in an activity- and PKC-dependent manner. *J Cell Biol, 204*(5), 759-775. doi:10.1083/jcb.201308026

Cisternas, F. A., Vincent, J. B., Scherer, S. W., & Ray, P. N. (2003). Cloning and characterization of human CADPS and CADPS2, new members of the Ca2+-dependent activator for secretion protein family. *Genomics, 81*(3), 279-291. doi:10.1016/s0888-7543(02)00040-x

Cone, R. D. (2005). Anatomy and regulation of the central melanocortin system. *Nat Neurosci, 8*(5), 571-578. doi:10.1038/nn1455

Crawford, I. L., & Connor, J. D. (1973). Localization and release of glutamic acid in relation to the hippocampal mossy fibre pathway. *Nature, 244*, 442-443.

Crawley, J. N. (2007). Mouse behavioral assays relevant to the symptoms of autism. *Brain Pathol, 17*(4), 448-459. doi:10.1111/j.1750-3639.2007.00096.x

Cruz, P. H. C., Kato, Y., Nakahama, T., Shibuya, T., & Kawahara, Y. (2020). A comparative analysis of ADAR mutant mice reveals site-specific regulation of RNA editing. *RNA, 26*, 454-469. doi:10.1261/rna

Daily, N. J., Boswell, K. L., James, D. J., & Martin, T. F. (2010). Novel interactions of CAPS (Ca2+-dependent activator protein for secretion) with the three neuronal SNARE proteins required for vesicle fusion. *J Biol Chem, 285*(46), 35320-35329. doi:10.1074/jbc.M110.145169

DiCarlo, G. E., Aguilar, J. I., Matthies, H. J., Harrison, F. E., Bundschuh, K. E., West, A., . . . Galli, A. (2019). Autism-linked dopamine transporter mutation alters striatal dopamine neurotransmission and dopamine-dependent behaviors. *J Clin Invest, 129*(8), 3407-3419. doi:10.1172/JCI127411

Dickinson, S. D., Sabeti, J., Larson, G. A., Giardina, K., Rubinstein, M., Kelly, M. A., . . . Zahniser, N. R. (1999). Dopamine D2 receptor-deficient mice exhibit decreased dopamine transporter function but no changes in dopamine release in dorsal striatum. *J Neurochem, 72*(1), 148-156. doi:10.1046/j.1471-4159.1999.0720148.x

Donovan, M. J., Paulino, G., & Raybould, H. E. (2007). CCK(1) receptor is essential for normal meal patterning in mice fed high fat diet. *Physiol Behav, 92*(5), 969-974. doi:10.1016/j.physbeh.2007.07.003

Dulubova, I., Sugita, S., Hill, S., Hosaka, M., Fernandez, I., Sudhof, T. C., & Rizo, J. (1999). A conformational switch in syntaxin during exocytosis: role of munc18. *EMBO J, 18*(16), 4372-4382. doi:10.1093/emboj/18.16.4372

Eckenstaler, R., Lessmann, V., & Brigadski, T. (2016). CAPS1 effects on intragranular pH and regulation of BDNF release from secretory granules in hippocampal neurons. *J Cell Sci, 129*(7), 1378-1390. doi:10.1242/jcs.178251

Elhamdani, A., Martin, T. F., Kowalchyk, J. A., & Artalejo, C. R. (1999). Ca(2+)-dependent activator protein for secretion is critical for the fusion of dense-core vesicles with the membrane in calf adrenal chromaffin cells. *J Neurosci, 19*(17), 7375-7383.

Eshel, N., & Roiser, J. P. (2010). Reward and punishment processing in depression. *Biol Psychiatry, 68*(2), 118-124. doi:10.1016/j.biopsych.2010.01.027

Farina, M., van de Bospoort, R., He, E., Persoon, C. M., van Weering, J. R., Broeke, J. H., . . . Toonen, R. F. (2015). CAPS-1 promotes fusion competence of stationary dense-core vesicles in presynaptic terminals of mammalian neurons. *Elife, 4*. doi:10.7554/eLife.05438

Filippini, A., Bonini, D., Lacoux, C., Pacini, L., Zingariello, M., Sancillo, L., . . . Barbon, A. (2017). Absence of the Fragile X Mental Retardation Protein results in defects of RNA editing of neuronal mRNAs in mouse. *RNA Biol, 14*(11), 1580-1591. doi:10.1080/15476286.2017.1338232

Fortin, G. D., Desrosiers, C. C., Yamaguchi, N., & Trudeau, L. E. (2006). Basal somatodendritic dopamine release requires snare proteins. *J Neurochem, 96*(6), 1740-1749. doi:10.1111/j.1471-4159.2006.03699.x

Foster, J. D., Yang, J. W., Moritz, A. E., Challasivakanaka, S., Smith, M. A., Holy, M., . . . Vaughan, R. A. (2012). Dopamine transporter phosphorylation site threonine 53 regulates substrate

reuptake and amphetamine-stimulated efflux. *J Biol Chem, 287*(35), 29702-29712. doi:10.1074/jbc.M112.367706

Fuccillo, M. V. (2016). Striatal Circuits as a Common Node for Autism Pathophysiology. *Front Neurosci, 10*, 27. doi:10.3389/fnins.2016.00027

Fujima, S., Amemiya, N., Arima, T., Sano, Y., & Furuichi, T. (2020). CAPS2 deficiency induces proopiomelanocortin accumulation in pituitary and affects food intake behavior in mice. *Neurosci Lett, 738*, 135335. doi:10.1016/j.neulet.2020.135335

Fujita, Y., Xu, A., Xie, L., Arunachalam, L., Chou, T. C., Jiang, T., . . . Sugita, S. (2007). Ca2+-dependent activator protein for secretion 1 is critical for constitutive and regulated exocytosis but not for loading of transmitters into dense core vesicles. *J Biol Chem, 282*(29), 21392-21403. doi:10.1074/jbc.M703699200

Gaisano, H. Y. (2017). Recent new insights into the role of SNARE and associated proteins in insulin granule exocytosis. *Diabetes Obes Metab, 19 Suppl 1*, 115-123. doi:10.1111/dom.13001

Gantz, S. C., Bunzow, J. R., & Williams, J. T. (2013). Spontaneous Inhibitory Synaptic Currents Mediated by a G Protein-Coupled Receptor. *Neuron, 78*, 807-812. doi:DOI10.1016

Gerber, S. H., Rah, J. C., Min, S. W., Liu, X., de Wit, H., Dulubova, I., . . . Sudhof, T. C. (2008). Conformational switch of syntaxin-1 controls synaptic vesicle fusion. *Science, 321*(5895), 1507-1510. doi:10.1126/science.1163174

Gowrishankar, R., Gresch, P. J., Davis, G. L., Katamish, R. M., Riele, J. R., Stewart, A. M., . . . Blakely, R. D. (2018). Region-Specific Regulation of Presynaptic Dopamine Homeostasis by D2 Autoreceptors Shapes the In Vivo Impact of the Neuropsychiatric Disease-Associated DAT Variant Val559. *J Neurosci, 38*(23), 5302-5312. doi:10.1523/JNEUROSCI.0055-18.2018

Grace, A. A., & Bunney, B. S. (1984a). The control of firing pattern in nigral dopamine neurons: burst firing. *J Neuro, 4*(11), 2877-2890.

Grace, A. A., & Bunney, B. S. (1984b). The control of firing pattern in nigral dopamine neurons: single spike firing. *J Neuro, 4*(11), 2866-2876.

Graybiel, A. M., & Grafton, S. T. (2015). The striatum: where skills and habits meet. *Cold Spring Harb Perspect Biol, 7*(8), a021691. doi:10.1101/cshperspect.a021691

Grishanin, R. N., Klenchin, V. A., Loyet, K. M., Kowalchyk, J. A., Ann, K., & Martin, T. F. (2002). Membrane association domains in Ca2+-dependent activator protein for secretion mediate plasma membrane and dense-core vesicle binding required for Ca2+-dependent exocytosis. *J Biol Chem, 277*(24), 22025-22034. doi:10.1074/jbc.M201614200

Grishanin, R. N., Kowalchyk, J. A., Klenchin, V. A., Ann, K., Earles, C. A., Chapman, E. R., . . . Martin, T. F. (2004). CAPS acts at a prefusion step in dense-core vesicle exocytosis as a PIP2 binding protein. *Neuron, 43*(4), 551-562. doi:10.1016/j.neuron.2004.07.028

Grove, J., Ripke, S., Als, T. D., Mattheisen, M., Walters, R. K., Won, H., . . . Borglum, A. D. (2019). Identification of common genetic risk variants for autism spectrum disorder. *Nat Genet, 51*(3), 431-444. doi:10.1038/s41588-019-0344-8

Gudelsky, G. A. (1981). Tuberoinfundibular Dopamine Neurons and the Regulation of Prolactin Secretion. *Psychoneuroendocrinology, 6*(1), 3-16.

Gundelfinger, E. D., Kessels, M. M., & Qualmann, B. (2003). Temporal and spatial coordination of exocytosis and endocytosis. *Nat Rev Mol Cell Biol, 4*(2), 127-139. doi:10.1038/nrm1016

Hata, Y., Slaughter, C. A., & Sudhof, T. C. (1993). Synaptic vesicle fusion complex contains unc-18 homologue bound to syntaxin. *Nature, 366*, 347-351.

Haynes, L. P., Fitzgerald, D. J., Wareing, B., O'Callaghan, D. W., Morgan, A., & Burgoyne, R. D. (2006). Analysis of the interacting partners of the neuronal calcium-binding proteins L-CaBP1, hippocalcin, NCS-1 and neurocalcin delta. *Proteomics, 6*(6), 1822-1832. doi:10.1002/pmic.200500489

Held, R. G., Liu, C., & Kaeser, P. S. (2016). ELKS controls the pool of readily releasable vesicles at excitatory synapses through its N-terminal coiled-coil domains. *Elife, 5*. doi:10.7554/eLife.14862

Herb, A., Higuchi, M., Sprengel, R., & Seeburg, P. H. (1996). Q/R site editing in kainate receptor GluR5 and GluR6 pre-mRNAs requires distant intronic sequences. *Proc Natl Acad Sci U S A, 93*, 1875-1880.

Hideyama, T., Yamashita, T., Aizawa, H., Tsuji, S., Kakita, A., Takahashi, H., & Kwak, S. (2012). Profound downregulation of the RNA editing enzyme ADAR2 in ALS spinal motor neurons. *Neurobiol Dis*, 1121-1128.

Higuchi, M., Single, F. N., Kohler, M., Sommer, B., Sprengel, R., & Seeburg, P. H. (1993). RNA editing of AMPA receptor subunit GluR-B: a base-paired intron-exon structure determines position and efficiency. *Cell, 75*(7), 1361-1370. doi:10.1016/0092-8674(93)90622-w

Hood, J. L., Morabito, M. V., Martinez, C. R., 3rd, Gilbert, J. A., Ferrick, E. A., Ayers, G. D., . . . Emeson, R. B. (2014). Reovirus-mediated induction of ADAR1 (p150) minimally alters RNA editing patterns in discrete brain regions. *Mol Cell Neurosci, 61*, 97-109. doi:10.1016/j.mcn.2014.06.001

Hosono, M., Shinoda, Y., Hirano, T., Ishizaki, Y., Furuichi, T., & Sadakata, T. (2016). Interaction of Ca(2+)-dependent activator protein for secretion 1 (CAPS1) with septin family proteins in mouse brain. *Neurosci Lett, 617*, 232-235. doi:10.1016/j.neulet.2016.02.035

Hough, R. F., & Bass, B. L. (1994). Purification of the *Xenopus laevis* Double-Stranded RNA Adenosine Deaminase. *J Biol Chem, 269*(13), 9933-9939.

Howe, M. W., & Dombeck, D. A. (2016). Rapid signalling in distinct dopaminergic axons during locomotion and reward. *Nature, 535*(7613), 505-510. doi:10.1038/nature18942

Howes, O. D., & Kapur, S. (2009). The dopamine hypothesis of schizophrenia: version III--the final common pathway. *Schizophr Bull, 35*(3), 549-562. doi:10.1093/schbul/sbp006

Imig, C., Min, S. W., Krinner, S., Arancillo, M., Rosenmund, C., Sudhof, T. C., . . . Cooper, B. H. (2014). The morphological and molecular nature of synaptic vesicle priming at presynaptic active zones. *Neuron, 84*(2), 416-431. doi:10.1016/j.neuron.2014.10.009

Ito, H., Atsuzawa, K., Morishita, R., Usuda, N., Sudo, K., Iwamoto, I., . . . Nagata, K. (2009). Sept8 controls the binding of vesicle-associated membrane protein 2 to synaptophysin. *J Neurochem, 108*(4), 867-880. doi:10.1111/j.1471-4159.2008.05849.x

James, D. J., Kowalchyk, J., Daily, N., Petrie, M., & Martin, T. F. (2009). CAPS drives trans-SNARE complex formation and membrane fusion through syntaxin interactions. *Proc Natl Acad Sci U S A, 106*(41), 17308-17313. doi:10.1073/pnas.0900755106

Jiao, J., He, M., Port, S. A., Baker, R. W., Xu, Y., Qu, H., . . . Zhang, Y. (2018). Munc18-1 catalyzes neuronal SNARE assembly by templating SNARE association. *Elife, 7*. doi:10.7554/eLife.41771

Jockusch, W. J., Speidel, D., Sigler, A., Sorensen, J. B., Varoqueaux, F., Rhee, J. S., & Brose, N. (2007). CAPS-1 and CAPS-2 are essential synaptic vesicle priming proteins. *Cell, 131*(4), 796-808. doi:10.1016/j.cell.2007.11.002

Jones, S. R., Gainetdinov, R. R., Jaber, M., Giros, B., Wightman, R. M., & Caron, M. G. (1998). Profound neuronal plasticity in response to inactivation of the dopamine transporter. *Proc Natl Acad Sci U S A, 95*, 4029-4034.

Jung, A. P., & Luthin, D. R. (2010). Wheel access does not attenuate weight gain in mice fed high-fat or high-CHO diets. *Med Sci Sports Exerc, 42*(2), 355-360. doi:10.1249/MSS.0b013e3181a6d88f

Kabachinski, G., Kielar-Grevstad, D. M., Zhang, X., James, D. J., & Martin, T. F. (2016). Resident CAPS on dense-core vesicles docks and primes vesicles for fusion. *Mol Biol Cell, 27*(4), 654-668. doi:10.1091/mbc.E15-07-0509

Kabachinski, G., Yamaga, M., Kielar-Grevstad, D. M., Bruinsma, S., & Martin, T. F. (2014). CAPS and Munc13 utilize distinct PIP2-linked mechanisms to promote vesicle exocytosis. *Mol Biol Cell, 25*(4), 508-521. doi:10.1091/mbc.E12-11-0829

Kaeser, P. S., Deng, L., Wang, Y., Dulubova, I., Liu, X., Rizo, J., & Sudhof, T. C. (2011). RIM proteins tether Ca2+ channels to presynaptic active zones via a direct PDZ-domain interaction. *Cell, 144*(2), 282-295. doi:10.1016/j.cell.2010.12.029

Kavalali, E. T., Klingauf, J., & Tsien, R. W. (1999). Activity-dependent regulation of synaptic clustering in a hippocampal culture system. *Proc Natl Acad Sci U S A, 96*(22), 12893-12900. doi:doi:10.1073/pnas.96.22.12893

Kawabe, H., Mitkovski, M., Kaeser, P. S., Hirrlinger, J., Opazo, F., Nestvogel, D., . . . Brose, N. (2017). ELKS1 localizes the synaptic vesicle priming protein bMunc13-2 to a specific subset of active zones. *J Cell Biol, 216*(4), 1143-1161. doi:10.1083/jcb.201606086

Khermesh, K., D'Erchia, A. M., Barak, M., Annese, A., Wachtel, C., Levanon, E. Y., . . . Eisenberg, E. (2016). Reduced levels of protein recoding by A-to-I RNA editing in Alzheimer's disease. *RNA, 22*(2), 290-302. doi:10.1261/rna.054627.115

Khodthong, C., Kabachinski, G., James, D. J., & Martin, T. F. (2011). Munc13 homology domain-1 in CAPS/UNC31 mediates SNARE binding required for priming vesicle exocytosis. *Cell Metab, 14*(2), 254-263. doi:10.1016/j.cmet.2011.07.002

Kim, U., Garner, T. L., Sanford, T., Speicher, D., Murray, J. M., & Nishikura, K. (1994). Purification and Characterization of Double-stranded RNA Adenosine Deaminase from Bovine Nuclear Extracts. *J Biol Chem, 269*(18), 13480-13489.

Kinoshita, A., Noda, M., & Kinoshita, M. (2000). Differential Localization of Septins in the Mouse Brain. *J Comp Neurol, 428*, 223-239.

Kreft, M., Krizaj, D., Grilc, S., & Zorec, R. (2003). Properties of Exocytotic Response in Vertebrate Photoreceptors. *J Neurophysiol, 90*, 218-225.

Kreft, M., Kuster, V., Grilc, S., Rupnik, M., Milisav, I., & Zorec, R. (2003). Synaptotagmin I increases the probability of vesicle fusion at low [Ca2+] in pituitary cells. *Am J Physiol Cell Physiol, 284*, C547-C554.

Kreutzberger, A. J. B., Kiessling, V., Liang, B., Seelheim, P., Jakhanwal, S., Jahn, R., . . . Tamm, L. K. (2017). Reconstitution of calcium-mediated exocytosis of dense-core vesicles. *Sci Adv, 3*(7), e1603208. doi:10.1126/sciadv.1603208

Lai, Y., Choi, U. B., Leitz, J., Rhee, H. J., Lee, C., Altas, B., . . . Brunger, A. T. (2017). Molecular Mechanisms of Synaptic Vesicle Priming by Munc13 and Munc18. *Neuron, 95*(3), 591-607 e510. doi:10.1016/j.neuron.2017.07.004

Le Moine, C., & Bloch, B. (1996). Expression of the d3 dopamine receptor in peptidergic neurons of the nucleus accumbens: Comparison with the D1 and D2 dopamine receptors. *Neuroscience, 73*(1), 131-143. doi:https://doi.org/10.1016/0306-4522(96)00029-2

Lee, Y., Kim, H., Kim, J. E., Park, J. Y., Choi, J., Lee, J. E., . . . Han, P. L. (2018). Excessive D1 Dopamine Receptor Activation in the Dorsal Striatum Promotes Autistic-Like Behaviors. *Mol Neurobiol, 55*(7), 5658-5671. doi:10.1007/s12035-017-0770-5

Levesque, D., Diaz, J. M., Pilon, C., Martres, M. P., Giros, B., Souil, E., . . . Sokoloff, P. (1992). Identification, characterization, and localization of the dopamine D3 receptor in rat brain using 7-[3H]hydroxy-N,N-di-n-propyl-2-aminotetralin. *Proc Natl Acad Sci U S A, 89*, 8155-8159.

Li, J. B., & Church, G. M. (2013). Deciphering the functions and regulation of brain-enriched A-to-I RNA editing. *Nat Neurosci, 16*(11), 1518-1522. doi:10.1038/nn.3539

Li, J. B., Levanon, E. Y., Yoon, J. K., Aach, J., Xie, B., Leproust, E., . . . Church, G. M. (2009). Genome-wide identification of human RNA editing sites by parallel DNA capturing and sequencing. *Science, 324*(5931), 1210-1213. doi:10.1126/science.1170995

Lin, L., Nuotio-Antar, A. M., Ma, X., Liu, F., Fiorotto, M. L., & Sun, Y. (2014). Ghrelin receptor regulates appetite and satiety during aging in mice by regulating meal frequency and portion size but not total food intake. *J Nutr, 144*(9), 1349-1355. doi:10.3945/jn.114.191171

Liu, C., Kershberg, L., Wang, J., Schneeberger, S., & Kaeser, P. S. (2018). Dopamine Secretion Is Mediated by Sparse Active Zone-like Release Sites. *Cell, 172*, 706-718.

Liu, Y., Peter, D., Roghani, A., Schuldiner, S., Prive, G. G., Eisenberg, D., . . . Edwards, R. H. (1992). A cDNA that suppresses MPP+ Toxicity encodes a vesicular amine transporter. *Cell, 70*, 539-551.

Livak, K. J., & Schmittgen, T. D. (2001). Analysis of Relative Gene Expression Data Using Real-Time Quantitative PCR and the 2^ - delta delta CT Method. *Methods, 25*, 402-408.

Lomeli, H., Mosbacher, J., Melcher, T., Hoger, T., Geiger, J. R. P., Kuner, T., . . . Seeburg, P. H. (1994). Control of Kinetic Properties of AMPA Receptor Channels by Nuclear RNA Editing. *Science, 266*(5191), 1709-1713.

Loyet, K. M., Kowalchyk, J. A., Chaudhary, A., Chen, J., Prestwich, G. D., & Martin, T. F. (1998). Specific binding of phosphatidylinositol 4,5-bisphosphate to calcium-dependent activator protein for secretion (CAPS), a potential phosphoinositide effector protein for regulated exocytosis. *J Biol Chem, 273*(14), 8337-8343.

Lu, J., Machius, M., Dulubova, I., Dai, H., Sudhof, T. C., Tomchick, D. R., & Rizo, J. (2006). Structural basis for a Munc13-1 homodimer to Munc13-1/RIM heterodimer switch. *PLoS Biol, 4*(7), e192. doi:10.1371/journal.pbio.0040192

Ma, C., Li, W., Xu, Y., & Rizo, J. (2011). Munc13 mediates the transition from the closed syntaxin-Munc18 complex to the SNARE complex. *Nat Struct Mol Biol, 18*(5), 542-549. doi:10.1038/nsmb.2047

Ma, C., Su, L., Seven, A. B., Xu, Y., & Rizo, J. (2013). Reconstitution of the Vital Functions of Munc18 and Munc13 in Neurotransmitter Release. *Science, 339*(6118), 421-425. doi:10.1126/science.1230473

Malik, T. N., Cartailler, J. P., & Emeson, R. B. (2021). Quantitative Analysis of Adenosine-to-Inosine RNA Editing. *Methods Mol Biol, 2181*, 97-111. doi:10.1007/978-1-0716-0787-9_7

McLachlan, S. M., Hamidi, S., Aliesky, H., Williams, R. W., & Rapoport, B. (2014). Sex, genetics, and the control of thyroxine and thyrotropin in mice. *Thyroid, 24*(7), 1080-1087. doi:10.1089/thy.2014.0003

Melcher, T., Maas, S., Herb, A., Sprengel, R., Higuchi, M., & Seeburg, P. H. (1996). RED2, a Brain-Specific Member of the RNA-specific Adenosine Deaminase Family. *J Biol Chem, 271*(50), 31795-31798.

Melcher, T., Maas, S., Herb, A., Sprengel, R., Seeburg, P. H., & Higuchi, M. (1996). A mammalian RNA editing enzyme. *Nature, 379*, 460-464.

Miller, K. G., Alfonso, A., Nguyen, M., Crowell, J. A., Johnson, C. D., & Rand, J. B. (1996). A genetic selection for Caenorhabditis elegans synaptic transmission mutants. *Proc Natl Acad Sci U S A, 93*(22), 12593-12598. doi:10.1073/pnas.93.22.12593

Misura, K. M., Scheller, R. H., & Weis, W. I. (2000). Three-dimensional structure of the neuronal-Sec1-syntaxin 1a complex. *Nature, 404*, 355-362.

Miyake, K., Ohta, T., Nakayama, H., Doe, N., Terao, Y., Oiki, E., . . . Kawahara, Y. (2016). CAPS1 RNA Editing Promotes Dense Core Vesicle Exocytosis. *Cell Rep, 17*(8), 2004-2014. doi:10.1016/j.celrep.2016.10.073

Morabito, M. V., Abbas, A. I., Hood, J. L., Kesterson, R. A., Jacobs, M. M., Kump, D. S., . . . Emeson, R. B. (2010). Mice with altered serotonin 2C receptor RNA editing display characteristics of Prader-Willi syndrome. *Neurobiol Dis, 39*(2), 169-180. doi:10.1016/j.nbd.2010.04.004

Mukherjee, K., Yang, X., Gerber, S. H., Kwon, H. B., Ho, A., Castillo, P. E., . . . Sudhof, T. C. (2010). Piccolo and bassoon maintain synaptic vesicle clustering without directly participating in vesicle exocytosis. *Proc Natl Acad Sci U S A, 107*(14), 6504-6509. doi:10.1073/pnas.1002307107

Nestvogel, D., Merino, R. M., Leon-Pinzon, C., Schottdorf, M., Lee, C., Imig, C., . . . Rhee, J. (2020). The Synaptic Vesicle Priming Protein CAPS-1 Shapes the Adaptation of Sensory Evoked Responses in Mouse Visual Cortex. *Cell Rep, 30*, 3261-3269. doi:10.1016/j.celrep.2020.02.045

Ng, E., Varaschin, R. K., Su, P., Browne, C. J., Hermainski, J., Foll, B. L., . . . Wong, A. H. C. (2016). Neuronal calcium sensor-1 deletion in the mouse decreases motivation and dopamine release in the nucleus accumbens *Behav Brain Res, 301*, 213-225.

Nusser, Z., Cull-Candy, S., & Farrant, M. (1997). Differences in Synaptic GABAA Receptor Number Unerlie Variation in GABA Mini Amplitude. *Neuron, 19*, 697-709.

O'Connell, M. A., & Keller, W. (1994). Purification and properties of double-stranded RNA-specific adenosine deaminase from calf thymus. *Proc Natl Acad Sci U S A, 91*, 10596-10600.

O'Connell, M. A., Krause, S., Higuchi, M., Hsuan, J. J., Totty, N. F., Jenny, A., & Keller, W. (1995). Cloning of cDNAs Encoding Mammalian Double-Stranded RNA-specific Adenosine Deaminase. *Mol Cell Biology, 15*(3), 1389-1397.

Ogura, T., Ogata, M., Akita, H., Jitsuki, S., Akiba, L., Noda, K., . . . Saji, M. (2005). Impaired acquisition of skilled behavior in rotarod task by moderate depletion of striatal dopamine

in a pre-symptomatic stage model of Parkinson's disease. *Neurosci Res, 51*(3), 299-308. doi:10.1016/j.neures.2004.12.006

Olah, M., Feher, P., Ihm, Z., Bacskay, I., Kiss, T., Freeman, M. E., . . . Vecsernyes, M. (2009). Dopamine-regulated adrenocorticotropic hormone secretion in lactating rats: functional plasticity of melanotropes. *Neuroendocrinology, 90*(4), 391-401. doi:10.1159/000232313

Park, E., Williams, B., Wold, B. J., & Mortazavi, A. (2012). RNA editing in the human ENCODE RNA-seq data. *Genome Res, 22*(9), 1626-1633. doi:10.1101/gr.134957.111

Parsaud, L., Li, L., Jung, C. H., Park, S., Saw, N. M., Kim, M. Y., & Sugita, S. (2013). Calcium-dependent activator protein for secretion 1 (CAPS1) binds to syntaxin-1 in a distinct mode from Munc13-1. *J Biol Chem, 288*(32), 23050-23063. doi:10.1074/jbc.M113.494088

Pavlos, N. J., Gronborg, M., Riedel, D., Chua, J. J., Boyken, J., Kloepper, T. H., . . . Jahn, R. (2010). Quantitative analysis of synaptic vesicle Rabs uncovers distinct yet overlapping roles for Rab3a and Rab27b in Ca2+-triggered exocytosis. *J Neurosci, 30*(40), 13441-13453. doi:10.1523/JNEUROSCI.0907-10.2010

Pei, J., Ma, C., Rizo, J., & Grishin, N. V. (2009). Remote homology between Munc13 MUN domain and vesicle tethering complexes. *J Mol Biol, 391*(3), 509-517. doi:10.1016/j.jmb.2009.06.054

Petrie, M., Esquibel, J., Kabachinski, G., Maciuba, S., Takahashi, H., Edwardson, J. M., & Martin, T. F. (2016). The Vesicle Priming Factor CAPS Functions as a Homodimer via C2 Domain Interactions to Promote Regulated Vesicle Exocytosis. *J Biol Chem, 291*(40), 21257-21270. doi:10.1074/jbc.M116.728097

Polson, A. G., Crain, P. F., Pomerantz, S. C., McCloskey, J. A., & Bass, B. L. (1991). The Mechanism of Adenosine to Inosine Conversion by the Double-Stranded RNA Unwinding/Modifying Activity: A High-Performance Liquid Chromatography- Mass Spectrometry Analysis. *Biochemistry, 30*, 11507-11514. doi:10.1021/bi00113a004,

Porath, H. T., Hazan, E., Shpigler, H., Cohen, M., Band, M., Ben-Shahar, Y., . . . Bloch, G. (2019). RNA editing is abundant and correlates with task performance in a social bumblebee. *Nat Commun, 10*(1), 1605. doi:10.1038/s41467-019-09543-w

Pothos, E. N., Davila, V., & Sulzer, D. (1998). Presynaptic recording of quanta from midbrain dopamine neurons and modulation of the quantal size. *J Neuro, 18*(11), 4106-4118.

Powell, L. M., Wallis, S. C., Pease, R. J., Edwards, Y. H., Knott, T. J., & Scott, J. (1987). A novel form of tissue-specific RNA processing produces apolipoprotein-B48 in intestine. *Cell, 50*(6), 831-840. doi:10.1016/0092-8674(87)90510-1

Puig, M. V., Rose, J., Schmidt, R., & Freund, N. (2014). Dopamine modulation of learning and memory in the prefrontal cortex: insights from studies in primates, rodents, and birds. *Front Neural Circuits, 8*, 93. doi:10.3389/fncir.2014.00093

Ramamoorthy, S., Shippenberg, T. S., & Jayanthi, L. D. (2011). Regulation of monoamine transporters: Role of transporter phosphorylation. *Pharmacol Ther, 129*(2), 220-238. doi:10.1016/j.pharmthera.2010.09.009

Ramaswami, G., Zhang, R., Piskol, R., Keegan, L. P., Deng, P., O'Connell, M. A., & Li, J. B. (2013). Identifying RNA editing sites using RNA sequencing data alone. *Nat Methods, 10*(2), 128-132. doi:10.1038/nmeth.2330

Ravussin, Y., Xiao, C., Gavrilova, O., & Reitman, M. L. (2014). Effect of intermittent cold exposure on brown fat activation, obesity, and energy homeostasis in mice. *PLoS One, 9*(1), e85876. doi:10.1371/journal.pone.0085876

Regehr, W. G. (2012). Short-term presynaptic plasticity. *Cold Spring Harb Perspect Biol, 4*(7), a005702. doi:10.1101/cshperspect.a005702

Rice, M. E., Richards, C. D., Nedergaard, S., Hounsgaard, J., Nicholson, C., & Greenfield, S. A. (1994). Direct monitoring of dopamine and 5-HT release in substantia nigra and ventral tegmental area in vitro. *Exp Brain Res, 100*, 395-406.

Rizo, J. (2018). Mechanism of neurotransmitter release coming into focus. *Protein Sci, 27*(8), 1364-1391. doi:10.1002/pro.3445

Rizo, J., & Sudhof, T. C. (1998). C2-domains, Structure and Function of a Universal Ca2+-binding domain. *J Biol Chem, 273*(26), 15879-15882.

Rueter, S. M., Burns, C. M., Coode, S. A., Mookherjee, P., & Emeson, R. B. (1995). Glutamate Receptor RNA Editing in Vitro by Enzymatic Conversion of Adenosine to Inosine. *Science, 267*(5203), 1491-1494.

Rueter, S. M., Dawson, T. R., & Emeson, R. B. (1999). Regulation of alternative splicing by RNA editing. *Nature, 399*(6731), 75-80. doi:10.1038/19992

Rupnik, M., Kreft, M., Sikdar, S. K., Grilc, S., Romih, R., Zupancic, G., . . . Zorec, R. (2000). Rapid regulated dense-core vesicle exocytosis requires the CAPS protein. *Proc Natl Acad Sci U S A, 97*(10), 5627-5632. doi:10.1073/pnas.090359097

Sadakata, T., Itakura, M., Kozaki, S., Sekine, Y., Takahashi, M., & Furuichi, T. (2006). Differential distributions of the Ca2+ -dependent activator protein for secretion family proteins (CAPS2 and CAPS1) in the mouse brain. *J Comp Neurol, 495*(6), 735-753. doi:10.1002/cne.20947

Sadakata, T., Kakegawa, W., Shinoda, Y., Hosono, M., Katoh-Semba, R., Sekine, Y., . . . Furuichi, T. (2013). CAPS1 deficiency perturbs dense-core vesicle trafficking and Golgi structure and reduces presynaptic release probability in the mouse brain. *J Neurosci, 33*(44), 17326-17334. doi:10.1523/JNEUROSCI.2777-13.2013

Sadakata, T., Washida, M., Iwayama, Y., Shoji, S., Sato, Y., Ohkura, T., . . . Furuichi, T. (2007). Autistic-like phenotypes in Cadps2-knockout mice and aberrant CADPS2 splicing in autistic patients. *J Clin Invest, 117*(4), 931-943. doi:10.1172/JCI29031

Sadakata, T., Washida, M., Morita, N., & Furuichi, T. (2007). Tissue distribution of Ca2+-dependent activator protein for secretion family members CAPS1 and CAPS2 in mice. *J Histochem Cytochem, 55*(3), 301-311. doi:10.1369/jhc.6A7033.2006

Salamone, J. D., & Correa, M. (2012). The mysterious motivational functions of mesolimbic dopamine. *Neuron, 76*(3), 470-485. doi:10.1016/j.neuron.2012.10.021

Sanjana, N. E., Levanon, E. Y., Hueske, E. A., Ambrose, J. M., & Li, J. B. (2012). Activity-dependent A-to-I RNA editing in rat cortical neurons. *Genetics, 192*(1), 281-287. doi:10.1534/genetics.112.141200

Sapiro, A. L., Freund, E. C., Restrepo, L., Qiao, H. H., Bhate, A., Li, Q., . . . Li, J. B. (2020). Zinc Finger RNA-Binding Protein Zn72D Regulates ADAR-Mediated RNA Editing in Neurons. *Cell Rep, 31*(7), 107654. doi:10.1016/j.celrep.2020.107654

Schaffer, A. A., Kopel, E., Hendel, A., Picardi, E., Levanon, E. Y., & Eisenberg, E. (2020). The cell line A-to-I RNA editing catalogue. *Nucleic Acids Res, 48*(11), 5849-5858. doi:10.1093/nar/gkaa305

Schmidt, H. D., McFarland, K. N., Darnell, S. B., Huizenga, M. N., Sangrey, G. R., Cha, J. H., . . . Sadri-Vakili, G. (2015). ADAR2-dependent GluA2 editing regulates cocaine seeking. *Mol Psychiatry, 20*(11), 1460-1466. doi:10.1038/mp.2014.134

Schoch, S., Deak, F., Konigstorfer, A., Mozhayeva, M., Sara, Y., Sudhof, T. C., & Kavalali, E. T. (2001). SNARE function analyzed in synaptobrevin/VAMP knockout mice. *Science, 294*, 1117-1122.

Shaib, A. H., Staudt, A., Harb, A., Klose, M., Shaaban, A., Schirra, C., . . . Becherer, U. (2018). Paralogs of the Calcium-Dependent Activator Protein for Secretion Differentially Regulate Synaptic Transmission and Peptide Secretion in Sensory Neurons. *Front Cell Neurosci, 12*, 304. doi:10.3389/fncel.2018.00304

Shinoda, Y., Ishii, C., Fukazawa, Y., Sadakata, T., Ishii, Y., Sano, Y., . . . Furuichi, T. (2016). CAPS1 stabilizes the state of readily releasable synaptic vesicles to fusion competence at CA3-CA1 synapses in adult hippocampus. *Sci Rep, 6*, 31540. doi:10.1038/srep31540

Shiotsuki, H., Yoshimi, K., Shimo, Y., Funayama, M., Takamatsu, Y., Ikeda, K., . . . Hattori, N. (2010). A rotarod test for evaluation of motor skill learning. *J Neurosci Methods, 189*(2), 180-185. doi:10.1016/j.jneumeth.2010.03.026

Shu, T., Jin, H., Rothman, J. E., & Zhang, Y. (2020). Munc13-1 MUN domain and Munc18-1 cooperatively chaperone SNARE assembly through a tetrameric complex. *Proc Natl Acad Sci U S A, 117*(2), 1036-1041. doi:10.1073/pnas.1914361117/-/DCSupplemental

Siciliano, C. A., Calipari, E. S., Ferris, M. J., & Jones, S. R. (2014). Biphasic mechanisms of amphetamine action at the dopamine terminal. *J Neurosci, 34*(16), 5575-5582. doi:10.1523/jneurosci.4050-13.2014

Siksou, L., Varoqueaux, F., Pascual, O., Triller, A., Brose, N., & Marty, S. (2009). A common molecular basis for membrane docking and functional priming of synaptic vesicles. *Eur J Neurosci, 30*(1), 49-56. doi:10.1111/j.1460-9568.2009.06811.x

Sollner, T., Bennett, M. K., Whiteheart, S. W., Scheller, R. H., & Rothman, J. E. (1993). A protein assembly-disassembly pathway in vitro that may correspond to sequential steps of synaptic vesicle docking, activation, and fusion. *Cell, 75*(3), 409-418. doi:10.1016/0092-8674(93)90376-2

Sommer, B., Kohler, M., Sprengel, R., & Seeburg, P. H. (1991). RNA editing in brain controls a determinant of ion flow in glutamate-gated channels. *Cell, 67*(1), 11-19. doi:10.1016/0092-8674(91)90568-j

Speidel, D., Bruederle, C. E., Enk, C., Voets, T., Varoqueaux, F., Reim, K., . . . Rettig, J. (2005). CAPS1 regulates catecholamine loading of large dense-core vesicles. *Neuron, 46*(1), 75-88. doi:10.1016/j.neuron.2005.02.019

Speidel, D., Salehi, A., Obermueller, S., Lundquist, I., Brose, N., Renstrom, E., & Rorsman, P. (2008). CAPS1 and CAPS2 regulate stability and recruitment of insulin granules in mouse pancreatic beta cells. *Cell Metab, 7*(1), 57-67. doi:10.1016/j.cmet.2007.11.009

Speidel, D., Varoqueaux, F., Enk, C., Nojiri, M., Grishanin, R. N., Martin, T. F., . . . Reim, K. (2003). A family of Ca2+-dependent activator proteins for secretion: comparative analysis of structure, expression, localization, and function. *J Biol Chem, 278*(52), 52802-52809. doi:10.1074/jbc.M304727200

Stevens, D. R., & Rettig, J. (2009). The Ca(2+)-dependent activator protein for secretion CAPS: do I dock or do I prime? *Mol Neurobiol, 39*(1), 62-72. doi:10.1007/s12035-009-8052-5

Sudhof, T. C. (2004). The synaptic vesicle cycle. *Annu Rev Neurosci, 27*, 509-547. doi:10.1146/annurev.neuro.26.041002.131412

Sutton, R. B., Fasshauer, D., Jahn, R., & Brunger, A. T. (1998). Crystal structure of a SNARE complex involved in synaptic exocytosis at 2.4 A resolution. *Nature, 395*(6700), 347-353. doi:10.1038/26412

Swallow, J. G., Koteja, P., Carter, P. A., & Garland, T. (2001). Food consumption and body composition in mice selected for high wheel-running activity. *J Comp Physiol B, 171*, 651-659. doi:10.1007/s003600100216

Tan, M. H., Li, Q., Shanmugam, R., Piskol, R., Kohler, J., Young, A. N., . . . Li, J. B. (2017). Dynamic landscape and regulation of RNA editing in mammals. *Nature, 550*(7675), 249-254. doi:10.1038/nature24041

Tandon, A., Bannykh, S., Kowalchyk, J. A., Banerjee, A., Martin, T. F., & Balch, W. E. (1998). Differential regulation of exocytosis by calcium and CAPS in semi-intact synaptosomes. *Neuron, 21*(1), 147-154.

Tang, A. H., Chen, H., Li, T. P., Metzbower, S. R., MacGillavry, H. D., & Blanpied, T. A. (2016). A trans-synaptic nanocolumn aligns neurotransmitter release to receptors. *Nature, 536*(7615), 210-214. doi:10.1038/nature19058

Thomas, P., Wong, J. G., Lee, A. K., & Almers, W. (1993). A low affinity calcium receptor controls the final steps of peptide secretion from pituitary melanotrophs. *Neuron, 11*, 93-104.

Thorn, P., Zorec, R., Rettig, J., & Keating, D. J. (2016). Exocytosis in non-neuronal cells. *J Neurochem, 137*(6), 849-859. doi:10.1111/jnc.13602

Threlfell, S., Lalic, T., Platt, N. J., Jennings, K. A., Deisseroth, K., & Cragg, S. J. (2012). Striatal Dopamine Release Is Triggered by Synchronized Activity in Cholinergic Interneurons. *Neuron, 75*(1), 58-64.

Tran, S. S., Jun, H. I., Bahn, J. H., Azghadi, A., Ramaswami, G., Van Nostrand, E. L., . . . Xiao, X. (2019). Widespread RNA editing dysregulation in brains from autistic individuals. *Nat Neurosci, 22*(1), 25-36. doi:10.1038/s41593-018-0287-x

Tsai, W.-H. (1985). Moment-Preserving Thresholding: A New Approach. *Computer Vision, Graphics, and Image Processing, 29*, 377-393.

Tsang, C. W., Estey, M. P., DiCiccio, J. E., Xie, H., Patterson, D., & Trimble, W. S. (2001). Characterization of presynaptic septin complexes in mammalian hippocampal neurons. *Biol Chem, 392*, 739-749. doi:10.1515/bc.2011.077sup

Uchigashima, M., Ohtsuka, T., Kobayashi, K., & Watanabe, M. (2016). Dopamine synapse is a neuroligin-2-mediated contact between dopaminergic presynaptic and GABAergic postsynaptic structures. *Proc Natl Acad Sci U S A, 113*(15), 4206-4211. doi:10.1073/pnas.1514074113

van Keimpema, L., Kooistra, R., Toonen, R. F., & Verhage, M. (2017). CAPS-1 requires its C2, PH, MHD1 and DCV domains for dense core vesicle exocytosis in mammalian CNS neurons. *Sci Rep, 7*(1), 10817. doi:10.1038/s41598-017-10936-4

Varoqueaux, F., Sigler, A., Rhee, J. S., Brose, N., Enk, C., Reim, K., & Rosenmund, C. (2002). Total arrest of spontaneous and evoked synaptic transmission but normal synaptogenesis in the absence of Munc13-mediated vesicle priming. *Proc Natl Acad Sci U S A, 99*(13), 9037-9042. doi:10.1073/pnas.122623799

Verhage, M., Maia, A. S., Plomp, J. J., Brussaard, A. B., Heeroma, J. H., Vermeer, H., . . . Sudhof, T. C. (2000). Synaptic assembly of the brain in the absence of neurotransmitter secretion. *Science, 287*(5454), 864-869. doi:10.1126/science.287.5454.864

Wagner, T., & Lipinski, H.-G. (2013). IJBlob: An ImageJ Library for Connected Component Analysis and Shape Analysis. *J Open Res Softw, 1*(1), e6. doi:http://doi.org/10.5334/jors.ae

Wahlstedt, H., Daniel, C., Enstero, M., & Ohman, M. (2009). Large-scale mRNA sequencing determines global regulation of RNA editing during brain development. *Genome Res, 19*(6), 978-986. doi:10.1101/gr.089409.108

Walent, J. H., Porter, B. W., & Martin, T. F. (1992a). A novel 145 kd brain cytosolic protein reconstitutes Ca(2+)-regulated secretion in permeable neuroendocrine cells. *Cell, 70*(5), 765-775.

Walent, J. H., Porter, B. W., & Martin, T. F. J. (1992b). A Novel 145 kd Brain Cytosolic Protein Reconstitutes Ca2+-Regulated Secretion in Permeable Neuroendocrine Cells. *Cell, 70*, 765-775.

Wang, J., Huang, J., Yang, X. H., Lui, S. S., Cheung, E. F., & Chan, R. C. (2015). Anhedonia in schizophrenia: Deficits in both motivation and hedonic capacity. *Schizophr Res, 168*(1-2), 465-474. doi:10.1016/j.schres.2015.06.019

Wang, S., Li, Y., Gong, J., Ye, S., Yang, X., Zhang, R., & Ma, C. (2019). Munc18 and Munc13 serve as a functional template to orchestrate neuronal SNARE complex assembly. *Nat Commun, 10*(1), 69. doi:10.1038/s41467-018-08028-6

Wang, Y., Okamoto, M., Schmitz, F., Hofmann, K., & Sudhof, T. C. (1997). Rim is a putative Rab3 effector in regulating synaptic-vesicle fusion. *Nature, 388*, 593-598.

Wassenberg, J. J., & Martin, T. F. (2002). Role of CAPS in dense-core vesicle exocytosis. *Ann N Y Acad Sci, 971*, 201-209.

West, D. B., Fey, D., & Woods, S. C. (1984). Cholecystokinin persistently suppresses meal size but not food intake in free-feeding rats. *American Journal of Physiology-Regulatory, Integrative and Comparative Physiology, 246*(5), R776-R787. doi:10.1152/ajpregu.1984.246.5.R776

Wojcik, S. M., Katsurabayashi, S., Guillemin, I., Friauf, E., Rosenmund, C., Brose, N., & Rhee, J. S. (2006). A shared vesicular carrier allows synaptic corelease of GABA and glycine. *Neuron, 50*(4), 575-587. doi:10.1016/j.neuron.2006.04.016

Wojcik, S. M., Rhee, J. S., Herzog, E., Sigler, A., Jahn, R., Takamori, S., . . . Rosenmund, C. (2004). An essential role for vesicular glutamate transporter 1 (VGLUT1) in postnatal development and control of quantal size. *Proc Natl Acad Sci U S A, 101*(18), 7158-7163.

Wu, B., Sun, D., Ma, L., Deng, Y., Zhang, S., Dong, L., & Chen, S. (2019). Exosomes isolated from CAPS1-overexpressing colorectal cancer cells promote cell migration. *Oncology Reports*. doi:10.3892/or.2019.7361

Xu, X., Wang, Y., & Liang, H. (2018). The role of A-to-I RNA editing in cancer development. *Curr Opin Genet Dev, 48*, 51-56. doi:10.1016/j.gde.2017.10.009

Yang, B., Steegmaier, M., Gonzalez Jr., L. C., & Scheller, R. H. (2000). nSec1 Binds a Closed Conformation of Syntaxin1a. *J Cell Biol, 148*(2), 247-252.

Yang, B., Steegmaier, M., Gonzalez, L. C., Jr., & Scheller, R. H. (2000). nSec1 binds a closed conformation of syntaxin1A. *J Cell Biol, 148*(2), 247-252. doi:10.1083/jcb.148.2.247

Yang, L., Zhao, L., Gan, Z., He, Z., Xu, J., Gao, X., . . . Liu, Y. (2010). Deficiency in RNA editing enzyme ADAR2 impairs regulated exocytosis. *FASEB J, 24*(10), 3720-3732. doi:10.1096/fj.09-152363

Yang, X., Wang, S., Sheng, Y., Zhang, M., Zou, W., Wu, L., . . . Ma, C. (2015). Syntaxin opening by the MUN domain underlies the function of Munc13 in synaptic-vesicle priming. *Nat Struct Mol Biol, 22*(7), 547-554. doi:10.1038/nsmb.3038

Yorgason, J. T., España, R. A., & Jones, S. R. (2011). Demon voltammetry and analysis software: analysis of cocaine-induced alterations in dopamine signaling using multiple kinetic measures. *Journal of Neuroscience Methods, 202*(2), 158-164.

Yorgason, J. T., Zeppenfeld, D. M., & Williams, J. T. (2017). Cholinergic Interneurons Underlie Spontaneous Dopamine Release in Nucleus Accumbens. *J Neurosci, 37*(8), 2086-2096. doi:10.1523/JNEUROSCI.3064-16.2017

Zhang, H., & Sulzer, D. (2004). Frequency-dependent modulation of dopamine release by nicotine. *Nat Neurosci, 7*(6), 581-582. doi:10.1038/nn1243

Zhao, G. X., Xu, Y. Y., Weng, S. Q., Zhang, S., Chen, Y., Shen, X. Z., . . . Chen, S. (2019). CAPS1 promotes colorectal cancer metastasis via Snail mediated epithelial mesenchymal transformation. *Oncogene*. doi:10.1038/s41388-019-0740-7

Zhou, F. M., Liang, Y., & Dani, J. A. (2001). Endogenous nicotinic cholinergic activity regulates dopamine release in the striatum. *Nat Neurosci, 4*(12), 1224-1229. doi:10.1038/nn769

Zhou, H., Wei, Z., Wang, S., Yao, D., Zhang, R., & Ma, C. (2019). Structural and Functional Analysis of the CAPS SNARE-Binding Domain Required for SNARE Complex Formation and Exocytosis. *Cell Rep, 26*(12), 3347-3359 e3346. doi:10.1016/j.celrep.2019.02.064